



**British
Geological Survey**

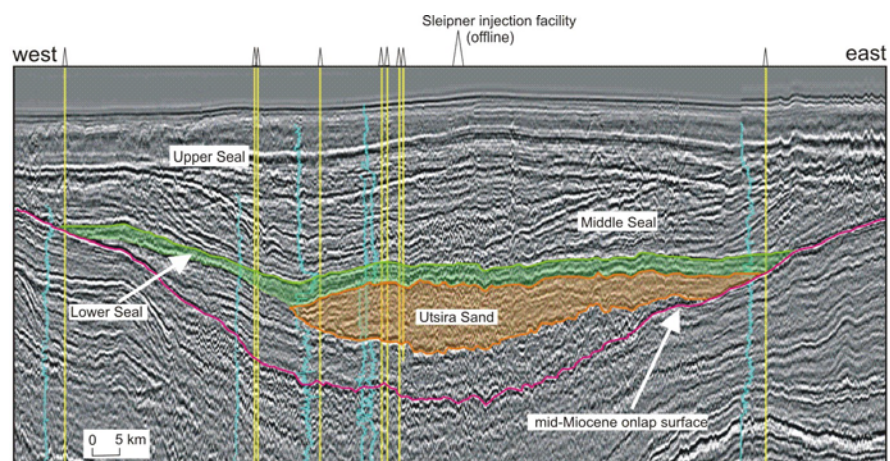
NATURAL ENVIRONMENT RESEARCH COUNCIL

Saline Aquifer CO₂ Storage (SACS2)

Final report: Geological characterisation of the
Utsira Sand reservoir and caprocks (Work Area 1)

Reservoir Geoscience Programme

Commissioned Report CR/02/153N



BRITISH GEOLOGICAL SURVEY

COMMISSIONED REPORT CR/02/153N

Saline Aquifer CO₂ Storage (SACS2)

Final report: Geological characterisation of the
Utsira Sand reservoir and caprocks (Work Area 1)

R A Chadwick, G.A. Kirby, S Holloway (BGS)

U. Gregersen, P.N. Johannessen (GEUS)

P. Zweigel (SINTEF)

R. Arts (NITG – TNO)

The National Grid and other
Ordnance Survey data are used
with the permission of the
Controller of Her Majesty's
Stationery Office.
Ordnance Survey licence number
GD 272191/1999

Key words

CO₂ storage, Seismic reflection
data, well data, depth and
isopach maps, porosity, sand
proportion, pore volume

*Front cover: Regional seismic
line through the Utsira Sand*

Bibliographical reference

CHADWICK, R. A., KIRBY, G.A.,
HOLLOWAY, S., GREGERSEN, U.,
JOHANNESSEN, P.N., ZWIEGEL, P.
& ARTS, R. 2002. Saline Aquifer
CO₂ Storage (SACS2). Final
Report: Geological
Characterisation (Work Area 1).
*British Geological Survey
Commissioned Report,
CR/02/153C.*

BRITISH GEOLOGICAL SURVEY

The full range of Survey publications is available from the BGS Sales Desks at Nottingham and Edinburgh; see contact details below or shop online at www.thebgs.co.uk

The London Information Office maintains a reference collection of BGS publications including maps for consultation.

The Survey publishes an annual catalogue of its maps and other publications; this catalogue is available from any of the BGS Sales Desks.

The British Geological Survey carries out the geological survey of Great Britain and Northern Ireland (the latter as an agency service for the government of Northern Ireland), and of the surrounding continental shelf, as well as its basic research projects. It also undertakes programmes of British technical aid in geology in developing countries as arranged by the Department for International Development and other agencies.

The British Geological Survey is a component body of the Natural Environment Research Council.

Keyworth, Nottingham NG12 5GG

☎ 0115-936 3241 Fax 0115-936 3488
e-mail: sales@bgs.ac.uk
www.bgs.ac.uk
Shop online at: www.thebgs.co.uk

Murchison House, West Mains Road, Edinburgh EH9 3LA

☎ 0131-667 1000 Fax 0131-668 2683
e-mail: scotsales@bgs.ac.uk

London Information Office at the Natural History Museum (Earth Galleries), Exhibition Road, South Kensington, London SW7 2DE

☎ 020-7589 4090 Fax 020-7584 8270
☎ 020-7942 5344/45 email: bgs-london@bgs.ac.uk

Forde House, Park Five Business Centre, Harrier Way, Sowton, Exeter, Devon EX2 7HU

☎ 01392-445271 Fax 01392-445371

Geological Survey of Northern Ireland, 20 College Gardens, Belfast BT9 6BS

☎ 028-9066 6595 Fax 028-9066 2835

Macleans Building, Crowmarsh Gifford, Wallingford, Oxfordshire OX10 8BB

☎ 01491-838800 Fax 01491-692345

Parent Body

Natural Environment Research Council, Polaris House, North Star Avenue, Swindon, Wiltshire SN2 1EU

☎ 01793-411500 Fax 01793-411501
www.nerc.ac.uk

Foreword

This report forms part of the international SACS (Saline Aquifer CO₂ Storage) project. The project aims to monitor and predict the behaviour of injected CO₂ in the Utsira Sand reservoir at the Sleipner field in the northern North Sea, to assess the regional storage potential of the Utsira reservoir, and to simulate and model likely chemical interactions of CO₂ with the host rock.

This is the final report of Work Area 1 in SACS, whose aims were to provide a full geological characterisation of the Utsira Sand and its caprock. The report summarises the key findings of the component subtasks of Work Area 1. The report also provides references to the various SACS Technical Reports wherein the full details of the scientific work can be found.

Acknowledgements

The authors would like to thank a number of colleagues whose work has contributed to the contents of this report namely J.M. Pearce, S J Kemp, J Bouch, H A Murphy, P.D. Wetton (BGS), N. Springer, L. Kristensen (GEUS), R. Bøe, E. Lindeberg and A. Lothe (SINTEF).

Forward	i
Acknowledgments	i
Summary.....	vii
1. Data Summary	1
1.1 Well Data	1
1.1.1 Core from the Utsira Sand	1
1.1.2 Cuttings from the Utsira Sand.....	1
1.1.3 Cuttings from the Nordland Shale	1
1.1.4 Core from a caprock analogue	1
1.1.5 Geophysical logs	2
1.1.6 Formation tops	2
1.1.7 Seismic data	2
1.1.8 Formation pressure data	2
2. The Utsira Sand Reservoir	2
2.1 Regional Structure	2
2.2 Structure around Sleipner	3
2.2.1 The coherency cube	3
2.3 Regional Stratigraphy	4
2.3.1 Well log correlations	4
2.3.2 Seismic stratigraphy	4
2.3.3 Core and cuttings	5
2.3.4 Biostratigraphy and depositional environment	6
2.4 Regional Reservoir Properties	7
3. Utsira Caprock	8
3.1 Regional Stratigraphy	8
3.1.1 The Lower Seal	8
3.1.2 The Middle Seal	9
3.1.3 The Upper Seal.....	9
3.2 Stratigraphy around Sleipner	10
3.3. Cuttings Analysis and Sealing Capacity.....	10
3.3.1 Lithology	10
3.3.2 Sealing capacity	10
3.4 Ekofisk Core	11
3.5 Seismic Amplitude Anomalies	11

3.5.1 Regional mapping	11
3.5.2 Mapping around Sleipner	12
4. Fluid Flow in the Utsira Sand	12
4.1 Natural Fluid Flow from Pressure Data.....	12
4.2 Fluid Flow from Basin Modelling	13
5. Utsira Reservoir Storage and Trapping Potential	14
5.1 Storage Capacity.....	14
5.1.1 Total storage volume.....	14
5.1.2 Volume in traps around Sleipner	14
5.2 CO ₂ migration away from the injection point	15
5.2.1 Migration at Top Utsira Sand.....	15
5.2.2 Migration at Top Sand-wedge.....	15
6. References and Bibliography	15
6.1 SACS Technical Reports	15
6.2 SACS Publications	16
6.3 Other References	17
Appendix I – Formation Tops in Wells.....	18

Table 1 Whole-rock XRD analysis of Utsira Sand core from UK well 15/9-A23

Table 2 Mineralogy of Utsira Sand core from UK well 15/9-A23 based on image analysis

Table 3 Possible overpressure in the Utsira Sand

Figure 1 Regional seismic and well datasets. Bold red lines denote geoseismic sections.

Figure 2 Seismic section across the southern Utsira depocentre, close to Sleipner (see Figure 1 for location).

Figure 3 Depth map to top of the Utsira Sand (scale in metres below OD). Dot denotes CO₂ injection point.

Figure 4 Depth map to base of the Utsira Sand (scale in metres below OD). Dot denotes CO₂ injection point.

Figure 5 Isopach map of the Utsira Sand (scale in metres). Dot denotes CO₂ injection point.

Figure 6 Synthetic seismograms derived from well log data (Norwegian well 15/9-7) compared to the actual seismic data.

Figure 7 3D seismic survey ST98M11, showing two-way time map of Top Utsira Sand and perspective view (top). Depth map to top Utsira Sand around injection point (bottom).

Figure 8 Seismic crossline (east to west) and inline (south to north) from survey ST98M11. Mud-volcanoes at the Base Utsira Sand are observed. Note the depressions just above them due to differential compaction. Amplitude anomalies possibly linked to the presence of shallow gas are observed in the thin shale drape just above the Top Utsira Sand in the lower Pliocene and also in the upper Pliocene.

Figure 9 3D seismic survey ST98M11, showing two-way time map of Base Utsira Sand. Note mud volcanoes.

Figure 10 Seismic inline showing 'pop-up' mud edifice, bounded by reverse faults. Note the identical seismic signature of the top part of the shales within and outside the mud edifice. Faults do not continue into the Utsira sand above the top level of the uplifted shales. The deeper shale layer, affected by polygonal normal faulting, has not been affected by the reverse faults.

Figure 11 Generalised stratigraphy of the Neogene of the northern North Sea. Principal sand units highlighted.

Figure 12 Regional well correlation diagrams a) through the Utsira southern depocentre. For simplicity the Sand-wedge is included in the Utsira Sand. b) through the Utsira northern depocentre. Note the sub-Utsira Sand unit in the north.

Figure 13 a) Detailed well logs through the Utsira Sand, showing a number of thin shale beds (Norwegian well 15/9-8). b) E-W well correlation diagram through the Utsira Sand and its caprock in the Sleipner area. Note the thin intra-reservoir shales and the Sand-wedge in the lowermost part of the caprock, pinching out to the west.

Figure 14 Thickness distribution of intra-reservoir shales, based on detailed interpretation of well log data from wells around Sleipner.

Figure 15 Interpreted geoseismic and well correlation section across the southern Utsira depocentre, showing the Utsira Sand and the main units of the caprock succession (see Figure 1 for location).

Figure 16 Interpreted geoseismic and well correlation section across the northern Utsira depocentre, showing the Utsira Sand and the main units of the caprock succession (see Figure 1 for location).

Figure 17 Complex distribution of the Utsira Sand at the western margin of the southern depocentre. Note the sand unit in UK well 16/29-4, formerly incorrectly identified as the Utsira Sand.

Figure 18 a) Photograph of 1m part of the Utsira Sand core from Norwegian well 15/9-A-23. b) Moderately well-sorted, subrounded to subangular, fine to medium-grained Utsira Sand c) Utsira Sand with calcareous shell and foraminifera fragments d) Typical examples of altered biotite (bottom) and muscovite flakes e) Typical example of rare glauconite grain, partially replaced by collophanic material and pyrite in cracks.

Figure 19 Whole-rock X-ray diffraction traces for samples E641A (black trace), E642 (red trace), E643 (magenta trace) and E644 (blue trace) showing major peak assignments and d spacings. Co-K α radiation.

Figure 20 Porosity of the Utsira Sand, computed from well logs (dot denotes CO₂ injection point).

Figure 21 Percentage clean sand in the Utsira Sand, computed from well logs (dot denotes CO₂ injection point).

Figure 22 Log correlation diagram across the southern Utsira depocentre, showing the lateral variation in shale content (percentage clean sand).

Figure 23 Schematic diagram of Pliocene prograding wedges and possible distribution of lithologies.

Figure 24 a) Seismic section across the southern Utsira depocentre showing the main caprock units. b) Interpreted geoseismic section across the northern Utsira depocentre showing the main caprock units.

Figure 25 a) Log detail of the Lower Seal around Sleipner b) Extent of the Lower Seal above the southern Utsira depocentre. Larger rectangle denotes survey ST98M11, smaller rectangle denotes 1999 time-lapse survey.

Figure 26 Distribution of minor sand units in the caprock succession.

Figure 27 a) The Sand-wedge on seismic b) Approximate extent of Sand-wedge picked out by high amplitudes

Figure 28 Thickness maps of the Sand-wedge (upper part of figure) reveal curved linear features interpreted as channels, visible on individual seismic lines (lower part of figure).

Figure 29 Wells with caprock cuttings samples. IP denotes CO₂ injection point. Green rectangle shows area of 1999 time-lapse seismic survey.

Figure 30 Typical examples of caprock cuttings a) shale fragments from Norwegian well 15/9-9, 615 m depth b) grey shale fragments from Norwegian well 15/9-14, 855 m depth.

Figure 31 SEM images of caprock cuttings material from wells in the UK sector a) Massive mudrock with several rounded fine-grained quartz grains (arrowed), UK well 16/29-1, 907 m depth b) Massive mudrock with large (up to 0.5 mm) voids (arrowed) where sand grains have been plucked out, UK well 16/28-3, 990 m depth c) High magnification detail of massive mudrock, showing tightly packed rather randomly-oriented clay particles. Note presence of clay mineral particles (arrowed), up to 20 µm in diameter, UK well 16/29-1, 907m depth.

Figure 32 a) Laminated mudrock with holes where fine sand grade grains have been plucked out, UK well 16/29-4, 1055 m depth b) High magnification detail of laminated mudrock showing tightly packed platelets with preferred orientation. Micropores (arrowed) are a few microns in diameter and poorly connected with each other, UK well 16/28-3, 970 m depth. c) Laminated mudrock, lamination defines terraced appearance of sample, UK well 16/29-1, 998 m.

Figure 33 X-ray diffraction traces from two caprock samples from Norwegian well 15/9-13, 795 and 805 m depth.

Figure 34 a) Mudrock with well-developed slickensides, UK well 16/28-5, 1100 m depth b) Mudrock with microfractures (arrowed), interpreted to result from sample shrinkage during drying out UK well 16/23-1 945 m depth.

Figure 35 Seismic amplitude anomalies around and above the Utsira Sand

Figure 36 Regional distribution of seismic amplitude anomalies in the Lower Seal and lower part of the Middle Seal.

Figure 37 Seismic amplitude anomalies at the top of the Utsira Sand a) depth map b) seismic amplitude map, note prominent blue anomalies c) d) seismic sections through the anomalies, showing structural control of higher amplitudes.

Figure 38 Survey ST98M11, seismic amplitude anomalies at top Utsira Sand (grey dashed arrow denotes potential migration path of CO₂ at top Utsira Sand if > 20MT CO₂ are injected).

Figure 39 Survey ST98M11, seismic amplitude anomalies in the Lower Seal

Figure 40 Survey ST98M11, seismic amplitude anomalies in the Middle Seal, note prominent NE-trending grain.

Figure 41 Survey ST98M11, seismic amplitude anomalies from the topmost Middle Seal, note the NNE linear trends, interpreted as channel features.

Figure 42 Formation fluid pressure data from the Utsira Sand

Figure 43 2D basin model a) Location map b) Porosity of the Utsira Sand and surrounding formations c) Permeability of the Utsira Sand and surrounding formations d) Predicted present-day fluid flow velocity (metres year⁻¹) due to sediment compaction.

Figure 44 The Utsira Sand, total pore-space thickness (metres). Dot denotes CO₂ injection point.

Figure 45 a) Survey ST98MT11 a) Utsira Sand thickness b) Structural traps at the top Utsira Sand. Colour scale gives height (metres) of trapped fluid column.

Figure 46 a) Detailed depth map of top Utsira Sand, showing potential initial migration paths from the injection point b) Final distribution of $30 \times 10^6 \text{ m}^3$ (~ 20 MT) of CO₂ assuming migration beneath the top of the Utsira Sand.

Figure 47 a) Final distribution of $7.4 \times 10^6 \text{ m}^3$ (~ 5 MT) of CO₂ assuming migration beneath the top of the Sand-wedge. Note if more CO₂ is injected it will migrate out of the mapped area. b) Image of the CO₂ accumulation beneath the top of the Sand-wedge from the 2001 time-lapse seismic data. Note linear northward migration feature beneath possible channel-related feature.

Figure 48 Regional migration trends from the Sleipner injection point. Large rectangle marks extent of ST98M11 survey, smaller rectangle marks extent of 1999 and 2001 time-lapse surveys.

Summary

This report summarises the results and highlights the main findings of SACS Work Area 1, the geological and reservoir characterisation of the Utsira Sand and its caprock. For more detailed technical information on each topic, the reader is directed to the relevant SACS Technical Reports and, in particular, two earlier Work Area 1 interim reports, Holloway et al. (1999) and Chadwick et al. (2000).

The Utsira Sand comprises a basinally-restricted deposit of Mio-Pliocene age forming a clearly defined seismic unit, pinching out to east and west, and seismically distinct from overlying and underlying strata. The reservoir is highly elongated, extending for more than 400 km from north to south and between 50 and 100 km from east to west, with an area of some 26100 km². Its eastern and western limits are defined by stratigraphical lap-out, to the southwest it passes laterally into shaly sediments, and to the north it occupies a narrow channel deepening towards the More Basin. Locally, particularly in the north, depositional patterns are quite complex with some isolated depocentres, and lesser areas of non-deposition within the main depocentre. The top Utsira Sand surface generally varies relatively smoothly, mainly in the range 550 to 1500 m, but mostly from 700 to 1000 m. The base of the sand is more irregular, disturbed by diapirism of the underlying shales. Isopachs of the reservoir sand show two main depocentres. One is in the south, around Sleipner, where thicknesses range up to more than 300 m. The second depocentre lies some 200 km to the north of Sleipner. Here the Utsira Sand is locally 200 m thick, with an underlying sandy unit adding further to the total reservoir thickness.

Macroscopic and microscopic analysis of core and cuttings samples of the Utsira Sand show that it consists of a largely uncemented fine-grained sand, with medium and occasional coarse grains. The grains are predominantly angular to sub-angular and consist primarily of quartz with some feldspar and shell fragments. Sheet silicates are present in small amounts (a few percent). The sand is interpreted as being deposited by mass flows in a marine environment in water depths of 100 m or more. The porosity of the Utsira Sand core ranges generally from 27% to 31%, but reaches values as high as 42%. Regional log porosities are quite uniform, in the range 35 to 40% over much of the reservoir.

Geophysical logs show a number of peaks on the γ -ray, sonic and neutron density logs, and also on some induction and resistivity logs. These are interpreted as mostly marking thin (~1m thick) intra-reservoir shale layers. The shale layers constitute important permeability barriers within the reservoir sand, and have proved to have a significant effect on CO₂ migration through, and entrapment within, the reservoir. The proportion of clean sand in the total reservoir thickness varies generally from about 0.7 to nearly 1.0.

The caprock succession overlying the Utsira reservoir is rather variable, and can be divided into three main units. The Lower Seal forms a shaly basin-restricted unit, some 50 to 100 m thick. The Middle Seal mostly comprises prograding sediment wedges of Pliocene age, dominantly shaly in the basin centre, but coarsening into a sandier facies both upwards and towards the basin margins. The Upper Seal comprises Quaternary strata, mostly glacio-marine clays and glacial tills. The Lower Seal extends well beyond the area currently occupied by the CO₂ injected at Sleipner and seems to be providing an effective seal at the present time. Cuttings samples comprise dominantly grey clay silts or silty clays. Most are massive although some show a weak sedimentary lamination. XRD analysis typically reveal quartz (30%), undifferentiated mica (30%), kaolinite (14%), K-feldspar (5%), calcite (4%), smectite (4%), albite (2%), chlorite (1%), pyrite (1%) and gypsum (1%) together with traces of drilling mud contamination. The clay fraction is generally dominated by illite with minor kaolinite and traces of chlorite and smectite. The cuttings samples are classified as non-organic mudshales and mudstones. Although the presence of small quantities of smectite may invalidate its predictions, XRD-determined quartz contents suggest displacement pore throat diameters in the range 14 to 40 nm. Such displacement pore throat diameters are consistent with capillary entry pressures of between about 2

and 5.5 MPa capable of trapping a CO₂ column several hundred metres high. In addition, the predominant clay fabric with limited grain support resembles caprocks which are stated in the literature to be capable of supporting a column of 35° API oil greater than 150 m in height. Empirically, therefore, the caprock samples suggest the presence of an effective seal at Sleipner, with capillary leakage of CO₂ unlikely to occur. Around and east of the injection point, a layer of sand, 0 - 50 m thick, lies close to the base of the Lower Seal and is termed the Sand-wedge. The geometry of this unit is likely to prove important in determining the long-term migration behaviour of the CO₂.

Fluid flow in the Utsira Sand, based on limited pressure measurements and basin-modelling, is likely to be low, in the range 0.3 – 4 metres per year, depending on assumed permeabilities.

The total pore-space within the Utsira Sand is estimated at $6.05 \times 10^{11} \text{ m}^3$. However not all of this can necessarily be utilised for CO₂ storage. The simplest assumption is that long-term storage of CO₂ can only be accomplished in structural traps at the top of the reservoir. A detailed study around Sleipner indicates that 0.3% of the reservoir porosity is actually situated within structural closures such as this. In practical terms moreover, with a small number of injection wells, it is unlikely that all of the small traps could be utilised in any case. Around Sleipner the most realistic estimate of the pore-space situated within accessible closed structures is just 0.11% of the total pore-volume. On the other hand, trapping of CO₂ beneath the intra-reservoir shales could significantly increase realisable storage volumes, particularly if it encouraged dissolution of CO₂ into the groundwater. Similarly trapping of CO₂ in the Sand-wedge, as well as beneath the top of the Utsira Sand, will increase the overall storage capacity significantly. In conclusion, the theoretical storage capacity of the Utsira Sand is very high, but how much of this can be utilised in reality is uncertain, and a function of several complex parameters.

Migration models have been constructed with $30 \times 10^6 \text{ m}^3$ of CO₂, injected into the Utsira Sand (approximating to the expected final injected mass of 20 million tonnes). They show that if the CO₂ is trapped at the top of the Utsira Sand it will migrate generally northwestward, reaching a maximum distance from the injection site of about 12 km. However, if the CO₂ is trapped within the Sand-wedge, migration is less well constrained, being northwards then northeastwards. Data limitations to the east of the injection point preclude quantitative estimates of the maximum migration distance in this case.

1 Data summary

Geological characterisation of the Utsira Sand and its caprock was based on the interpretation of 2D and 3D seismic reflection data and various types of well information (Figure 1).

1.1 WELL DATA

A variety of data, from a total of 430 wells, were available to the project (Figure 1).

1.1.1 Core from the Utsira Sand

Prior to commencing the SACS project, the Sleipner licence group cut 9 m of core from the Utsira Sand in Norwegian well 15/9-A23, a Sleipner field development well. This was done specifically to provide data for the project. The drilled depth of the core was 1079-1088 m, corresponding to 905.4 - 910.8 m TVDSS. Sections of core were distributed as follows:

- Two 1m long segments of core were sent to SINTEF Petroleum Research (1080-1081 m and 1087-1088 m drilled depth; 906.0 - 906.6 m and 910.2 - 910.8 m TVDSS).
- One 1m segment was sent to BGS (1085 -1086 m drilled depth; 909.0 - 909.6 m TVDSS).
- One 0.9m segment was sent to GEUS (1084.1 – 1085.0m drilled depth, 908.47 - 909.0 m TVDSS).

Core analysis included photography, microscopy, petrography, mineralogical modal analysis, X-ray diffraction (XRD) scanning electron microscopy (SEM) including backscattered scanning electron microscopy (BSEM), and limited electron probe microanalyses (EMPA) of selected minerals. Core samples were also examined micropalaeontologically, to obtain information on the age and sedimentary environment of the Utsira Formation.

1.1.2 Cuttings from the Utsira Sand

Washed cuttings from 39 wells in the UK sector of the North Sea were inspected, and selected samples were collected. The cuttings samples were examined by binocular microscope to check and supplement existing descriptions in well reports and on composite logs.

Cuttings from 3 Statoil-owned wells in the Norwegian sector of the North Sea were sampled. Several of the samples were washed and examined. Modal analyses on thin sections from some sand-rich samples were carried out.

1.1.3 Cuttings from the Nordland Shale

Twenty cuttings samples were obtained from wells in the UK sector and 23 from the Norwegian sector. The samples were examined by binocular microscope and subjected to a range of analyses including XRD, SEM, and assessed in terms of particle-size, cation exchange capacity (CEC) and total organic carbon (TOC).

1.1.4 Core from a caprock analogue

No core was available from the Nordland Shale itself. Core material from the Pleistocene succession from the Ekofisk field was examined as a possible caprock analogue.

1.1.5 Geophysical Logs

A total of 234 wells had geophysical log data, mostly γ -ray and sonic logs. Of these, 190 had well velocity surveys utilised to tie between the well and seismic data.

1.1.6 Formation tops

Formation top information was available prior to the start of the project for many of the wells. 132 wells were initially recorded as penetrating the Utsira Sand. As the project progressed it was necessary to modify some formation information, particularly the top and base of the Utsira Sand, which had been misidentified in a number of wells.

1.1.7 Seismic data

Seismic data available to the project comprised a number of regional 2D surveys (CNST82RE, NNST84, NVGT88, VGST89) that cover much of the central and northern North Sea basins (Figure 1). In addition the ST98M11 3D survey around Sleipner was also utilised.

1.1.8 Formation pressure data

Formation pressure measurements were available from the Sleipner and Brage fields.

2 The Utsira Sand Reservoir

The current lithostratigraphic scheme used in the Norwegian sector of the North Sea is not well-suited to the detailed interpretation of the Utsira reservoir. This is because the Utsira Formation as lithostratigraphically defined (Isaksen & Tonstad 1989) includes both the main sandy reservoir unit (up to 300 m of clean sand) and also overlying shaly strata which form a cap rock to the storage reservoir in parts of the North Sea. Consequently, the SACS project adopted a seismic stratigraphical framework to subdivide the storage reservoir and surrounding strata into depositional units. The main storage reservoir is referred to as the Utsira Sand throughout this account and corresponds to the thick Mio-Pliocene sand unit penetrated in wells at and around the Sleipner field in the northern North Sea.

2.1 REGIONAL STRUCTURE

Regional interpretation of the Utsira Sand was carried out utilising the regional 2-D seismic datasets and all available well data (Kirby et al. 2001). Around Sleipner the Utsira Sand forms a clearly defined basin-restricted seismic unit, pinching out to east and west, and seismically distinct from overlying and underlying strata (Figure 2). Farther north the Utsira Sand is less distinct, due to an underlying sand of similar seismic character, termed by SACS the sub-Utsira Sand. Careful mapping of the reflectors, paying particular attention to the lap out positions of the Utsira Sand enable its limits to be determined.

Detailed structural information from the ST98M11 3D survey around Sleipner was also incorporated into the regional interpretation prior to depth conversion and mapping (Figures 3, 4 and 5). The Utsira Sand has a highly elongated form, extending for more than 400 km from north to south and between 50 and 100 km from east to west, with an area of some 26100 km². Its eastern and western limits are defined by stratigraphical lap-out. The southwestern limit of the reservoir marks a lateral transition into shaly sediments and its northern limit a narrow, deepening channel. Locally, particularly in the north, depositional patterns are quite complex with some isolated depocentres, and lesser areas of non-deposition within the main depocentre.

Isopachs of the Utsira Sand (Figure 5) show three main depocentres. The principal one is in the south, around Sleipner. Here, thicknesses range up to more than 300 m in a generally irregular pattern, although there is a significant north-trending thicker area just north of the injection point (Figure 5).

The second depocentre lies some 200 km to the north, above the North Viking Graben. Here the Utsira Sand itself locally reaches 200 m in thickness, with the sub-Utsira Sand adding considerably to the total reservoir thickness. This is typified by the Brage – Oseberg area, where the Utsira plus sub-Utsira sand bodies total more than 210 m (Norwegian well 30/6-20). A broad saddle, where the Utsira Sand is generally thin, separates these two depocentres. The third, minor, depocentre, lies in the far north where the depositional extent is very narrow. Thicknesses in the minor depositional protuberances and isolated outliers in the north are generally very low.

The top Utsira Sand surface (Figure 3) generally varies relatively smoothly, mainly in the range 550 to 1500 m, but mostly from 700 to 1000 m. Depths to the base of the Utsira Sand (Figure 4) vary from 600 to 1700 m, but mostly lie between 700 and 1200 m. The form of the base Utsira Sand surface is generally more complex than that of the top Utsira Sand, due to a combination of channelling, loading and shale diapirism. There is also commonly a correspondence between the downwardly concave features at the base, and upwardly convex features at the top Utsira Sand. This is suggestive of features formed by syn- and post-depositional loading and is particularly well-imaged around the Sleipner area, where seismic coverage is very dense (see Section 2.2).

2.2 STRUCTURE AROUND SLEIPNER

The 3D seismic survey ST98M11 provides important insights into the local geology in the area immediately surrounding the injection site (Lothe & Zweigel, 1999; Zweigel et al. 2000a). The correlation of the geophysical well logs with the seismic data was established through synthetic seismograms (Figure 6).

Around Sleipner, the top of the Utsira Sand (Figure 7) shows a general southward dip, in accordance with the regional structural configuration. The base of the Utsira Sand is structurally more complex, and is characterised by the presence of numerous mounds (Figure 8). The mounds are typically about 100 m high and in map view constitute isolated, near circular domes or irregular, elongate bodies with varying orientations (Figure 9). The mounds are typically 1 – 2 km in diameter, with the elongated bodies up to 10 km long. These features are interpreted as being due to mud diapirism, whereby mobilisation of the underlying Hordaland shales has uplifted the base of the Utsira Sand, and/or locally injected fluidised mud into its lower layers. The detailed relationship of these features to the Utsira Sand (Zweigel et al. 2000a) suggests that they developed during deposition of the lower part of the Utsira Sand. In addition to the mud diapirism, and probably connected with it, the base of the Utsira Sand is locally faulted, small reverse faults predominating (Figure 10), but in cases identified up to now, faulting has not affected the Utsira Sand itself or its cap rock.

The presence of these shale mounds induced compaction and subsidence anomalies which led to depressions of the Utsira Sand and overlying units above the mud diapirs (Figure 8a). These depressions constitute local modifications of the general southward dip of the top Utsira Sand, including local domal and anticlinal structures which probably will act as traps and/or channels during CO₂ migration. The detailed perspective view of the top Utsira Sand (Figure 7) illustrates the structural closure above the injection point and the presence of ridges trending north and northwest from the closure. The detailed depth map (Figure 7) around the injection point shows the local closure to have an amplitude of about 12 m.

2.2.1 The coherency cube

Part of the ST98M11 3D dataset have been processed to enhance coherency, with the objective of identifying ‘edge’ features such as faults. The coherency cube has been interpreted to map lineaments in and above the Utsira Sand that potentially could be faults. Most lineaments strike NE-SW and are likely to be artefacts, mirroring velocity anomalies in the shallower overburden. So far, none of the lineaments has been clearly identified as a fault.

2.3 REGIONAL STRATIGRAPHY

The Utsira Sand comprises the mainly sandy, lower part of the Utsira Formation (Isaksen & Tonstad 1989). It lies within the Nordland Group and is of late Miocene to earliest late Pliocene in age (Figure 11).

2.3.1 Well log correlations

The Utsira Sand is clearly identifiable on geophysical well logs, being generally characterised by low gamma-ray values (except locally in the northern part, where it is glauconitic; Eidvin et al., 2000), sonic velocities, induction and resistivity. This is well-illustrated by two regional correlation diagrams (Figure 12). The section through the southern depocentre near Sleipner (Figure 12a) shows the Utsira Sand ranging in thickness up to about 300m. Its top and base are sharply defined, particularly on the γ -ray logs. γ -ray peaks in the Utsira Sand are interpreted as thin beds of shale or clay. The section through the northern depocentre (Figure 12b) shows rather thinner Utsira Sand, up to 150 m thick, with a less sharply defined top. A further complication lies in the occurrence of a sub-Utsira Sand unit. This has similar log properties to the Utsira Sand itself, and, in the literature outwith SACS, is commonly referred to as the Utsira Sand. The SACS interpretation, based on the seismic data, is that this is a distinct, older sandy unit. A characteristic break in the γ -ray and sonic logs supports this interpretation.

More detailed geophysical well logs around the Sleipner area show the characteristic log motif of the Utsira Sand, with a very sharp top and base (Figure 13). The logs show a number of peaks on the γ -ray, sonic and neutron density logs, and also on some induction and resistivity logs. These are interpreted as mostly marking thin (~1m thick) shale layers. Some γ -ray peaks which do not correspond to peaks in other logs may be due to the presence of glauconite. Analysis of the shale bed γ -ray signatures, indicates thicknesses in the range 0.5 - ~5 m, strongly clustered around mean and modal thicknesses of 1 - 1.5 m (Figure 14).

2.3.2 Seismic stratigraphy

Seismically the Utsira Sand is most clearly distinguishable from surrounding units in the southern depocentre, around Sleipner. Regional geoseismic cross-sections around Sleipner (Gregersen & Johannessen 2001) show a basin restricted unit with internal, stacked mounded structures (Figure 15). In the northern depocentre, the overall configuration is similar, but an underlying sandy unit, here termed the sub Utsira Sand, is also evident (Figure 16). Its more or less direct contact with the overlying Utsira Sand indicates that the two sand units are likely to be in hydraulic continuity.

The sub Utsira Sand, which may represent the first sandy deposition after the mid Miocene hiatus, also contains internal mounded features similar to those of the Utsira Sand. The origin of these features is uncertain. They may represent primary depositional structures or, perhaps more likely, they may be a secondary feature due to differential compaction above the base-Utsira shale diapirs.

The oldest mounded units within the Utsira Sand are located centrally, in the deepest part of the basin, downlapping onto the Lowermost shale/sand unit (Figures 15 and 16). This downlap surface is locally very irregular (Section 2.2) and disturbed by diapiric shale diapirs and mud volcanoes (Heggland, 1997; Gregersen et al., 1997; Zweigel et al, 2000a). With time, the depositional area of the Utsira Sand expanded, onlapping the mid-Miocene unconformity, towards the pinch out at the eastern limit. In the west, the Utsira Sand successively onlaps Miocene clays and shales, pinching out at the toes of eastward prograding wedges (Figure 16). Locally these wedges contain sandy material referred to as the Hutton Sand (Figure 11), derived from the British Isles and deposited along the eastern margin of the East Shetland Platform (Gregersen et al., 1997).

The western margin of the Utsira Sand is complex and irregular and in places difficult to map. The seismic data show that sandy units which, prior to SACS, had been identified as the Utsira Sand, are in fact stratigraphically distinct (Figure 17). Thus the sand unit in well 16/29-4 (highlighted in yellow)

was formerly identified as Utsira Sand, but is clearly not the equivalent of the seismically correlated Utsira Sand that pinches out either side of the well.

At its northern limit, the Utsira Sand narrows and deepens markedly, appearing to occupy a north-trending channel feature deepening northwards into the More Basin (Figure 3). The interpretation of channelised Utsira Sand was also suggested by Jordt et al. (1995), Rundberg et al. (1995), Gregersen et al. (1997), Gregersen (1998) and Martinsen et al. (1999). However, Eidvin et al. (2000) interpreted this channel to have been cut into the Utsira Sand, based on seismic correlation to biostratigraphically dated wells, and give a late Pliocene age for the channel formation.

Towards the south, in the southern Norwegian sector, the Utsira Sand passes southward into a more basinal clay facies, to be absent south of 57° 50'. South of 57° 50' minor isolated sands occur such as the upper Oligocene Vade Formation (blocks 2/2 & 2/3), locally up to about 70 m thick (Norwegian well 2/2-2) and some minor Pliocene, probably massflow sands in the central North Sea. Further to the east, towards the coasts of southern Norway and Denmark, more significant Oligocene and Miocene sands occur. New analyses by Eidvin et al. (2000) suggest that some of these sandy units could be incorporated into the Skade Formation.

2.3.3 Core and cuttings

Macroscopic and microscopic analysis of core and cuttings samples of the Utsira Sand show that it consists mainly of a fine-grained sand, with medium and occasional coarse grains (Figure 18). The sand grains are predominantly angular to sub-angular and consist primarily of quartz with some feldspar and organic components (shell fragments). They are almost completely uncemented. Sheet silicates are present in small amounts (a few percent). The cores through the Utsira Sand show no visible layering or preferred orientation of minerals. Shell fragments are common and seem to be randomly oriented. This lack of layering and other primary sediment structures might be due to high energy deposition (e.g. as a turbidite) or due to bioturbation. The possible disturbance of loose sediment whilst coring may also have destroyed or obscured internal core fabrics.

The core sample from UK well 15/9-A23, depths 1085 – 1086 m (Pearce et al. 1999), is a medium grained, moderately to well sorted, very poorly cemented and friable subarkosic sand. It comprises predominant quartz with minor plagioclase, K-feldspar, calcite (probably shell fragments) and common bioclastic debris including foraminifera, radiolaria and sponge spicules. Some detrital grains are covered in a thin, <10 µm, clay coating which XRD indicates comprises mainly smectite with minor illite and chlorite. Limited SEM evidence indicates that some smectite morphologies are indicative of authigenic development. Pyrite is a minor but commonly distributed authigenic mineral occurring as framboidal aggregates, especially within foraminifera tests. The most notable diagenetic modification is the development of two minor zeolites, phillipsite and clinoptilolite. Both zeolites have developed through precipitation directly from porewaters with the dissolution of radiolaria and sponge spicules providing a likely source of biogenic silica. Although common the zeolites only form a very small component of the sand and do not represent a significant modification to porosity and permeability. The general description agrees with that from Isaksen & Tonstad (1989).

Whole-rock XRD analysis (Pearce et al. 1999) on a number of samples shows a quite uniform whole-rock mineralogy, with dominant quartz, minor feldspar and traces of albite, calcite, aragonite and undifferentiated mica species (Figure 19, Table 1).

Whole-rock analyses are comparable to the modal composition of the samples (Table 2) estimated using a petrographic image analysis method (Pearce et al. 2002).

Sample	% mineral					
	Quartz	Calcite	K-feldspar	Albite	Aragonite	'Mica'
E641A	75	2	14	3	3	3
E642	75	3	13	3	3	3
E643	75	2	14	3	3	3
E644	76	3	12	3	4	3

Table 1 Whole-rock XRD analysis of Utsira Sand core from UK well 15/9-A23

Phase	Volumetric %		Mineral %
	(Average)	Std. Deviation	(Average)
Quartz	44.19	2.410	76.36
K-feldspar	4.01	1.268	6.92
Plagioclase	1.74	0.228	3.00
Chlorite	0.77	0.217	1.33
Mica	3.02	0.877	5.22
Zeolite	0.13	0.088	0.22
Calcite	3.90	0.707	6.73
Ti Oxides	0.02	0.031	0.04
Apatite	0.01	0.004	0.00
Illmenite	0.07	0.038	0.11
Pyrite	0.03	0.014	0.05
Porosity	41.99	0.834	-

Table 2 Mineralogy of Utsira Sand core from UK well 15/9-A23 based on image analysis

2.3.4 Biostratigraphy and depositional environment

Biostratigraphical analyses (Wilkinson, 1999, Piasecki et al., 2002) from the core samples in well 15/9-A23 indicate that the Utsira Sand has an age in the range early Late Miocene to Early Pliocene.

Analysis of foraminifera and dinoflagellates (Wilkinson 1999, Piasecki et al. 2002) indicate a marine, neritic environment, possibly with oceanic influence during deposition, with water depths characteristic of the middle to outer shelf, around 100 m or more. The mixed content of nearshore indicators (lignite fragments) and marine indicators (bivalve shell fragments, glauconite, dinoflagellates), and the subangular, mature quartz sediments without visible layering from core samples (Pearce et al., 2000), is consistent with deposition in an environment with some energy. The tabular to mounded morphology of the sand bodies, corresponding to blocky low gamma-ray values, separated by thin shale layers, indicates several events of high energy deposition, separated by relaxation times with clay deposition. The sharp-based, mounded nature of the sand bodies deposited with mixed near-shore and more open-marine indicators in the deepest central part of the Viking Graben area points toward mass-flow/gravity-flow deposition, possibly turbidites or other processes (Gregersen et al., 1997; Eidvin et al., 1999). The total period of deposition of the Utsira Sand, from

early Late Miocene to Early Pliocene, may span as much as 7.5 million years (Eidvin et al 2000). Given the average sand thickness of about 200 m, an average sedimentation rate about 30 metres per million years, is implied. However, the actual sedimentation rate during each depositional event was probably much higher.

In the north, deposition of the Utsira Sand succeeded an earlier sand unit, the sub Utsira Sand (Figure 13), above the regional mid Miocene unconformity. The oldest and lowermost mounds of the Utsira Sand are located centrally in the basin and successive mounds are more extensive, gradually onlapping to east and west. This may indicate that the first mounds of the Utsira Sand were deposited as basinal lowstand deposits succeeded by more extensive onlapping transgressive sand units. The transgressive nature may be indicated by upward fining units and glauconitic deposits, locally in the northern Viking Graben area, where they interdigitate with or drape the main Utsira Sand (Eidvin et al., 2000).

The Utsira Sand differs lithologically from stratigraphically equivalent units in the Central North Sea. Whereas the Utsira Sand was deposited in a narrow, elongate basin, deposition in the Central North Sea occurred over a much area. Thin, sandy Utsira sediments which almost completely lack a mud component, pass southwards into thick, mud dominated sediments in the Central North Sea. These differences might be explained by a filtering process in the area of Utsira Sand deposition, where strong currents in the narrow rather linear basin washed out the finer sedimentary fraction which was then deposited in neighbouring, more distal areas.

2.4 REGIONAL RESERVOIR PROPERTIES

The porosity of the Utsira Sand core determined by microscopic modal analysis of thin sections ranges generally from 27% to 31%, but reaches values as high as 42% (Pearce et al. 1999, Lothe & Zweigel 1999). Liquid invasion, using water and helium, yielded effective porosities ranging from 35 to 42.5 % (Lindeberg et al. 2000). However, these measurements were made from prepared samples of frozen loose sand from a single part of the reservoir. As a guide to regional reservoir properties they may therefore be less reliable than *in situ* porosities derived from wireline logs.

A study of regional porosity variation in the Utsira Sand, based on density and sonic logs was carried out (Kirby et al. 2001). Overall, log-derived porosities are quite uniform, in the range 35 to 40% over much of the reservoir (Figure 20). Only in the far north do values appear to fall below 35%, and here well control is very sparse; the effect of increased glauconite in these northern sediments may also lead to decreased reliability of the log-derived porosity values.

The porosity figures quoted above refer to the clean sand portions of the Utsira reservoir. In reality the proportion of the unit which actually comprises clean sand varies quite markedly. This has important consequences in terms of reservoir volumetrics and migration modelling. Clean sand proportion was defined on the basis of γ - ray log readings (Kirby et al. 2001). The proportion of clean sand in the Utsira reservoir varies from about 0.7 to 1.0 in the main southern and northern depocentres, to less than 0.5 in the thin reservoir sands between the two main reservoirs (Figure 21). The implication is that the two depocentres are probably not in good hydraulic continuity.

Local variation is also quite evident and can be mapped in some detail in the southern depocentre where there is good well coverage (Figure 22). Thus just north of Sleipner, the proportion of sand decreases from nearly 1.0 at the eastern reservoir margin, to less than 0.5 in the west. Around Sleipner itself, values are generally in the range 0.7 to 0.9, though Zweigel et al. (2000a) report values in the range 0.90 to 0.96 in selected wells around Sleipner.

3 Utsira Caprock

3.1 REGIONAL STRATIGRAPHY

The succession overlying the Utsira Sand, referred to here as the ‘caprock succession’, is rather variable, principally comprising prograding deltaic wedges of Pliocene age (Figure 23), overlain by Pleistocene deposits.

The Pliocene strata form a succession coarsening upwards from shales, in the deeper, central parts of the basin to silt and sand in the shallower and more marginal parts. The height of the prograding clinoforms, 300 - 400 m, corresponds to the approximate water depth at the time of deposition (not compensated for subsequent compaction/subsidence). Therefore a major relative sea-level rise must have taken place in latest Miocene or during the Early Pliocene. Subsequently, huge amounts of Upper Pliocene sediments were deposited by major deltaic systems, first mainly from east and west or southwest, presumably due to relative uplift of southern Scandinavia and Scotland/Shetland, and later more dominantly from the south. Nearly all the easterly-derived clinoforms have been truncated by Pleistocene strata beneath the Norwegian Channel, parallel to the Norwegian coast and the most eastward clinoforms seem to be lacking their offlap breaks, meaning deep and significant glacial erosion and/or late Cenozoic uplift.

Lithologically the caprock succession consists mainly of clays, with local minor sands. It has been divided into three seismic units (Gregersen & Johannessen 2001), here termed the Lower Seal, draping the Utsira Sand, the progradational Middle Seal and finally the erosive Upper Seal (Figures 15, 16 and 24).

3.1.1 The Lower Seal

Around Sleipner, the lowermost part of the caprock succession comprises the Lower Seal, a well defined shale unit formerly referred to in SACS as the Shale Drape (Chadwick et al., 2000). It has the form of a tabular, basin-restricted unit, some 50 – 100 m thick, lying immediately above the Utsira Sand and overlapping the reservoir to east and west. It pinches out against the mid-Miocene onlap surface, and is bounded to the top by a regional downlap surface, beneath the progradational Middle Seal (Figure 24a). Drill cuttings from the Sleipner area indicate a grey mudstone with a high content of clay minerals, supported by log analysis (e.g. Figure 25a) which indicates at least 80 % shale volume.

The Lower Seal can be mapped over much of the southern depocentre of the Utsira Sand (Figure 25). South of the Sleipner area it is less clearly identifiable, as the Utsira Sand itself shales out rendering the lithological contrast less clear. Towards the north, the upper boundary of the Lower Seal locally cannot be identified as a downlap surface, and it may pass laterally into progradational units. However, over much of the northern Utsira depocentre the Lower Seal has a dominantly draping geometry, with an upper bounding regional downlap surface (Figure 24b) The most basal parts of the Lower Seal were probably subjected to marine condensation, prior to the progradation of the succeeding Middle Seal clinoforms. In these basal draping areas, the Lower Seal probably constitutes the most efficient sealing unit of the caprock succession, due to its concordant stratification and generally very low sand content.

Two sand bodies have been identified, the West and East Sand units, which, stratigraphically are most referable to the Lower Seal (Figure 26).

The West Sand unit

The West Sand unit (Figure 26) is located west of the Utsira Sand, at a similar stratigraphical level, in a small area around UK well 211/28-2. It is not connected with the Utsira Sand. The limited lateral and stratigraphical extent of this sand will probably have little effect on the regional seal efficacy.

The East Sand unit

The East Sand forms part of a prograding wedge, just east of the Utsira Sand (Figures 24 and 26). It is locally more than 80 m thick (Norwegian well 35/11-5), is dated as Late Miocene to Early Pliocene age and in the literature is taken as the Utsira Sand (Gregersen et al. 1997; Eidvin & Rundberg 2001). However the SACS seismic interpretation indicates that the unit terminates east of the Utsira Sand proper, and is slightly younger than it. The East Sand unit is wedgelike, pinching out westwards just east of the Utsira Sand and eastwards, just beneath unconformable base of the Upper Seal (Figure 24). With available data it is uncertain if there is a direct contact between the Utsira and the East Sand units. If this were the case the East Sand could provide a possible hydraulic connection from the Utsira Sand to much shallower depths beneath the Norwegian Trench.

3.1.2 The Middle Seal

The Middle Seal is of Late Pliocene to Pleistocene age (Eidvin et al., 2000). It is characterised by inclined reflections, indicating progradation from both the east and the west (Figures 23 and 24). The basal bottom-set beds of the Middle Seal downlap the Lower Seal, and its upper parts are truncated by the erosive Upper Seal, particularly beneath the Norwegian Channel (Figures 15 and 16). The variations in thickness and dip of the internal clinoforms are limited and indicate mainly balanced rates between sediment supply and creation of accommodation space, though internal erosional surfaces, interpreted as sequence boundaries (Gregersen et al., 1997), indicate breaks in the overall progradation.

Cuttings descriptions from NPD papers and well logs (Figures 15 and 16) show mainly clay lithologies, but minor sands do occur locally. High amplitude reflections, which onlap the toe-sets of the prograding clinoforms, may be interpreted as more sandy beds, perhaps deposited as turbidites (Figure 23). Sandy parts of the Middle Seal have been identified above the northern Utsira depocentre, these are termed the Bottom-set Sands (Figure 26).

The Bottom-set Sands

Around the northwesternmost extent of the Utsira Sand (Figure 26), minor mounded features or wedges with moderate to high seismic amplitudes are found within the Middle Seal, at the slope toe or bottom-set of the prograding reflections. These correlate with minor sands in wells and are termed the Bottom-set Sands. Six such sand bodies, which are proven by wells, have been mapped (Figure 26), they are up to 60 m thick, irregular in form and typically 5 -10 km across. The stratigraphical position of the sand wedges at the slope-toes or bottom-sets of the prograding clinoforms indicates that they probably represent massflow deposits. The limited lateral and stratigraphical extent of these sands will probably have little effect on the efficacy of the regional seal.

3.1.3 The Upper Seal

The Upper Seal, of Pleistocene age, is here defined as the uppermost seismic unit between a basal regional unconformity and the sea floor (Figures 15, 16, 24). The unit cannot everywhere be mapped with confidence; where it is shallow the seabed multiple obscures interpretation. Beneath the Norwegian Channel the unit is almost concordantly stratified and onlaps dipping parts of the basal unconformity, while shallower strata prograde towards east and downlap the lower concordant part (Figure 16). Core information from southwest of the investigated area and also in the central part of the Norwegian Trench, prove glacio-marine clays, deposited under shallow-marine, arctic conditions and glacial tills (Sejrup et al., 1991). Scattered high seismic amplitude anomalies may indicate locally sandy lithologies.

3.2 STRATIGRAPHY AROUND SLEIPNER

In the Sleipner area the stratigraphy of the Lower seal is complicated by the presence of a thin sandy unit here termed the Sand-wedge (Lothe & Zweigel 1999; Zweigel et al. 2000a). The Sand-wedge is evident in the eastern half of the area covered by the 3D seismic survey ST98M11 where low γ -ray measurements and other wireline log data indicate a sand body assigned by SACS to the lowermost part of the Nordland Shale i.e. the Lower Seal caprock unit.

The Sand-wedge is separated from the main Utsira Sand by a thin bed of shale about 6.5 m thick. It has a wedge-like form, thickening eastwards and pinching out to the west in the central part of the survey (Figure 27a). The top of the Sand-wedge corresponds to a strong reflection (Figure 27a), making it possible to map the rough extent of the wedge from seismic amplitudes on the 3D seismic data (Figure 27b). Detailed mapping of the Sandwedge from the seismic shows its overall form (Figure 27c). The greatest thickness proved by wells is about 25 m, around Sleipner, but it thickens eastwards of this to between 30 and 50 m at the eastern limit of the survey.

The Sand-wedge is likely to have an important influence on the sealing characteristics of the caprock at Sleipner. The time-lapse seismic data indicate that the injected CO₂ had migrated into the sand-wedge by 1999, with considerably more accumulating by 2001. The geometry of the Sand-wedge will therefore exert important control on medium term migration of the CO₂. Initial studies indicate that CO₂ migration directions at the top of the Sand-wedge differ considerably from migration directions at the top of the Utsira Sand (Section 5.2).

Detailed mapping of sand-wedge thicknesses on the 3D dataset reveals the presence of curvi-linear features (Figure 28). These appear to be related to channelling effects at the top of the Sand-wedge. It is notable moreover that the latest 2001 time-lapse seismic dataset indicates CO₂ migration at the top of the Sand-wedge along the north-trending linear feature Channel A (Figure 28).

3.3 CUTTINGS ANALYSIS AND SEALING CAPACITY

Caprock cuttings from the shales of the Nordland Group were obtained from wells in both the Norwegian and UK sectors (Figure 29). Samples are concentrated in the caprock directly overlying the Utsira Sand and the Sand-wedge (the Lower Seal), but in some wells the whole Pliocene shale sequence has been sampled.

The samples were subjected to a range of analyses including X-ray diffraction and scanning-electron microscopy. They were also analysed for particle-size, cation exchange capacity and total organic carbon (Kemp et al. 2001, Boe & Zweigel, 2001).

3.3.1 Lithology

The caprock samples dominantly comprise grey clayey silts or silty clays (Figure 30). Petrographic analysis suggests that most of the samples are massive (Figure 31) although some present evidence of a weak sedimentary lamination (Figure 32). XRD analysis (Figure 33) shows the samples to be typically composed of quartz (30%), undifferentiated mica (30%), kaolinite (14%), K-feldspar (5%), calcite (4%), smectite (4%), albite (2%), chlorite (1%), pyrite (1%) and gypsum (1%) together with traces of drilling mud contamination. The clay fraction is generally dominated by illite with minor kaolinite and traces of chlorite and smectite.

3.3.2 Sealing capacity

The samples are non-organic and are classified as non-organic mudshales and mudstones according to the Krushin (1997) classification. Although the presence of small quantities of smectite in the Nordland Shale may invalidate its predictions, XRD-determined quartz contents suggest displacement pore throat diameters in the range 14 to 40 nm. Such displacement pore throat diameters predict

capillary entry pressures of between about 2 and 5.5 MPa, which would be capable of trapping a CO₂ column ranging from 667 to 1833 m high.

The predominant clay fabric with limited grain support resembles the type 'A' or type 'B' seals illustrated in Sneider et al. (1997), predicted to be capable of supporting a column of 35° API oil greater than 150 m in height.

Empirically, therefore, the caprock samples suggest the presence of an effective seal, where capillary leakage of CO₂ is unlikely to occur. Despite this, seismic data indicate that CO₂ has penetrated into the Sand-wedge above the Utsira Sand. This is likely to have necessitated the CO₂ passing through a number of thin clay/silt barriers (mostly about 1 m thick, but some may be thicker) within the reservoir sand. Assuming these intra-reservoir shales have a similar mineralogy and fabric to the overlying Nordland Shale, the CO₂ must be passing through by some means other than capillary entry. Such means would be afforded by faulting, microfracturing or through holes where the shales pinchout in some way. The cuttings samples show occasional slickensides (Figure 34a), providing evidence of shear deformation, consistent with faulting. The lack of clear caprock faulting on the seismic data however suggest that any structures are beneath the limit of seismic resolution. Microfractures were also seen in the cuttings (Figure 34b). It is unlikely that these are real geological features, they are instead interpreted as forming during drying-related shrinkage of the sample. Nevertheless, it is believed that supercritical CO₂ is a dehydrating agent, which by implication may be capable of inducing shrinkage cracks in clays with which it comes into contact. Such a process may lead to enhanced permeability, particularly in thin shale layers.

3.4 EKOFISK CORE

At the time of writing no caprock core material is available around Sleipner. A possible analogue for the caprock is available from Ekofisk where an Early Pleistocene clay/shale section has been cored in Norwegian well 2/4-C11. The clay core was still damp and found to be in a good condition, and 3 small samples were taken for mineralogical analysis, including XRD, N₂BET (gas absorption/specific surface area) and grain size determination (Lindgren et al. 2001).

The samples are mineralogically similar to the caprock cuttings samples from around Sleipner. Grain size analysis indicates that clay fractions (<2µm) constitute between 26 and 50% of the whole-rock. The clay mineralogy comprises approximately equal amounts of smectite, illite and kaolinite, with minor amounts of vermiculite and quartz and traces of chlorite. BET surface area is in the range 20 – 40 m²g⁻¹.

3.5 SEISMIC AMPLITUDE ANOMALIES

Mud logs from several wells in the Sleipner field indicate the presence of shallow gas in the Utsira Sand and the overlying caprock succession. Seismic amplitude anomalies are common above and around the Utsira Sand (Figure 35), and may provide a means of identifying routes of possible gas migration.

3.5.1 Regional mapping

Regional analysis of amplitude anomalies was restricted to the lower 500 ms (about 500 metres) of the caprock succession, incorporating the Lower Seal and part of the Middle Seal (Figure 36). Minor anomalies are observed above the southern part of the Utsira Sand, in the injection area and towards northwest. However, these minor anomalies seem to be isolated and may represent local sands or shallow gas.

The highest concentration of high seismic amplitudes is seen in the northernmost part, where they coincide with the mapped bottom-set sands in the Middle seal. Above the northern depocentre of the

Utsira Sand a number of linear anomaly trends are evident. These trends can be correlated from seismic section to section and may reflect sandy channel systems in the caprock.

3.5.2 Mapping around Sleipner

Closer to Sleipner, seismic amplitude anomalies were identified on the 3-D seismic survey ST98M11 (Zweigel et al. 2000a), both at the top of the Utsira Sand itself and also in the caprock (Figure 35).

Anomalies at the tops of the reservoir units (the Utsira Sand and the Sand-wedge) all correspond to structural traps (e.g. Figure 37 and Figure 38) and are most likely caused by the presence of gas. They attest to the sealing potential of the caprock (Lower Seal), but the fact that the anomalies are only present in a small number of the traps, and that they do not fill these traps completely, may imply that migration into the caprock does occur in places. On the other hand, the presence of a channel-like structure in the sand-wedge (Figure 28) and the observation that seismic anomalies at the reservoir tops are partly displaced from the structural culminations (Figure 37), may suggest that reservoir heterogeneity, rather than seal efficacy, is the controlling factor on gas accumulation. It is notable that the highest seismic amplitude anomalies lie some distance to the NW of the CO₂ injection point (Figure 38), perhaps suggesting that the area around the CO₂ injection point is not particularly characterised by significant gas flux.

Within the caprock succession amplitude anomalies are likely to signify the presence of sand units, possibly filled with gas (see also Hegglund 1997). Anomalies are scattered within the lower part of the caprock (the Lower Seal), and are manifest as discrete sub-circular features (Figure 39). At this level, the amplitude anomalies are roughly uniformly distributed over the area of ST98M11, though slightly less abundant in the SE, above the CO₂ injection point. Higher in the caprock succession, in the upper Pliocene shales (the Middle Seal), the distribution of anomalies shows a weak tendency for NE-NNE alignment (Figure 40). In addition, some (but by no means all) of the anomalies seem to be linked to mud volcanoes at the base of the Utsira Sand by zones of weak amplitudes interpreted as 'gas chimneys' (Zweigel et al. 2000a). Immediately beneath the top of the Middle Seal amplitude anomalies show a strong NNE linear alignment, presumably associated with channelling (Figure 41). Anomalies also occur within the Quaternary Upper Seal (Figure 35).

4 Fluid Flow in the Utsira Sand

4.1 NATURAL FLUID FLOW FROM PRESSURE DATA

Only three formation pressure measurements are available from the Utsira Sand, two from the Sleipner 15/9-A-23 well, and a single measurement from the Brage Field, approximately 250 km north of the Sleipner (Figure 42).

Fluid pressure at Brage is close to hydrostatic pressure, whereas the Sleipner data indicate pressures slightly above hydrostatic (Figure 42). However, Statoil consider the accuracy of the pressure gauge used at Sleipner to be suspect, Baklid et. al. (1996) state moreover that the Utsira Sand is water filled and the pressure is hydrostatic. If the pressure gradient is hydrostatic both at Sleipner and Brage the natural water flow in the Utsira reservoir will be negligible.

If, on the other hand, the pressure figures for Sleipner are taken as accurate and representative, the overpressure can be calculated (Table 3).

Area	Formation pressure (bar)	Depth, TVDss (m)	Overpressure (m) (bar)	Comments

Sleipner	106.1	853.6	196.8	19.8	slightly overpressured
Sleipner	108.0	854.4	214.8	21.7	slightly overpressured
Brage	65	638	5.5	0.56	no overpressure

Table 3 Possible overpressure in the Utsira Sand

The overpressure at Sleipner with respect to Brage is approximately 20 bar, the distance between the two fields being about 250 km. If it is assumed that there are no hydrogeological barriers between Sleipner and Brage, then a very approximate estimate of the natural fluid flow can be calculated from Darcy's Law. Assuming a permeability of 1 Darcy (average for the Utsira Sand) and a formation fluid (brine) viscosity of 0.9 cP, a flow velocity of approximately 10^{-8} m s⁻¹ is obtained. This approximates to 0.3 metres per year or about 3 km in 10000 years.

In fact it is likely that the Sleipner and Brage fields are not in good hydraulic contact, due to the thin, shaly reservoir on the structural saddle between them (Figures 5 and 21), so this calculation may in any case not be reliable. All in all, it is perhaps best to conclude that the pressure data, sparse and possibly unreliable, are in any case, consistent with very low rates of natural flow.

4.2 FLUID FLOW FROM BASIN MODELLING

In view of the very limited pressure data available from the Utsira Sand, a basin modelling study was set up to simulate the natural burial and compaction of the sand. From this it is possible to calculate the velocity of compaction-driven fluid flow in the Utsira Sand, and to evaluate the range of natural flow velocities (Kristensen & Bidstrup 2000).

A simple 2D model, based on well and seismic data, was established along a section running NNW through Sleipner and into the UK sector (Figure 43a). The preferred input model comprised 50 layers and events, from the seabed to the top of the Zechstein, with porosities and permeabilities based on well log data (Figures 43b and 43c). The Utsira Sand was sandwiched between layers of much lower permeability, the caprock directly above the Utsira Sand, the Lower Seal, being assigned a permeability of 0.0001 mDarcy.

Initial boundary conditions assumed no-flow boundaries at the top of Zechstein salt and at the southern end of the section, where the Utsira Sand passes southwards into shales. At the NNW end of the section, where the sediments are much more sandy, an open-flow boundary was assumed. Fluid pressures calculated with these preferred boundary conditions (Kristensen & Bidstrup 2000) are consistent with observed data in the North Sea, indicating potential overpressure in the Cenozoic shales and in the Jurassic and Triassic formations, but no overpressure in the Chalk.

A number of simulations were carried out using the above boundary conditions (Kristensen & Bidstrup 2000). The preferred model assumes that the Utsira Sand is sealed above by the Lower Seal, but is in hydraulic contact with a sandy wedge at the NNW end of the model. Results from the preferred model (Figure 43d) indicate NNW-directed flow in the Utsira Sand with flow velocities in the range 2 – 4 metres per year around the Sleipner injection point. These increase updip to more than 10 metres per year at the NNW end of the model, principally due to updip pinchout of the Utsira reservoir, which results in narrowing of the hydraulic system. Other model scenarios were simulated, but the overall results remained similar with flow values generally less than 5 metres per year around the injection point, but higher farther north. These results are higher than the natural flow modelling results (Section 4.1), even those which assume slight overpressuring in the Utsira Sand. This is mainly due to the higher permeabilities (10 Darcy) assumed in the basin modelling. However if similar permeabilities had been assumed in the two modelling approaches, results would have been closely comparable. In

any event, the values calculated here probably represent the highest possible flow values in the Utsira Sand reservoir.

5 Utsira reservoir storage and trapping potential

To assess the storage capacity and migration paths of CO₂ in the Utsira Sand it is necessary to take into account the physical properties of the reservoir unit, in particular the porosity of the sand and proportion of shale units within the reservoir, and also the topography and 'roughness' of the top Utsira Sand surface.

5.1 STORAGE CAPACITY

5.1.1 Total storage volume

The total porespace within the Utsira Sand can be calculated by multiplying the Utsira Sand isopachs (Figure 5), by the sand porosity (Figure 20) and by the proportion of clean sand (Figure 21). This gives a map showing the total porespace thickness variation for the Utsira Sand (Figure 44). By integrating this with the area of Utsira Sand deposition, a figure for the total pore volume of $6.05 \times 10^{11} \text{ m}^3$ is obtained. [This compares with an earlier estimate by SACS, based on a single assumed porosity value and approximate depth conversion, of $5.5 \times 10^{11} \text{ m}^3$ (Chadwick et al. 2000)].

5.1.2 Volume in traps around Sleipner

The thickness of the Utsira Sand in the area of the 3D seismic survey ST98M11 varies from about 50 m to slightly over 300 m (Figure 45a), local variations being due to the presence of mud mounds at the base and corresponding depressions at the top of the Utsira Sand. The thickness outside the areas affected by mud mobilisation ranges mainly from 240 to 270 m. The total volume of the Utsira Sand in the survey area is $1.485 \times 10^{11} \text{ m}^3$.

The volume of structural traps at the top of the Utsira Sand was determined using the secondary hydrocarbon migration simulator SEMI (Zweigel et al. 2000b). The simulations made the artificial assumption that vertically migrating CO₂ was available in excess such that it could fill all available traps up to their spill point. The positions of traps and the maximum column height are indicated in Figure 45b. The total calculated volume of these traps, assuming a sweep efficiency of 0.85, amounts to about $1.35 \times 10^8 \text{ m}^3$.

Taking an average porosity of 30%, the total pore volume of the Utsira Sand in the ST98M11 survey area is $4.455 \times 10^{10} \text{ m}^3$. This means that, in the survey area, only 0.3% of the available pore space lies within available structural traps at top Utsira level. In practical terms, with a small number of injection wells, it is unlikely that all of the small traps could be utilised in any case. To illustrate this, the calculated storage volume of all traps reached on the current Sleipner CO₂ injection migration path (Section 5.2) would amount to about $5.0 \times 10^7 \text{ m}^3$ (Zweigel et al. 2000b). This would account for no more than 0.11% of the total pore volume in the survey area. In fact other large trap structures exist to the south and west of the injection point, which might be used for CO₂ storage in the future, increasing the utilisable volume somewhat.

The fact that (see Section 5.2) CO₂ will also be stored beneath the top of the Sand-wedge, as well as beneath the top of the Utsira Sand, will increase the overall storage capacity significantly, perhaps by a factor of up to two. Additional storage potential beneath the intra-reservoir shales is a possibility, but the long-term significance of this is as yet uncertain.

Irrespective of the details, if it is required that the CO₂ is sequestered in structurally closed features, then the real storage capacity of the Utsira Sand is much lower than its total pore volume. Further detailed regional analysis is required to quantify the real, practical storage capacity of the Utsira Sand.

Taking into account the general situation whereby only a proportion of these traps can be reached by economic placement of injection wells, the results are not inconsistent with the contention of Holloway et al. (1996), that the typical total storage efficiency of an aquifer, in terms of structural traps, might be only a fraction of one percent.

5.2 CO₂ MIGRATION AWAY FROM THE INJECTION POINT

The future distribution of CO₂ injected into the Utsira Sand at Sleipner has been simulated using the secondary hydrocarbon migration modelling tool SEMI (Zweigel et al. 2000b). The approach addresses the medium-term (decades to centuries) geometrical aspects of CO₂ migration. Migration is assumed to be driven solely by buoyancy and to take place instantaneously. CO₂ was taken as the only phase present in the pore space, so any effects of dissolution, chemical reaction or capillary pressure were disregarded.

Long-term migration at two surfaces was considered, Top Utsira Sand and Top Sand-wedge. No lower barrier was imposed for migration at Top Utsira Sand, whereas for migration at Top Sand-Wedge, the base of the Sand-wedge was taken as a barrier.

5.2.1 Migration at Top Utsira Sand

The depth map of Top Utsira Sand illustrates the potential migration paths from the injection point. (Figure 46a). Two saddles, one to the north and one to the west, link the local injection dome with a larger complex domal structure to the west and northwest. The northerly saddle represents the most likely migration path, though, given the uncertainty of depth conversion, migration along the western saddle cannot be ruled out. SEMI modelling of $30 \times 10^6 \text{ m}^3$ of CO₂ (approximating to the final projected amount of 20 MT of injected CO₂), shows that the migration direction is predominantly to the northwest, reaching a maximum distance from the injection site of about 12 km (Figure 46b).

5.2.2 Migration at Top Sand-wedge

If, as the time-lapse seismic indicates (Arts et al in press), CO₂ invades the Sand-wedge in the lowermost part of the Lower Seal, CO₂ migration will be affected quite radically, due to the different structural configuration. SEMI modelling (Figure 47a), indicates that initial northward migration is succeeded by northeastward migration. This is supported by the 2001 time-lapse seismic image of the CO₂ accumulation beneath the top of the Sand-wedge (Figure 47b), which shows general northward migration with particularly rapid advance along a north-trending linear feature possibly related to channelling (cf Figure 28). A prediction of the projected 20 MT of injected CO₂ was not possible in detail because the CO₂ would leave the mapped area via its eastern edge (Figure 47a). The volume accounted for in the illustrated model is only $7.4 \times 10^6 \text{ m}^3$ of CO₂. More regional extrapolation of top Sand-wedge migration (Figure 48) predicts that, following northeastwards migration to the edge of the ST98M11 survey the migration pathway would then deviate back northwards, beneath the main part of the Lower Seal.

It is likely that for either migration scenario, CO₂ will stay well within the limits of the Lower Seal (Figure 48), remaining effectively isolated from the overlying prograding wedges of the Middle Seal. A third migration scenario, whereby CO₂ is partitioned beneath both the top of the Sand-wedge and the top of the Utsira Sand was not modelled. However, if this were the case in the long-term (quite likely in view of the results of the time-lapse seismic data), migration distances would be shorter.

6 References and Bibliography

6.1 SACS TECHNICAL REPORTS

- Boe, R. & Zweigel, P. 2001. Characterisation of the Nordland Shale in the Sleipner area by XRD analysis. SINTEF Petroleum Research Report 33.0764.00/01/01.
- Gregersen, U. & Johannessen, P.N. 2001. The Neogene Utsira Sand and its seal in the Viking Graben area, North Sea. GEUS Report 2001/100.
- Holloway, S., Chadwick, R.A., Kirby, G.A., Pearce, J.M., Gregersen, U., Johannessen, P.N., Kristensen, L., Zweigel, P., Lothe, A. & Arts, R. 2000. Final Report of the SACS 1 project - Saline Aquifer CO₂ Storage: A Demonstration Project at the Sleipner Field: Work Area 1 – Geology. BGS Technical Report WH/2000/21C.
- Kemp, S.J. Bouch, J. & Murphy, H.A. 2001. Mineralogical characterisation of the Nordland Shale, UK Quadrant 16, northern North Sea. BGS Commissioned Report CR/01/136.
- Kirby, G.A., Chadwick, R.A. & Holloway, S. 2001. Depth mapping and characterisation of the Utsira Sand saline aquifer, central and northern North Sea. BGS Commissioned Report CR/01/218.
- Kristensen, L. & Bidstrup, T. 2001. Determination of the natural fluid flow in the Utsira Sand reservoir using basin modelling. SACS Project: Final Technical Report of Task 1.6. GEUS Report 2001/2.
- Lindeberg, E., Van de Meer, B., Moen, A., Wessel-Berg, D & Ghaderi, A. 2000. Saline Aquifer CO₂ storage: Task 2: Fluid and core properties and reservoir simulation. Report period 01/11/98 to 31/12/99. SINTEF Petroleum Research Confidential Report 54.5148.00/02/00.
- Lindgren, H., Fries, K. & Springer, N. 2002. Clay Mineralogical Investigation of core and cuttings from the Ekofisk and Sleipner areas. Danmarks og Grønlands Geologiske Undersøgelse Rapport nr. 3, 2002
- Lothe, A.E., & Zweigel, P. 1999. Saline Aquifer CO₂ Storage (SACS). Informal annual report 1999 of SINTEF Petroleum Research's results in work area 1 'Reservoir Geology'. Sintef Petroleum Research Confidential Report 23.43000.00/03/99.
- Pearce, J.M., Kemp, S.J. & Wetton, P.D. 2000. Mineralogical and petrographical characterisation of a 1 m core from the Utsira Formation, central North Sea. BGS Technical Report WG/99/24C.
- Wilkinson, I.P. 1999. The biostratigraphical and palaeo-ecological application of calcareous microfaunas from the Utsira Formation in Norwegian well 15/9-A-23. BGS Technical Report WH99/124R.
- Zweigel, P., Lothe, A.E, Arts, R. & Hamborg, M. 2000a. Reservoir geology of the storage units in the Sleipner CO₂-injection case. A contribution to the Saline Aquifer CO₂ Storage project (SACS). SINTEF Petroleum Research Confidential Report 23.4285.00/02/00. (CD-ROM).
- Zweigel, P., Hamborg, M., Arts, R., Lothe, A.E., Sylta, O., Tommeras, A. & Causse, E. 2000b. Simulation of migration of injected CO₂ in the Sleipner case by means of a secondary migration modelling tool. A contribution to the Saline Aquifer CO₂ Storage Project (SACS). SINTEF Petroleum Research Confidential Report 23.4285.00/01/00.

6.2 SACS PUBLICATIONS

- Chadwick, R.A., Holloway, S., Kirby, G.A., Gregersen, U. & Johannessen, P.N. 2000. The Utsira Sand, Central North Sea – an assessment of its potential for regional CO₂ disposal. Proceedings of the 5th International Conference on Greenhouse Gas Control Technologies (GHGT-5), Cairns, Australia, 349 – 354.
- Zweigel, P., Hamborg, M., Arts, R., Lothe, A.E., Sylta, O., & Tommeras, A. 2000c. Prediction of migration of CO₂ injected into a underground depository: reservoir geology and migration modelling in the Sleipner case (North Sea). Proceedings of the 5th International Conference on Greenhouse Gas Control Technologies (GHGT-5), Cairns, Australia, 360 – 365.
- Zweigel, P., Arts, R., Bidstrup, T., Chadwick, A., Eiken, O., Gregersen, U., Hamborg, M., Johannessen, P., Kirby, G., Kristensen, L., & Lindeberg, E., 2001: Results and experiences from the first Industrial-scale underground CO₂ sequestration case (Sleipner Field, North Sea). American Association of Petroleum Geologists, Annual Meeting, June 2001, Denver, Abstract Volume (CD) 6pp.

6.3 OTHER REFERENCES

Baklid, A., Korbøl, R. and Owren, G., 1996: Sleipner vest CO₂ disposal, injection into a shallow underground aquifer. SPE paper no. 36600.

Eidvin, T., Jansen, E., Rundberg, Y., Brekke, H. & Grogan, P., 2000. The upper Cainozoic of the Norwegian continental shelf correlated with the deep sea record of the Norwegian Sea and the North Atlantic. *Marine and Petroleum Geology*, 17, 579 - 600.

Eidvin, T. & Rundberg, Y. 2001. Late Cainozoic stratigraphy of the Tampen area (Snorre and Visund fields) in the northern North Sea, with emphasis on the chronology of early Neogene sands. *Norsk Geologisk Tidsskrift*, 81, 119-160.

Gregersen, U., Michelsen, O. & Sørensen, J.C. 1997. Stratigraphy and facies distribution of the Utsira Formation and the Pliocene sequences in the northern North Sea. *Marine and Petroleum Geology*, 14, 893 - 914.

Gregersen, U., 1998. Upper Cenozoic channels and fans on 3D seismic data in the northern Norwegian North Sea, *Petroleum Geoscience*, vol. 4, 67-80.

Heggland, R. 1997. Detection of gas migration from a deep source by use of exploration 3D seismic data. *Marine Geology*, 37, 41-47.

Holloway, S. (Ed.). 1996. The Underground Disposal of Carbon Dioxide. Final Report of Joule II Project No. CT92-0031. 355 pp. British Geological Survey, Keyworth, UK.

Isaksen, D. & Tonstad, K. 1989. A revised Cretaceous and Tertiary lithostratigraphic nomenclature for the Norwegian North Sea, *NPD Bulletin* 5, Oljedirektoratet.

Jordt, H., Faleide, J.I., Bjørlykke, K. & Ibrahim, M.T. 1995. Cenozoic sequence stratigraphy of the central and northern North Sea Basin: tectonic development, sediment distribution and provenance areas, *Marine and Petroleum Geology*, 12, 845-879.

Krushin, J T. 1997. Seal capacity of nonsmectite shale. In: Surdam, R C. (Ed.) *Seals, traps, and the petroleum system*. AAPG Memoir 67, 31-47.

Piasecki, S., Gregersen, U. & Johannessen, P.N. 2002. Lower Pliocene dinoflagellate cysts from cored Utsira Formation in the Viking Graben, northern North Sea, *Marine and Petroleum Geology*, 19, 55-67.

Rundberg, Y., Olaussen, S. and Gradstein, F, 1995. Incision of Oligocene strata; Evidence for Northern North Sea Miocene uplift and key to the formation of the Utsira sand. *Geonytt*, 22, 62.

Sejrup, H.P., Aarseth, I. and Haflidason, H., 1991. The Quaternary succession in the northern North Sea. *Marine Geology*, 101, 103-111.

Sneider, R M, Sneider, J.S., Bolger, G.W. & Neasham, J.W. 1997. Comparison of seal capacity determinations: conventional cores vs. cuttings. In: Surdam, R C. (Ed.) *Seals, traps, and the petroleum system*. AAPG Memoir 67, 1-12.

Appendix I – Formation tops in wells

SACS WELLS - Utsira Sand								
All depths are relative to sea-level								
UK wells no prefix Norwegian wells have N prefix								
TUS - Top Utsira Sand BUS - Base Utsira Sand								
Well	TUS (mSL)	BUS (mSL)	Well	TUS (mSL)	BUS (mSL)	Well	TUS (mSL)	BUS (mSL)
16/12A-3	-710	-771	N15/9-12	-797	-1041			
16/13-1	-800	-926	N15/9-13	-822	-1028	N16/7-1	-783	-901
16/13A-2	-787	-909	N15/9-15	-867	-1104	N16/7-2	-769	-1071
16/13A-3	-776	-849	N15/9-16	-818	-1065	N16/7-3	-810	-980
16/13A-4	-771	-862	N15/9-17	-810	-1023	N16/7-4	-823	-1036
16/18-1	-872	-1061	N15/9-18	-844	-1084	N16/7-5	-843	-990
16/18-4	-833	-959	N15/9-19A	-818	-1035	N26/4-1	-745	-801
16/22-2	-957	-1090	N15/9-19B-T2	-818	-1035	N30/3-1	-801	-925
16/22-3	-1026	-1049	N15/9-19SR	-818	-1034	N30/3-2R	-728	-883
16/23-1	-935	-1189	N15/9-21S	-818	-1063	N30/3-3	-711	-861
16/23-2	-900	-1078	N15/9-3	-777	-1009	N30/4-1	-568	-601
16/23-3	-912	-1115	N15/9-4	-821	-1087	N30/6-1	-659	-817
16/27A-2	-1062	-1153	N15/9-5	-812	-1068	N30/6-10	-642	-791
16/27A-3	-1095	-1172	N15/9-6	-809	-1038	N30/6-11	-696	-825
16/28-1	-1040	-1148	N15/9-7	-831	-1080	N30/6-14	-702	-832
16/28-3	-958	-1157	N15/9-8	-838	-1093	N30/6-16	-659	-787
16/28-4	-978	-1121	N15/9-9	-819	-1067	N30/6-20	-664	-766
16/28-5	-1034	-1104	N15/9-A-10	-810	-995	N30/6-23	-707	-864
16/28-6	-1029	-1115	N15/9-A-16	-831	-1083	N30/6-5	-701	-853
16/29-1	-974	-1058	N15/9-A-19	-814	-1057	N30/9-11	-628	-804
16/29-2	-951	-1101	N15/9-A-22	-811	-995	N30/9-12	-621	-817
16/29-3	-942	-1156	N15/9-A-26	-813	-1114	N30/9-2	-631	-815
16/29A-5	-951	-1044	N15/9-A-27	-815	-982	N30/9-5	-619	-790
16/6A-1	-630	-675	N15/9-A-28	-812	-990	N30/9-9	-639	-794
16/8-1	-695	-785	N15/9-A-2T2	-812	-1116	N31/4-1	-682	-832
16/8B-5	-734	-779	N15/9-A-6	-811	-995	N31/4-4	-738	-829
22/3A-1	-1174	-1240	N15/9-A-9	-810	-1044	N31/4-7	-706	-748
N15/12-2	-958		N15/9-B-10	-813	-1054	N34/10-30	-891	-925
N15/12-3	-883	-1106	N15/9-B-14	-815	-1054	N34/11-1	-876	-972
N15/2-1	-680	-801	N15/9-B-17	-816	-1071	N34/7-15S	-1087	-1126
N15/3-1S	-647	-821	N15/9-B-24	-811	-1065	N34/7-2	-974	-990
N15/3-3	-652	-826	N15/9-B-6	-818	-1058	N34/7-4	-1057	-1090
N15/3-4	-663	-895	N15/9-B-7	-816	-1056	N34/8-1	-1001	-1057
N15/3-5	-677	-933	N15/9-C-2H	-819	-1030	N34/8-4A	-1047	-1084
N15/5-3	-694	-859	N15/9-D-1H	-813	-1055	N34/8-5	-1040	-1094
N15/5-4	-757	-871	N15/9-D-3H	-811	-1095	N34/8-6	-1136	-1155
N15/6-2	-761	-996	N16/01-1	-717	-787	N34/8-8	-1091	-1140
N15/6-3	-772	-1014	N16/10-2	-953	-1079	N35/11-1	-633	-694
N15/6-5	-789		N16/1-2	-741	-822	N35/11-3S	-842	-869
N15/6-6	-782	-1018	N16/1-3	-707	-898	N35/11-5	-821	-843
N15/6-7	-747	-968	N16/2-1	-772	-840	N35/11-6	-813	-861
N15/8-1	-854	-1063	N16/3-2	-754	-821	N35/8-1	-898	-939
N15/9-1	-799	-1040	N16/4-1	-735	-973			
N15/9-10	-859	-1077	N16/4-2	-753	-1043			
N15/9-11	-800	-1074	N16/5-1	-730	-818			

TEXT FIGURES

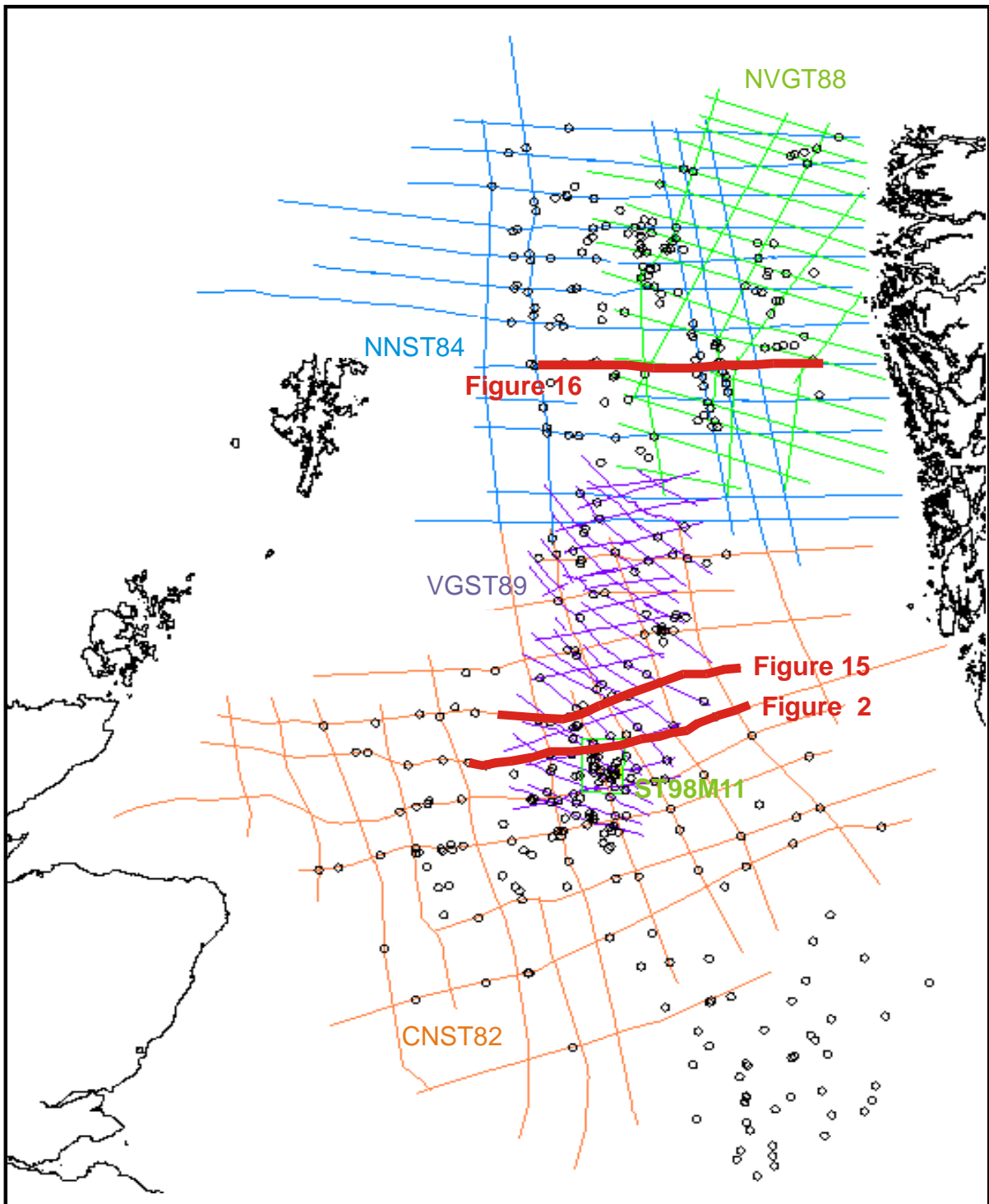


Figure 1 Regional seismic and well datasets. Bold red lines denote geoseismic sections.

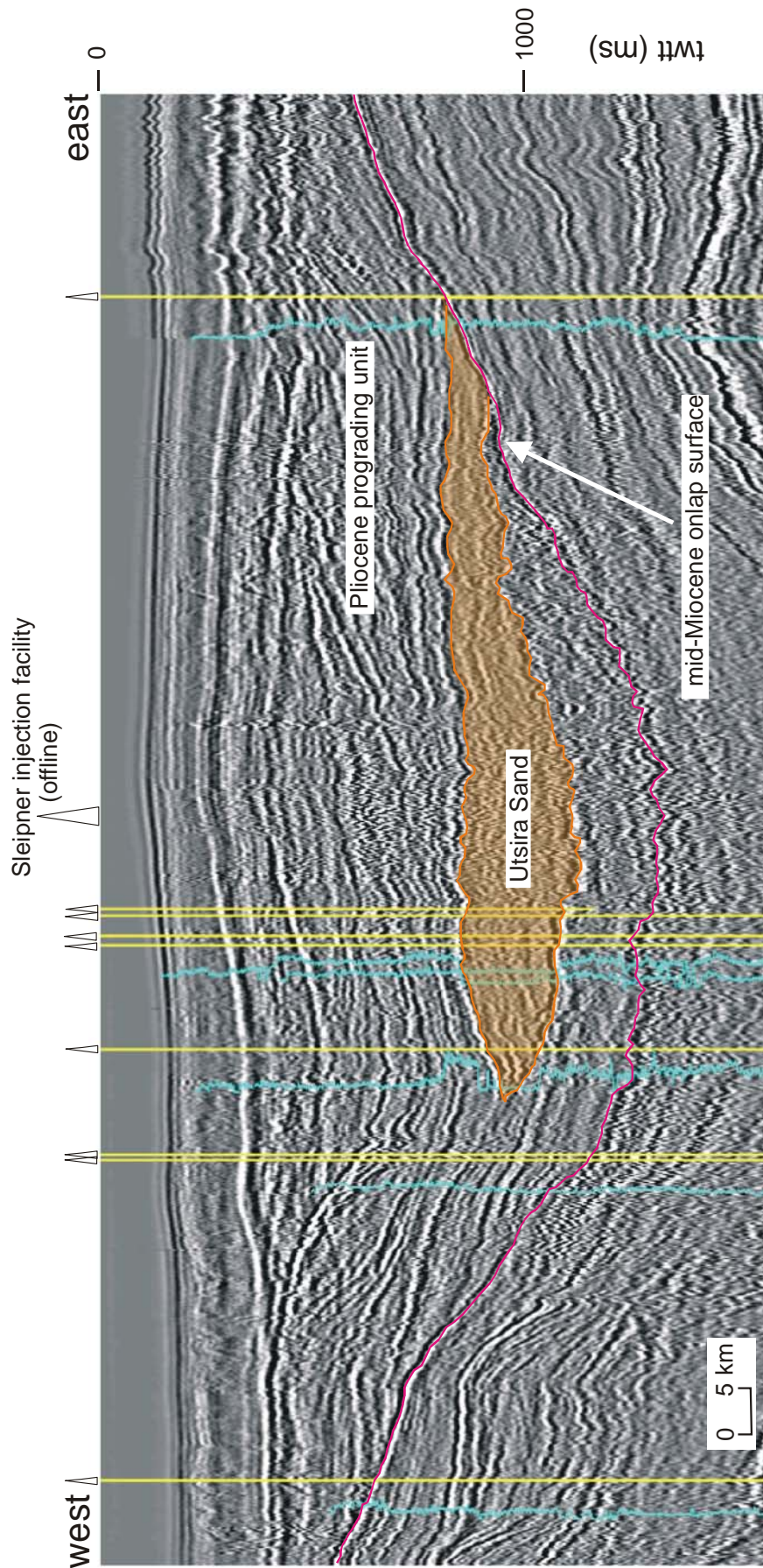


Figure 2. Seismic section across the southern Utsira depocentre, close to Sleipner (see Figure 1 for location).

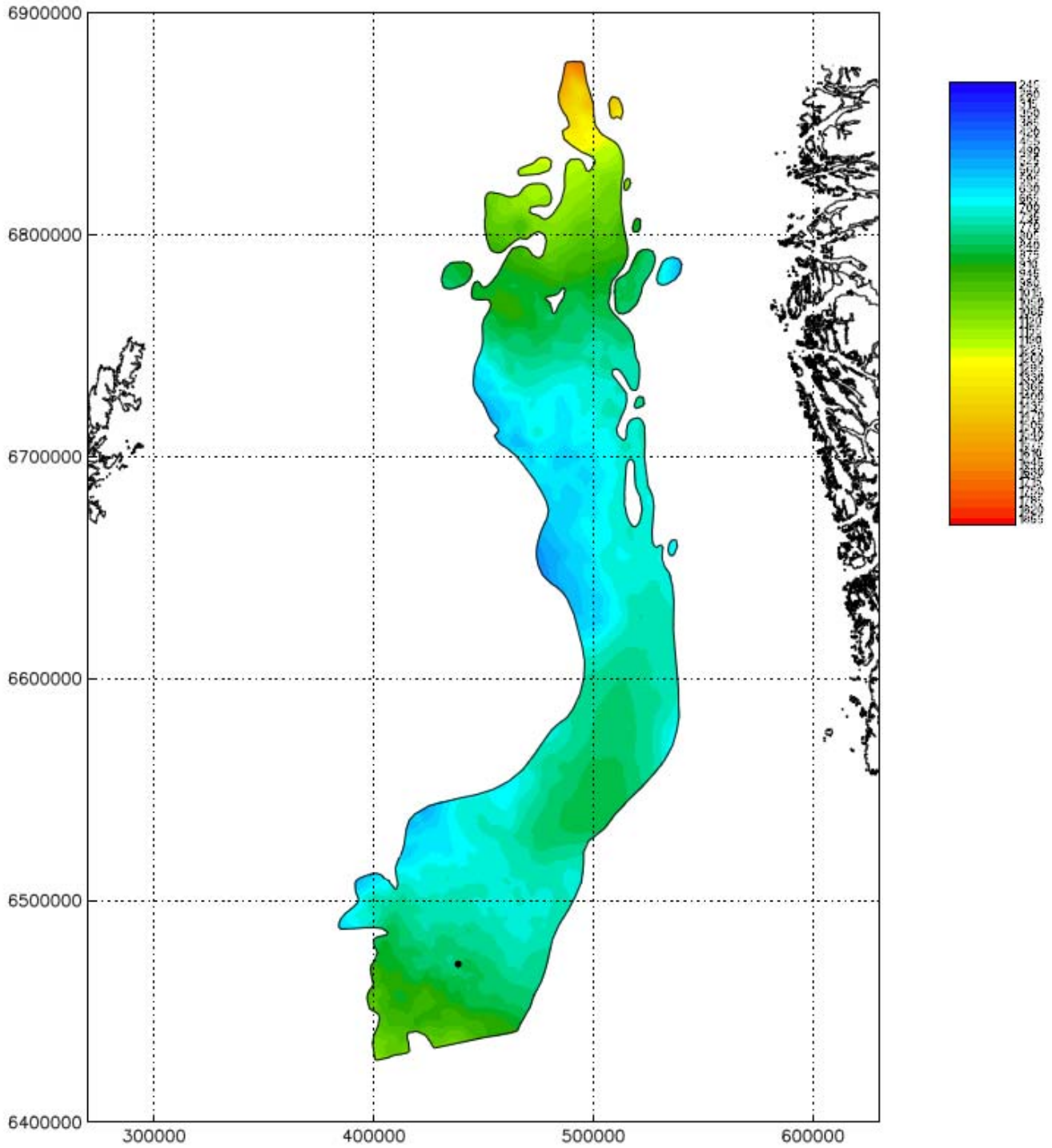


Figure 3. Depth map to top of the Utsira Sand (scale in metres below OD). Dot denotes CO₂ injection point.

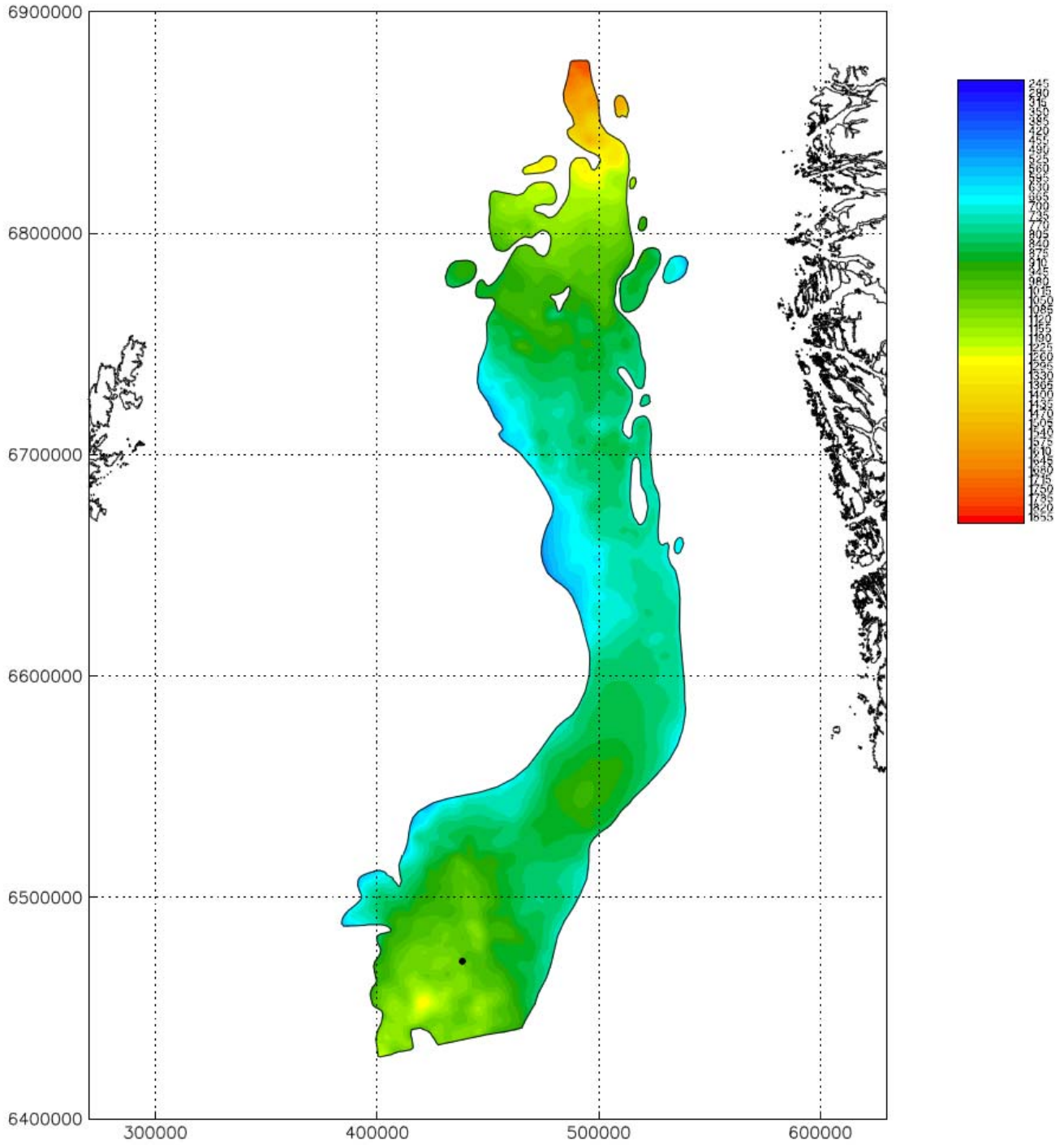


Figure 4. Depth map to base of the Utsira Sand (scale in metres below OD). Dot denotes CO₂ injection point.

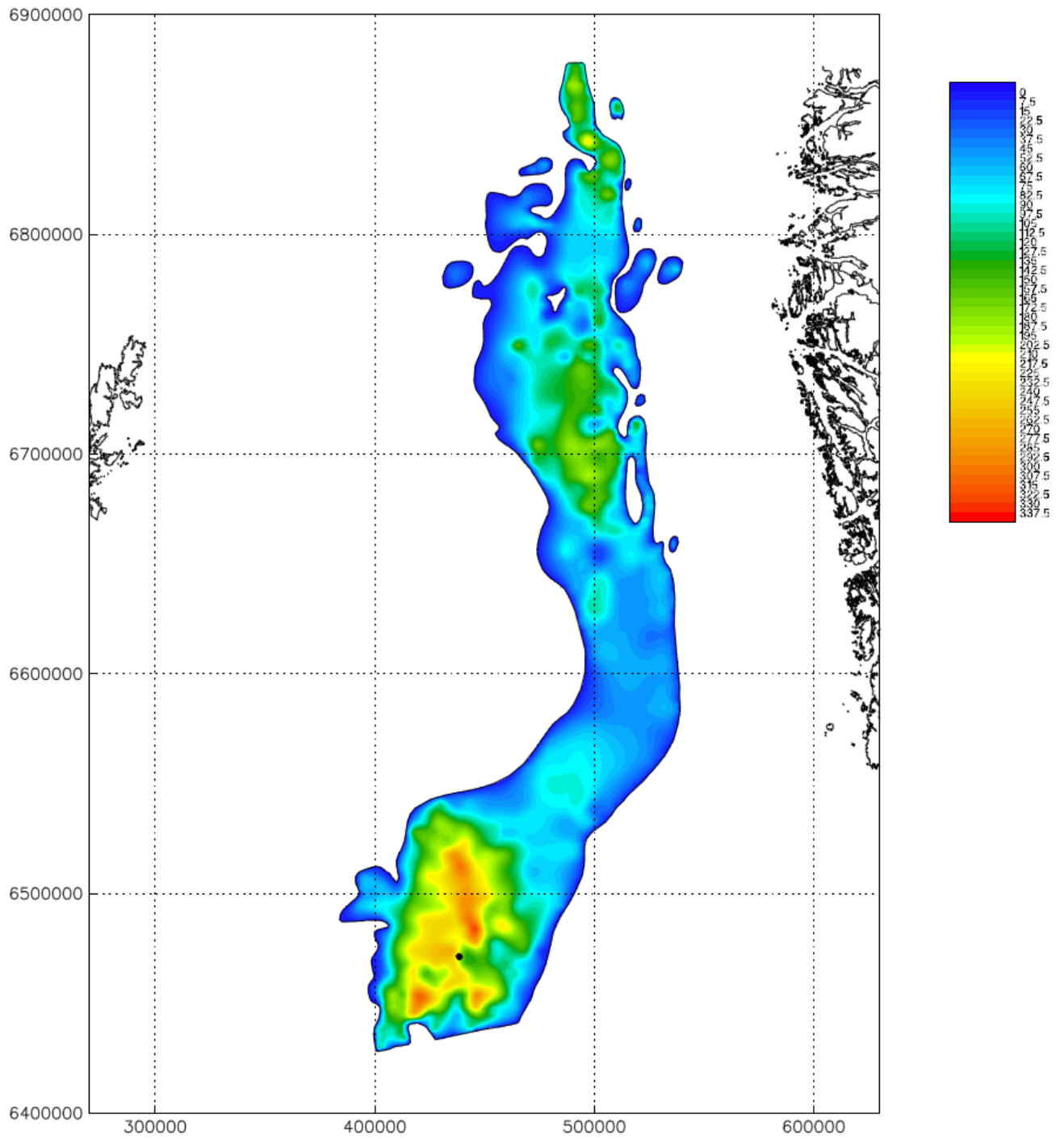


Figure 5. Isopach map of the Utsira Sand (scale in metres). Dot denotes CO₂ injection point.

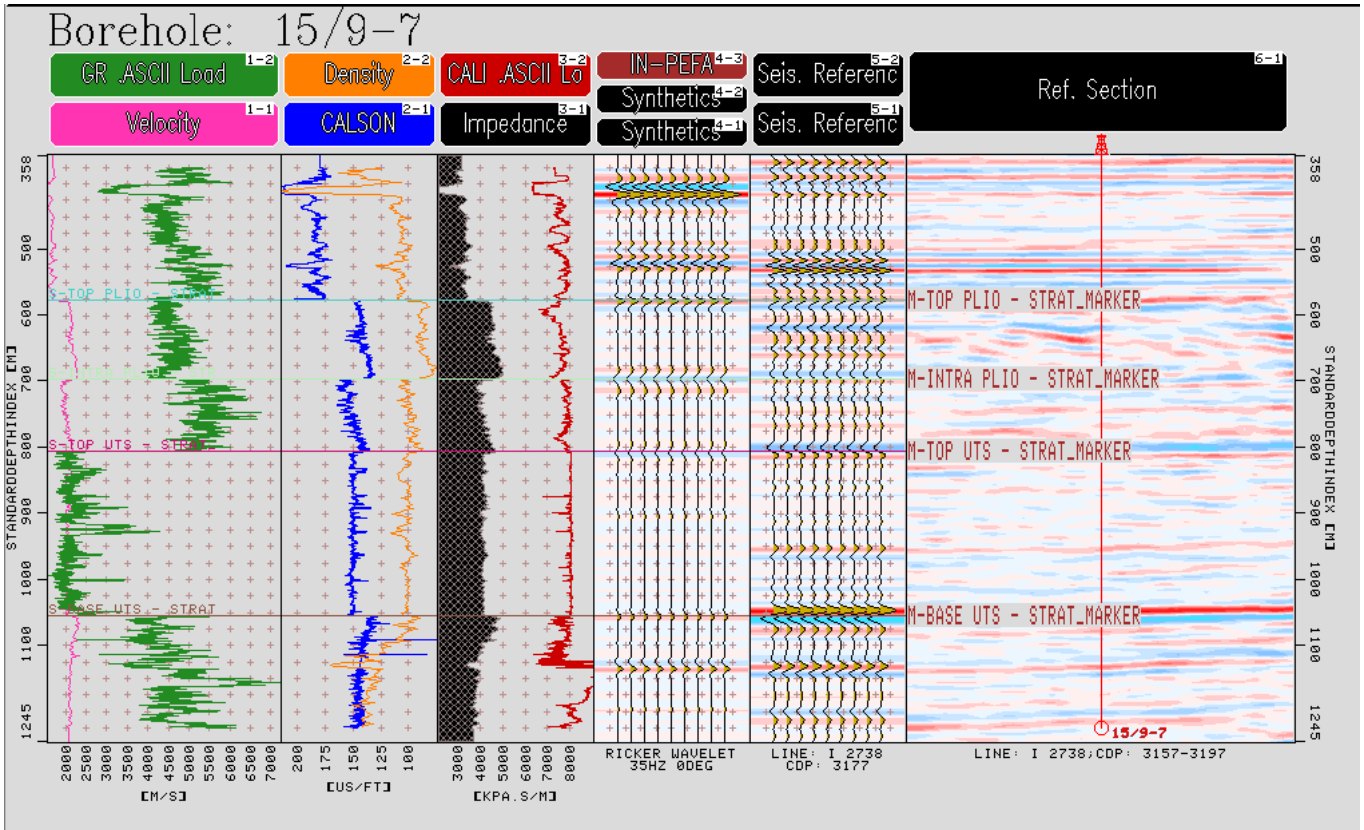


Figure 6. Synthetic seismograms derived from well log data (Norwegian well 15/9-7) compared to the actual seismic data.

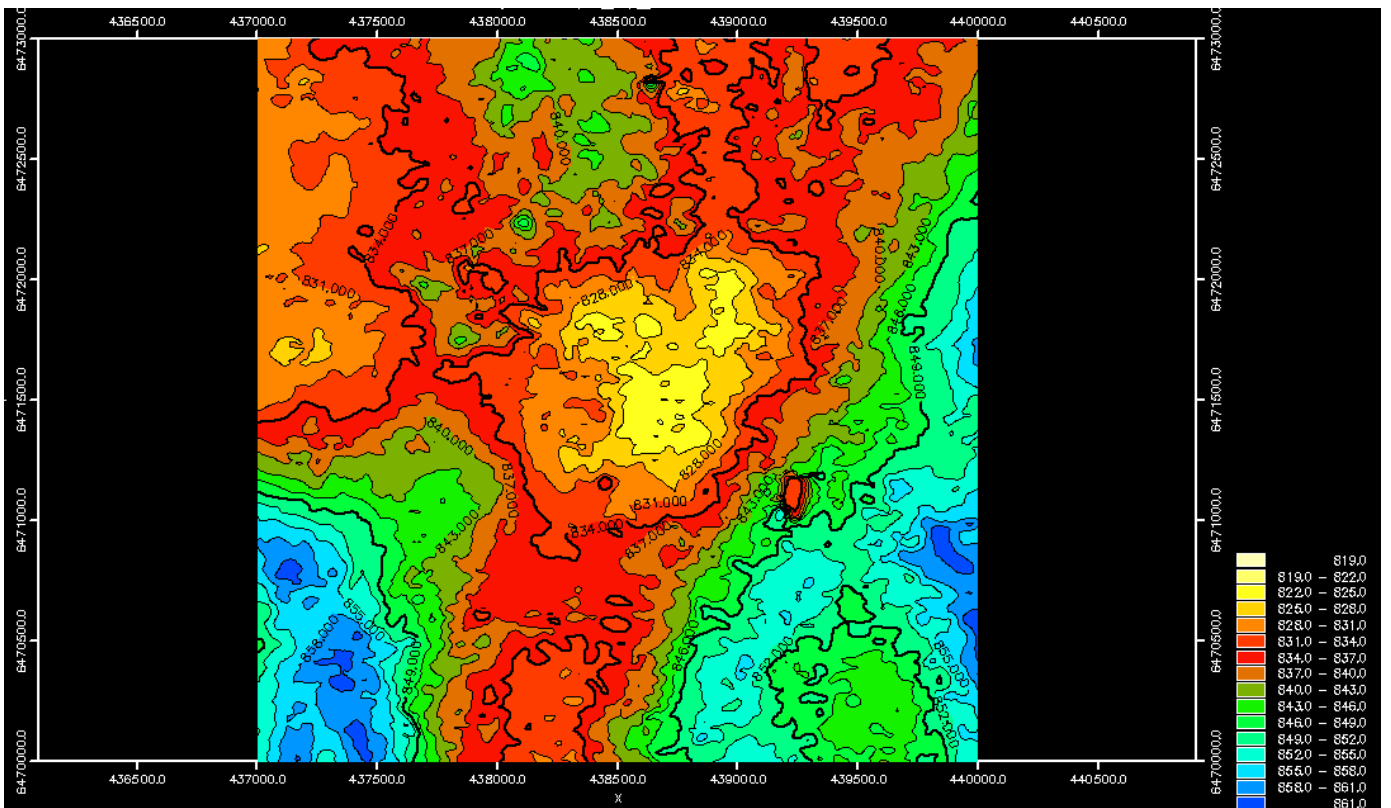
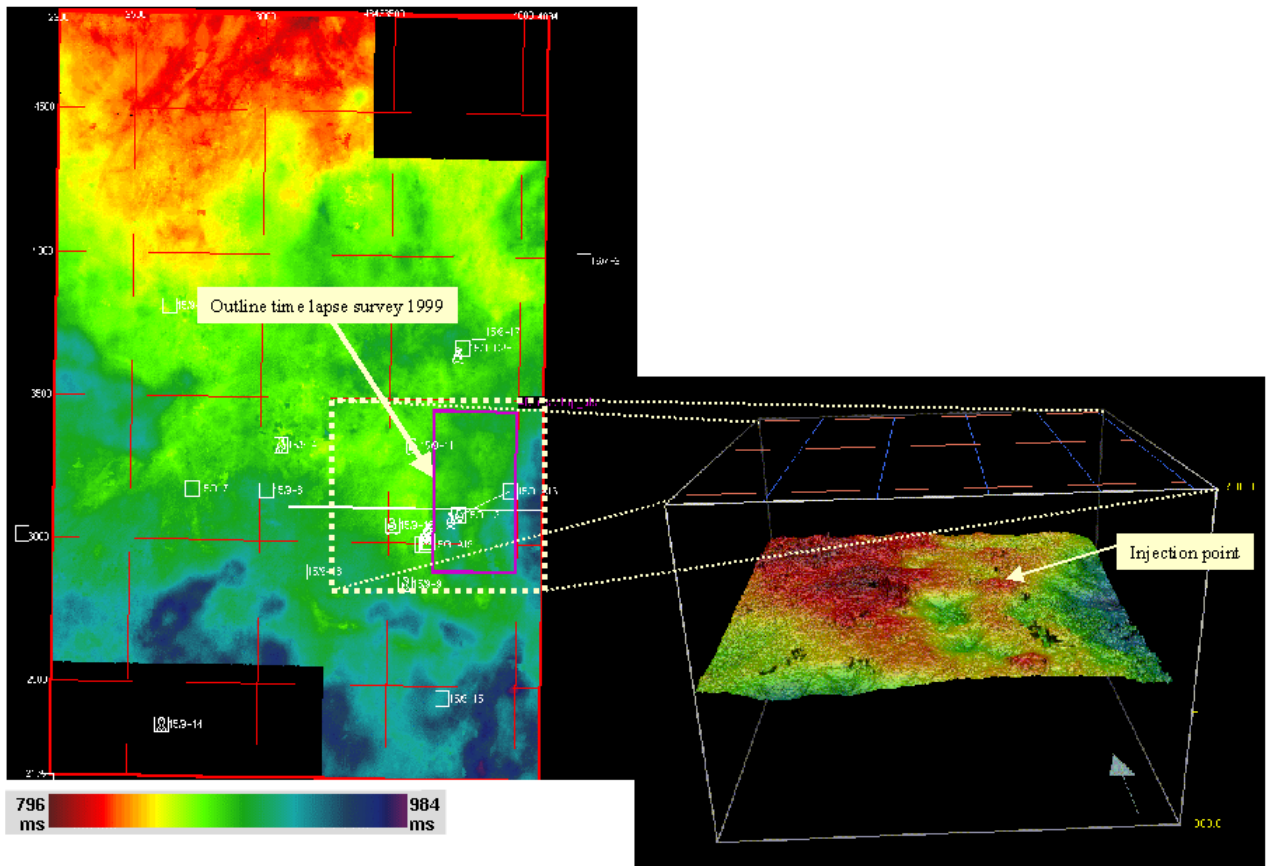


Figure 7. 3D seismic survey ST98M11, showing two-way time map of Top Utsira Sand and perspective view (top). Depth map to top Utsira Sand around injection point (bottom).

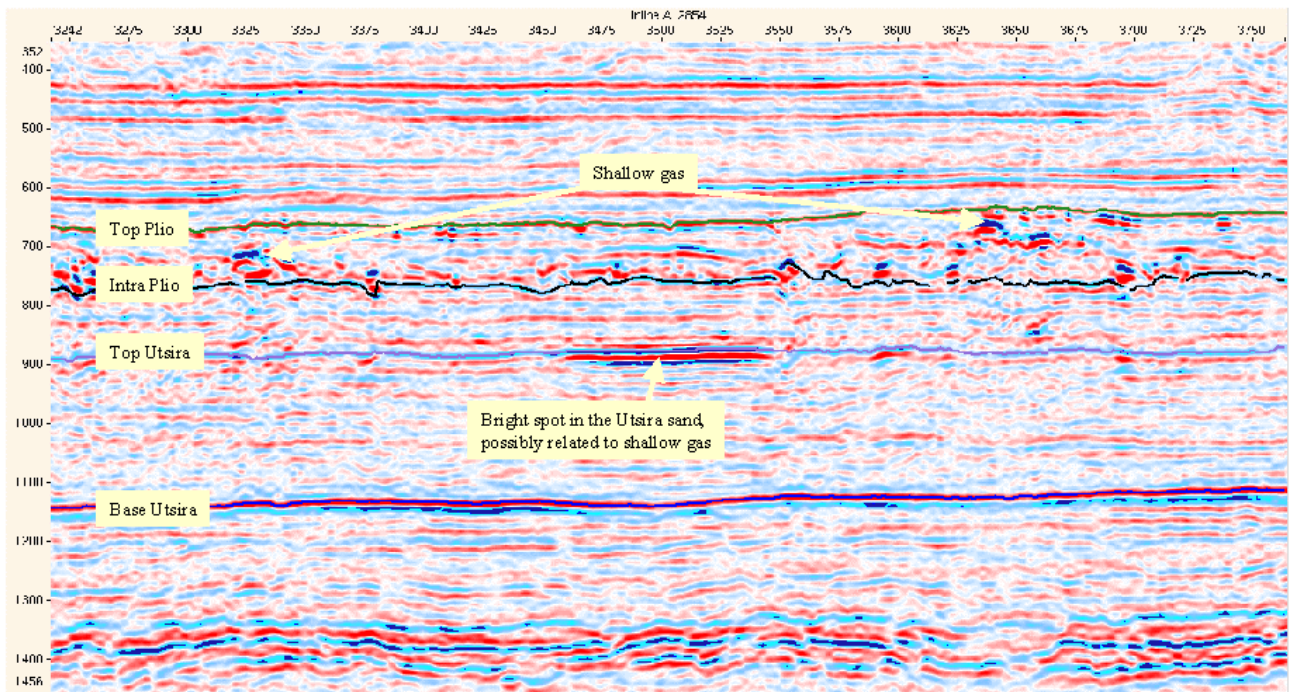
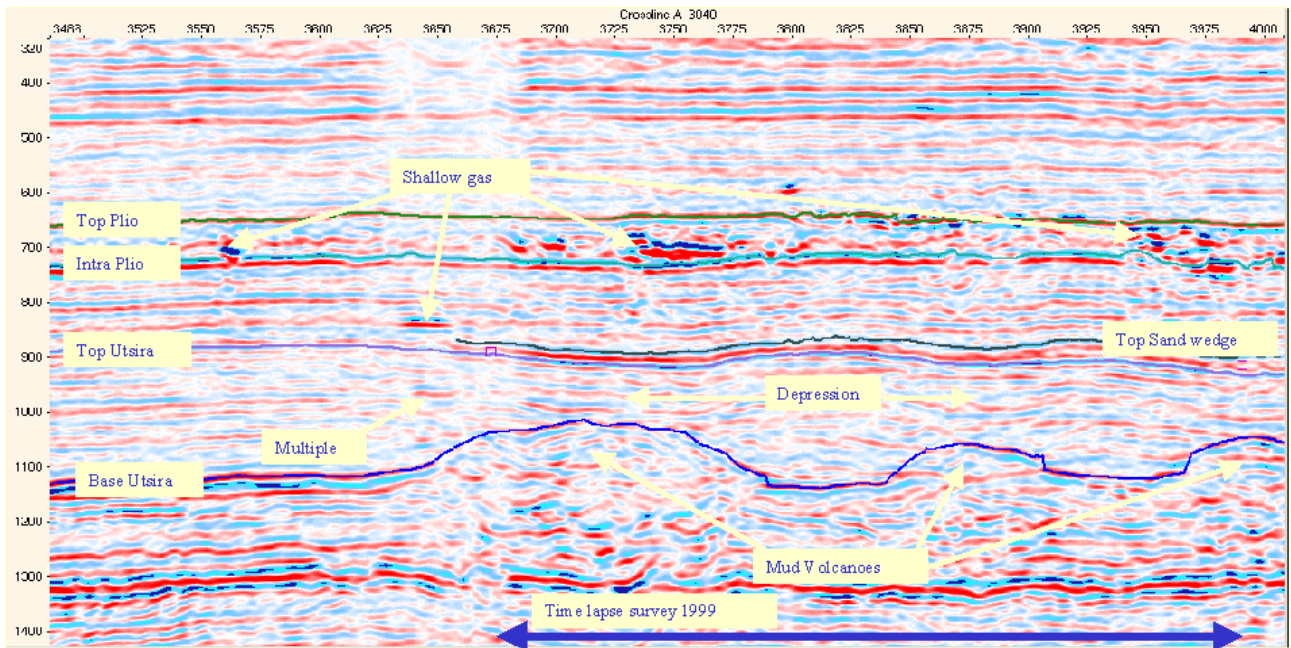


Figure 8. Seismic crossline (east to west) and inline (south to north) from survey ST98M11. Mud-volcanoes at the Base Utsira Sand are observed. Note the depressions just above them due to differential compaction. Amplitude anomalies possibly linked to the presence of shallow gas are observed in the thin shale drape just above the Top Utsira Sand in the lower Pliocene and also in the upper Pliocene.

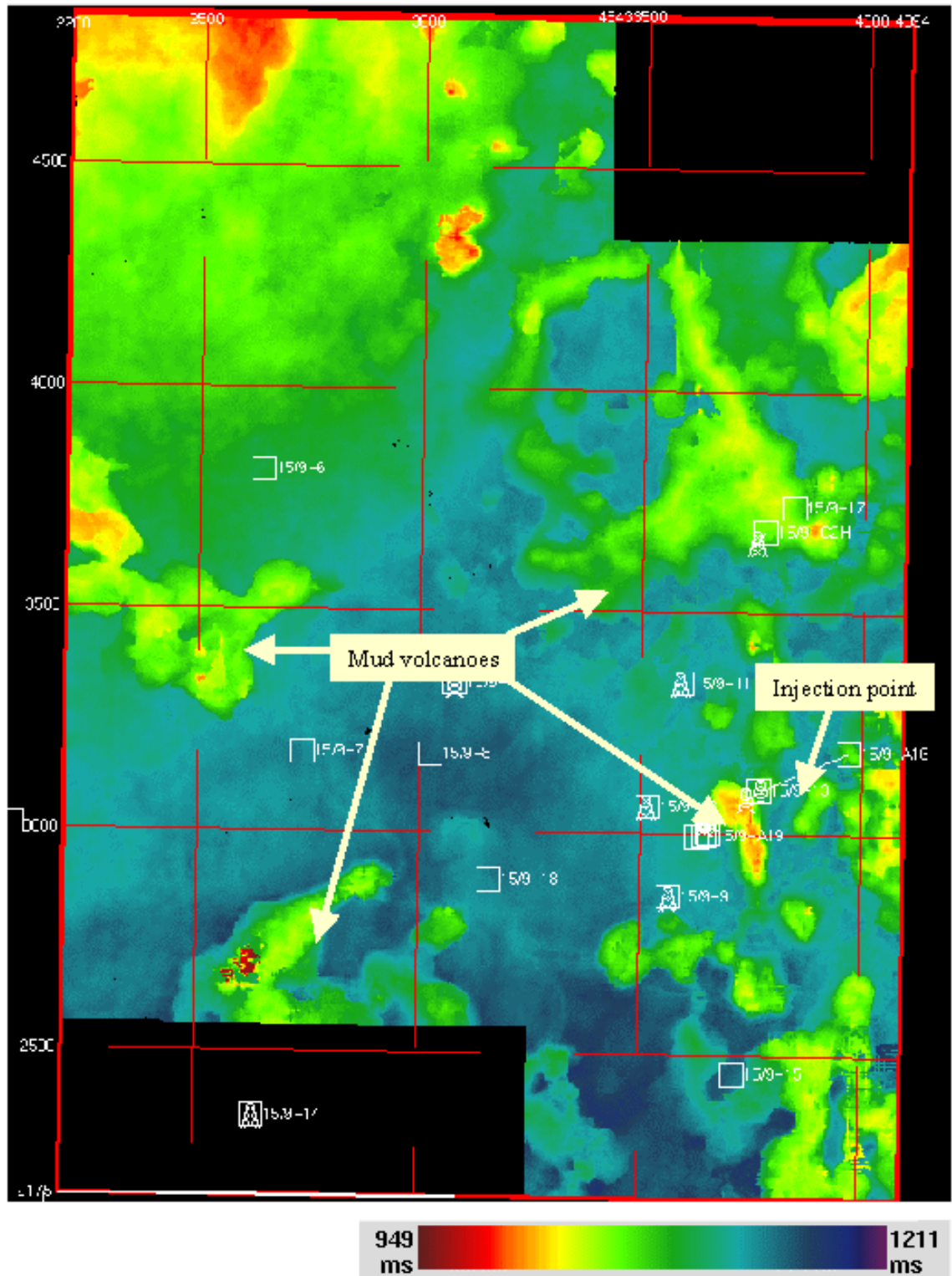


Figure 9. 3D seismic survey ST98M11, showing two-way time map of Base Utsira Sand. Note mud volcanoes.

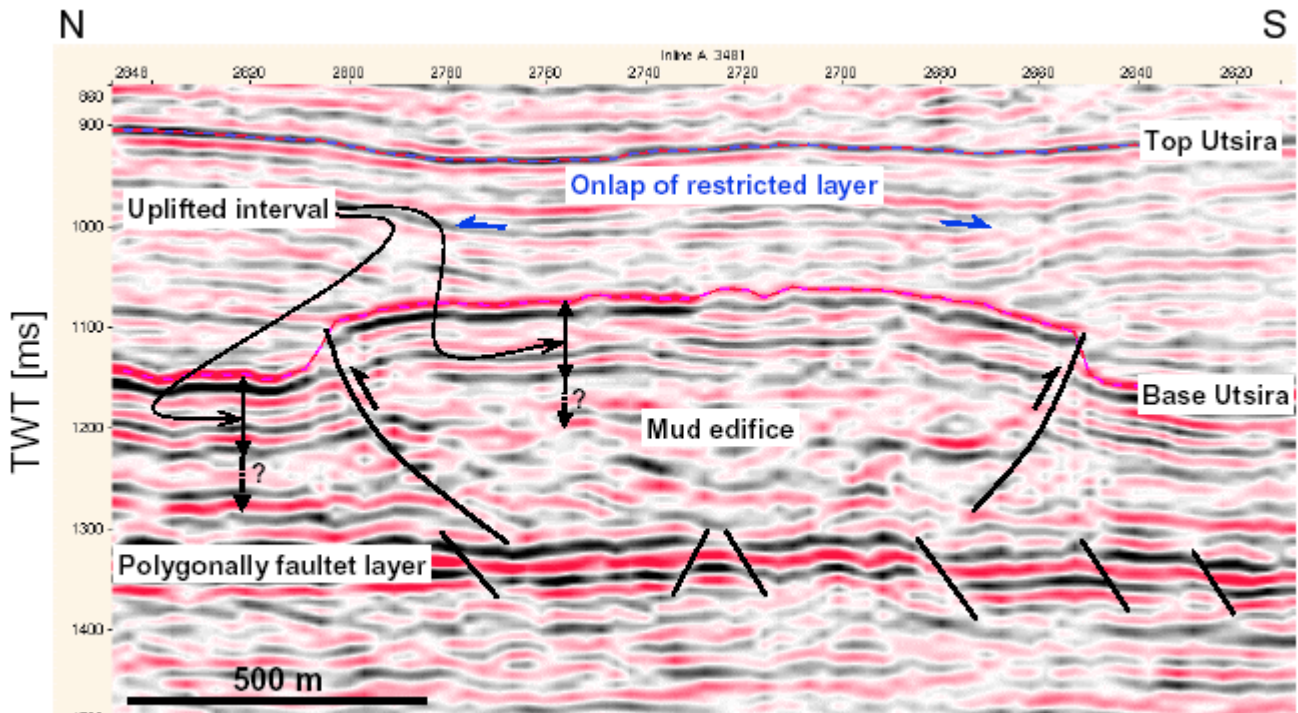


Figure 10. Seismic inline showing ‘pop-up’ mud edifice, bounded by reverse faults. Note the identical seismic signature of the top part of the shales within and outside the mud edifice. Faults do not continue into the Utsira sand above the top level of the uplifted shales. The deeper shale layer, affected by polygonal normal faulting, has not been affected by the reverse faults.

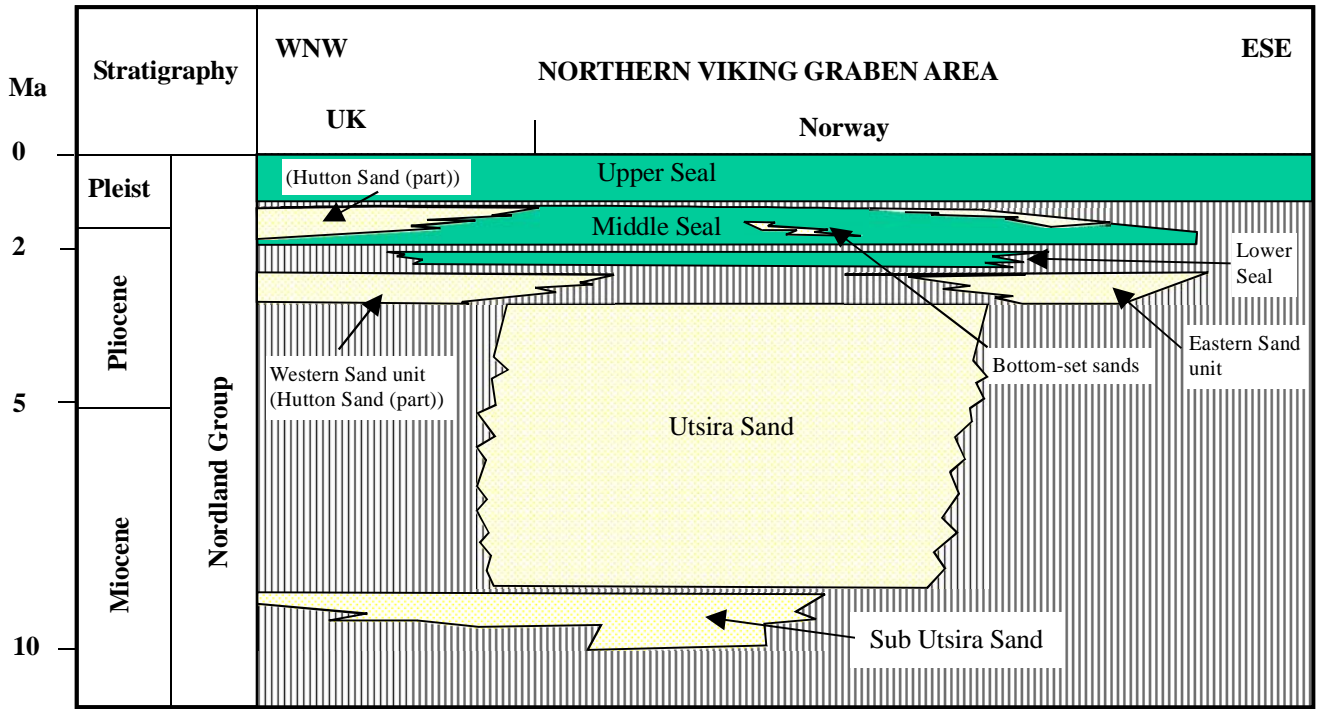


Figure 11. Generalised stratigraphy of the Neogene of the northern North Sea. Principal sand units highlighted.

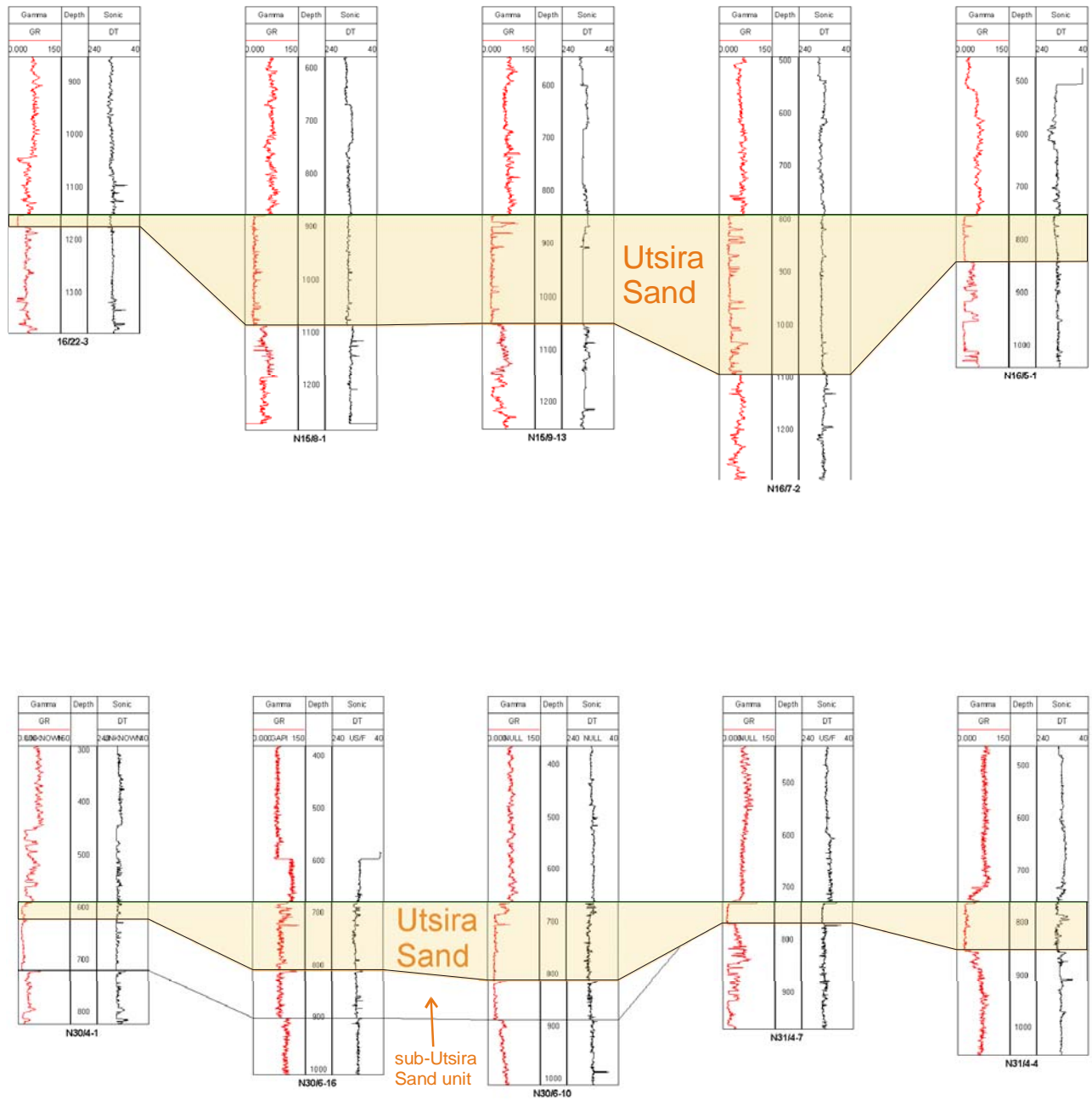


Figure 12. Regional well correlation diagrams a) through the Utsira southern depocentre. For simplicity the Sand-wedge is included within Utsira Sand. b) through the Utsira northern depocentre. Note the sub-Utsira Sand unit in the north.

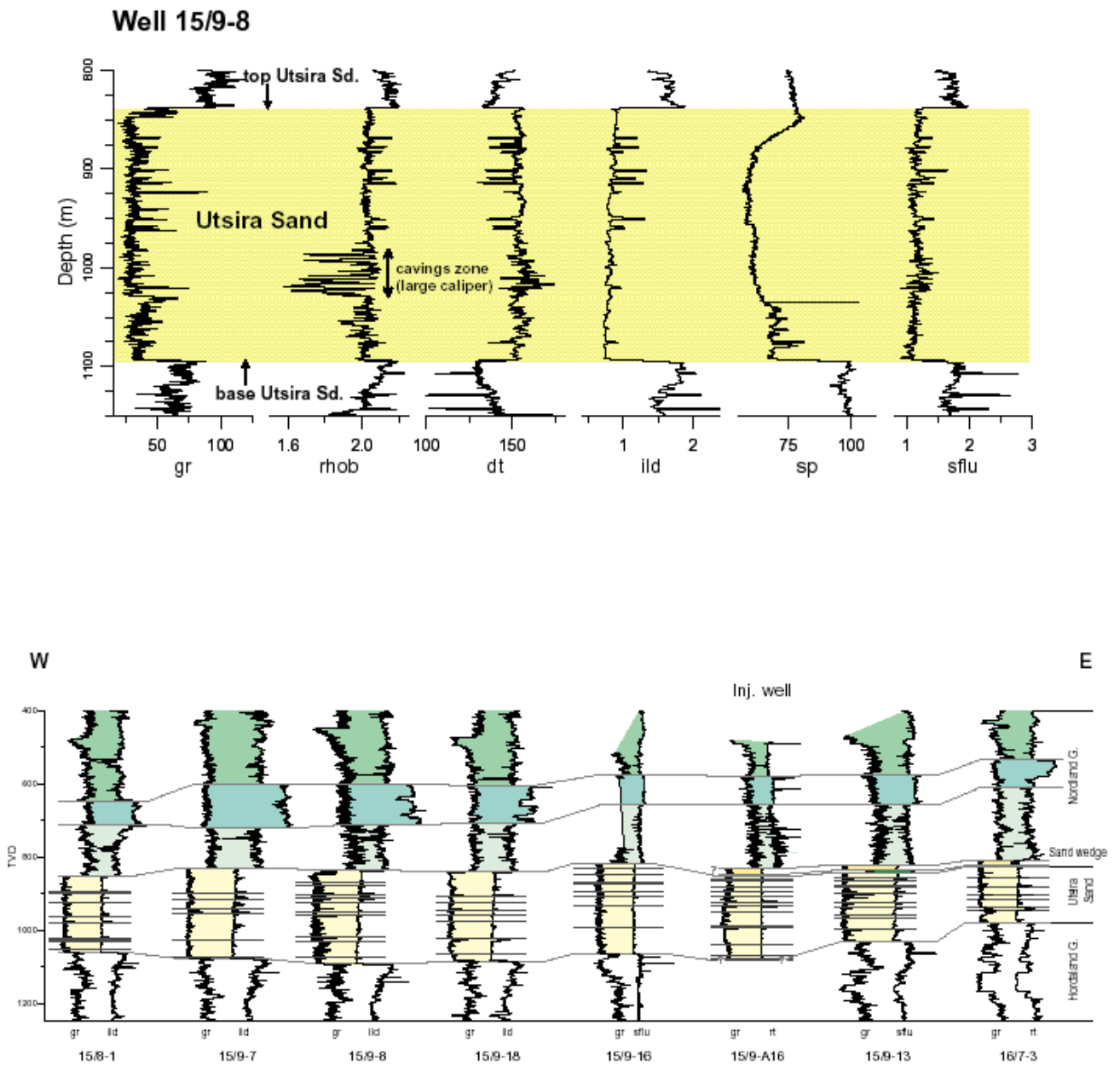


Figure 13. a) Detailed well logs through the Utsira Sand, showing a number of thin shale beds (Norwegian well 15/9-8). b) E-W well correlation diagram through the Utsira Sand and its caprock in the Sleipner area. Note the thin intra-reservoir shales and the Sand-wedge in the lowermost part of the caprock, pinching out to the west.

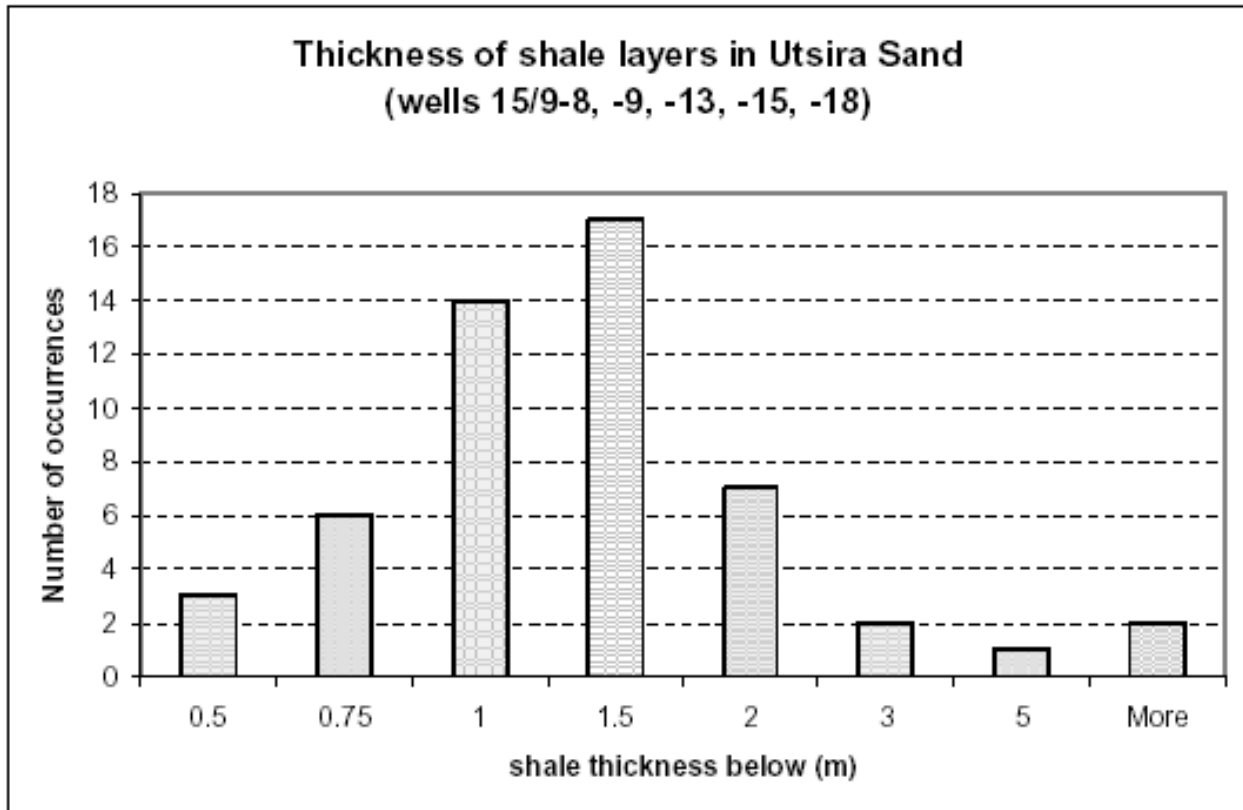


Figure 14. Thickness distribution of intra-reservoir shales, based on detailed interpretation of well log data from wells around Sleipner.

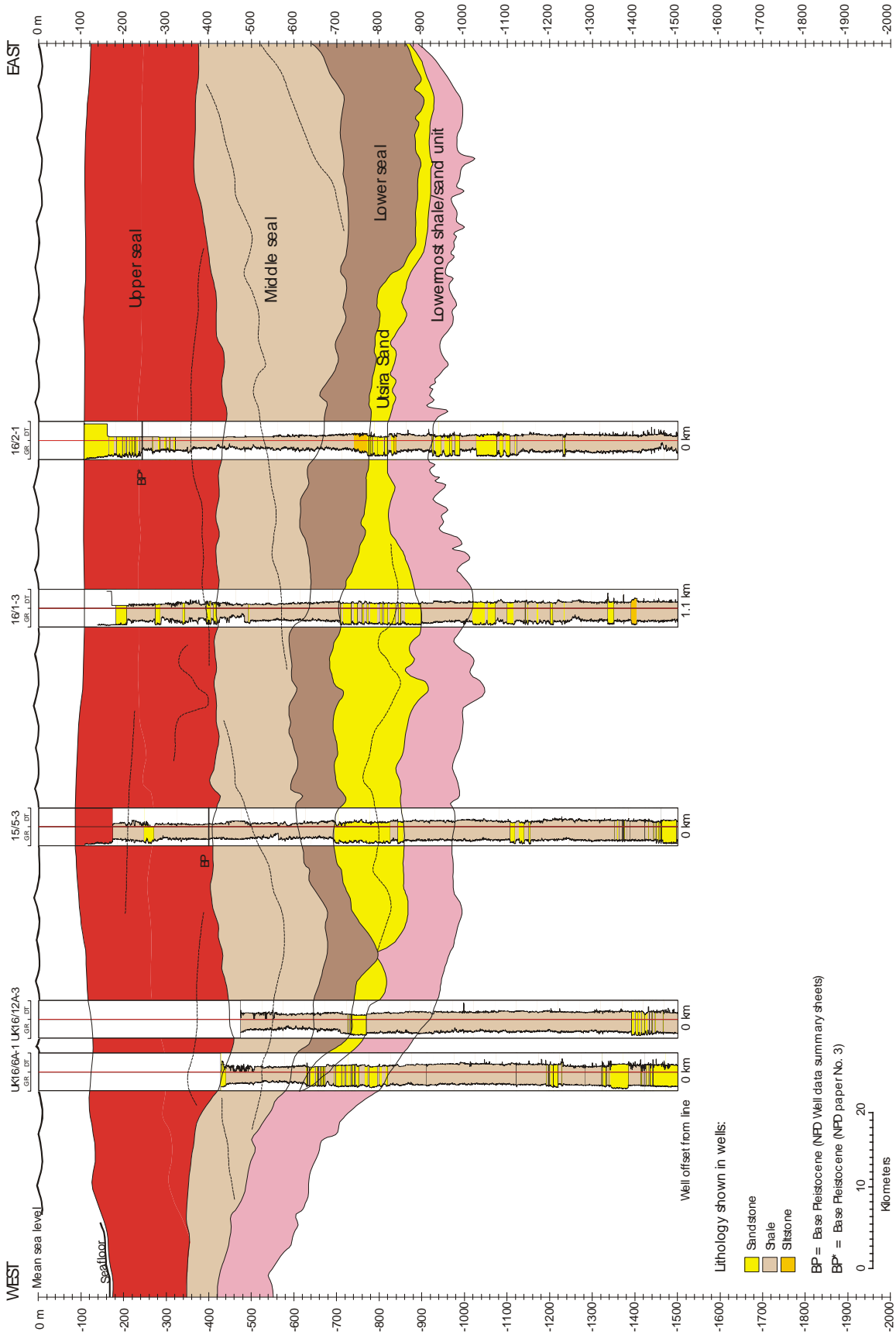


Figure 15. Interpreted geoseismic and well correlation section across the southern Utsira depocentre, showing the Utsira Sand and the main units of the caprock succession (see Figure 1 for location).

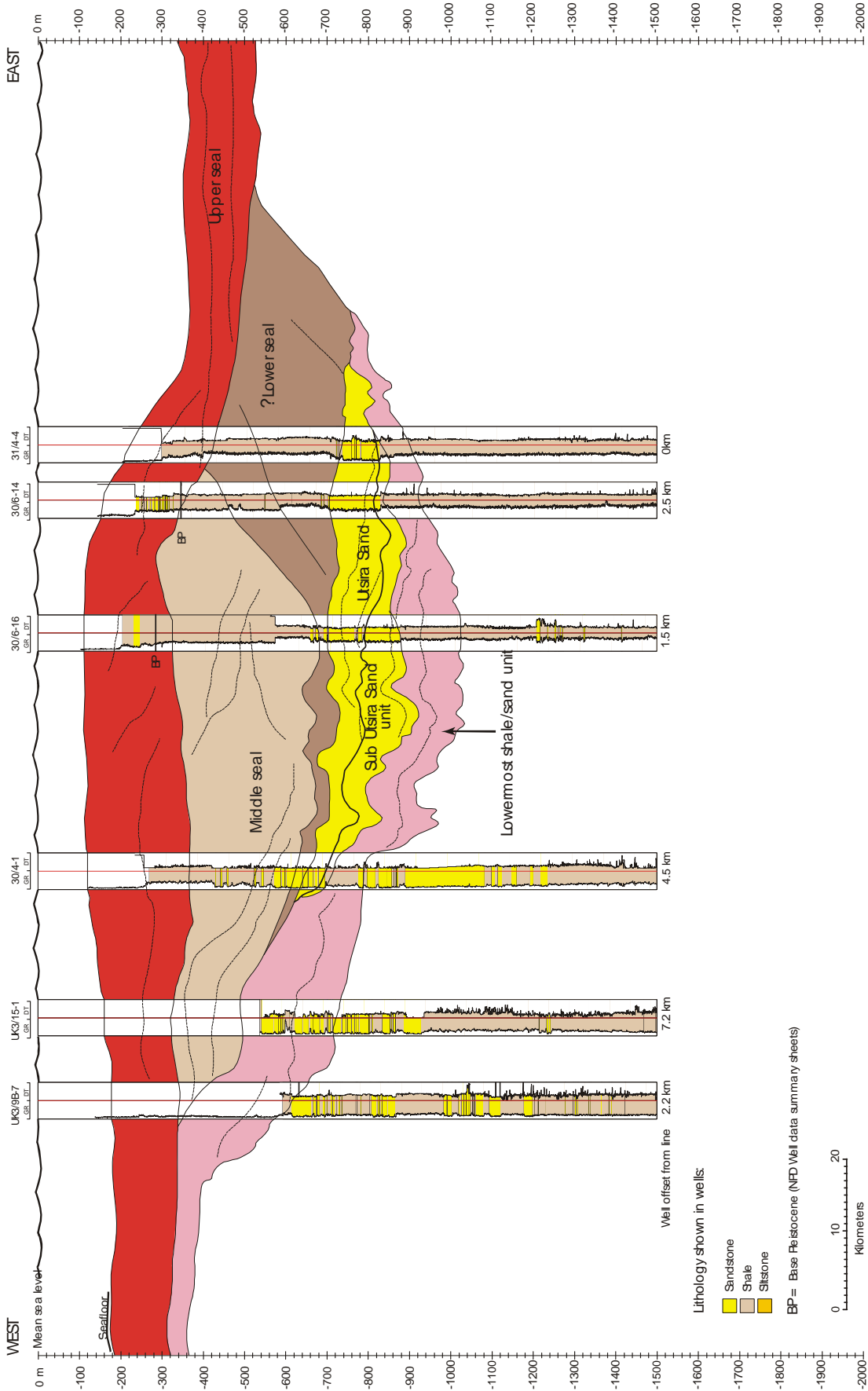


Figure 16. Interpreted geoseismic and well correlation section across the northern Utsira depocentre, showing the Utsira Sand and the main units of the caprock succession (see Figure 1 for location).

W

E

16/29-4

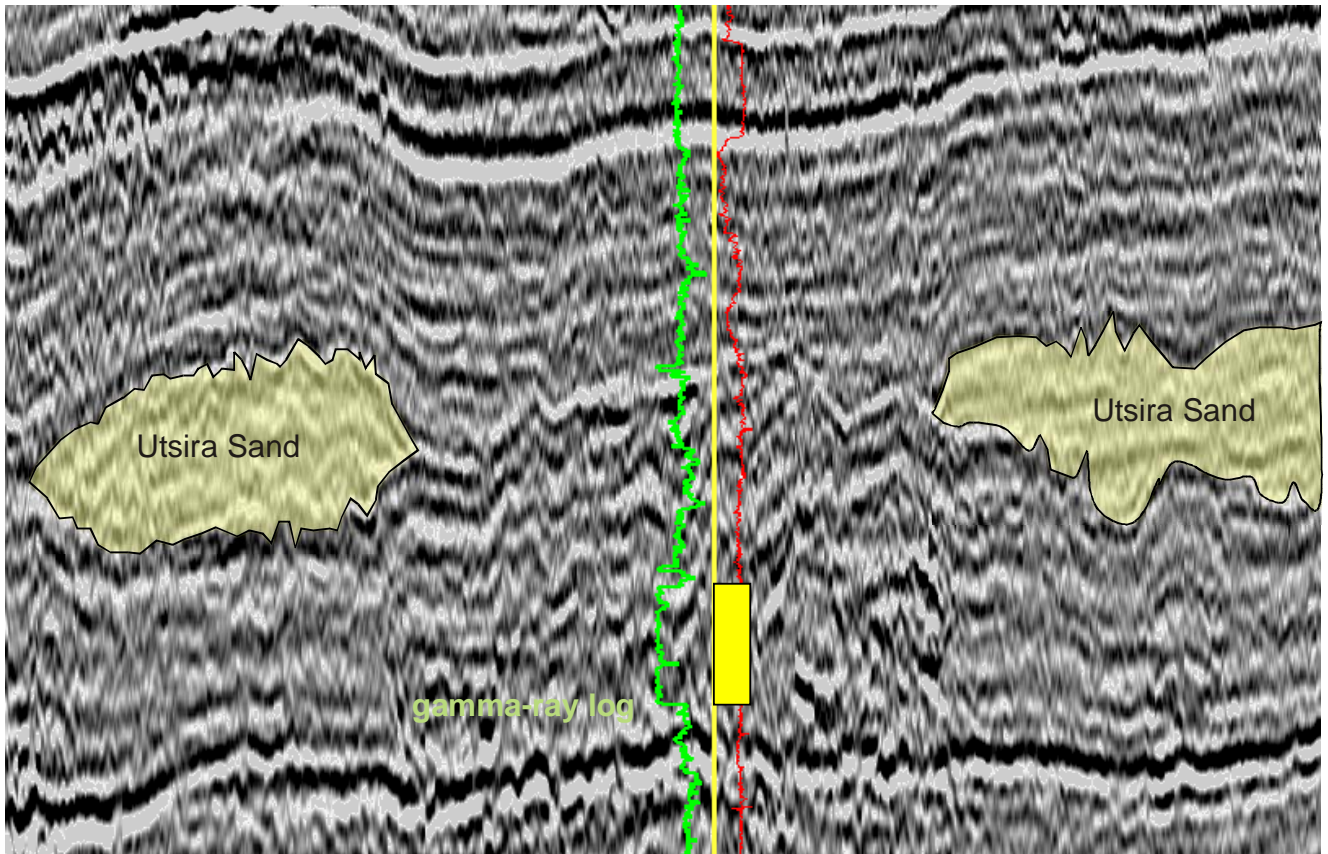
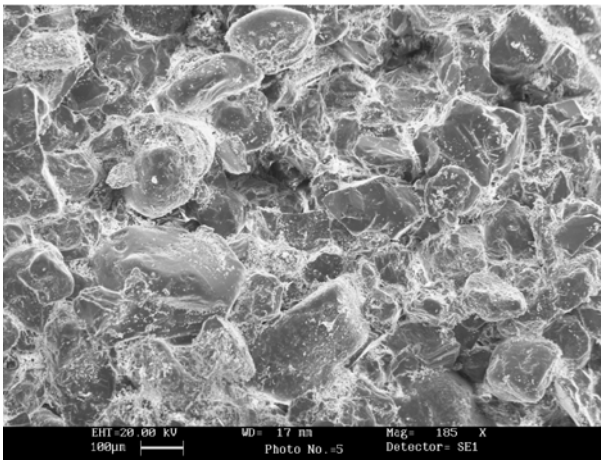


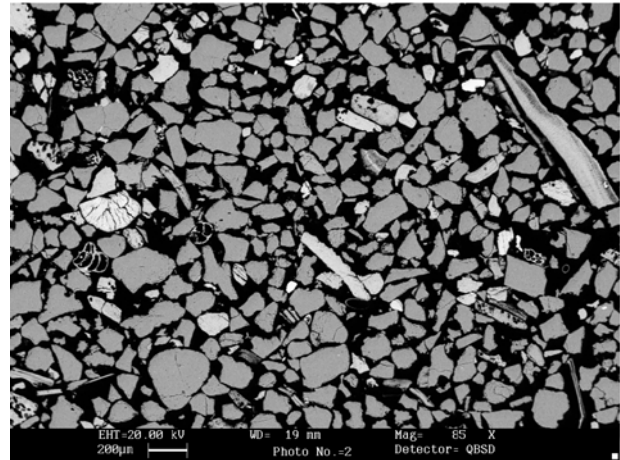
Figure 17. Complex distribution of the Utsira Sand at the western margin of the southern depocentre. Note the sand unit in UK well 16/29-4, formerly incorrectly identified as the Utsira Sand.



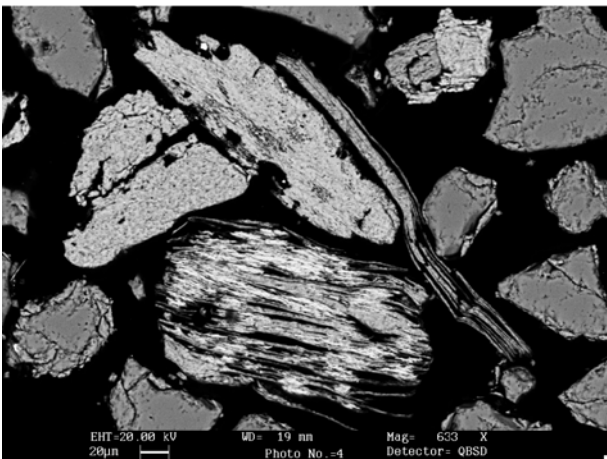
a



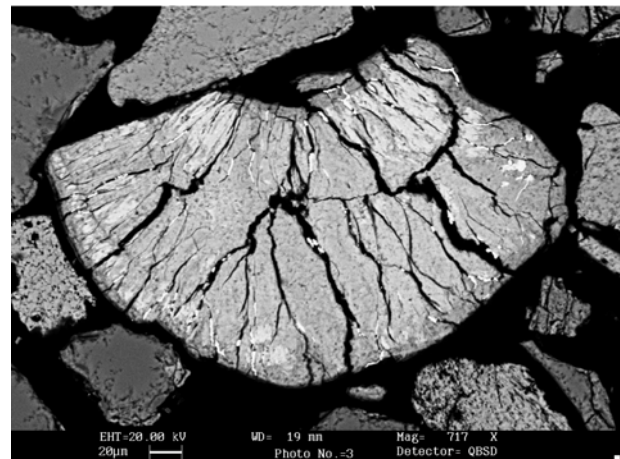
b



c



d



e

Figure 18. a) Photograph of 1m part of the Utsira Sand core from Norwegian well 15/9-A-23. b) Moderately well-sorted, subrounded to subangular, fine to medium-grained Utsira Sand c) Utsira Sand with calcareous shell and foraminifera fragments d) Typical examples of altered biotite (bottom) and muscovite flakes e) Typical example of rare glauconite grain, partially replaced by collophanic material and pyrite in cracks.

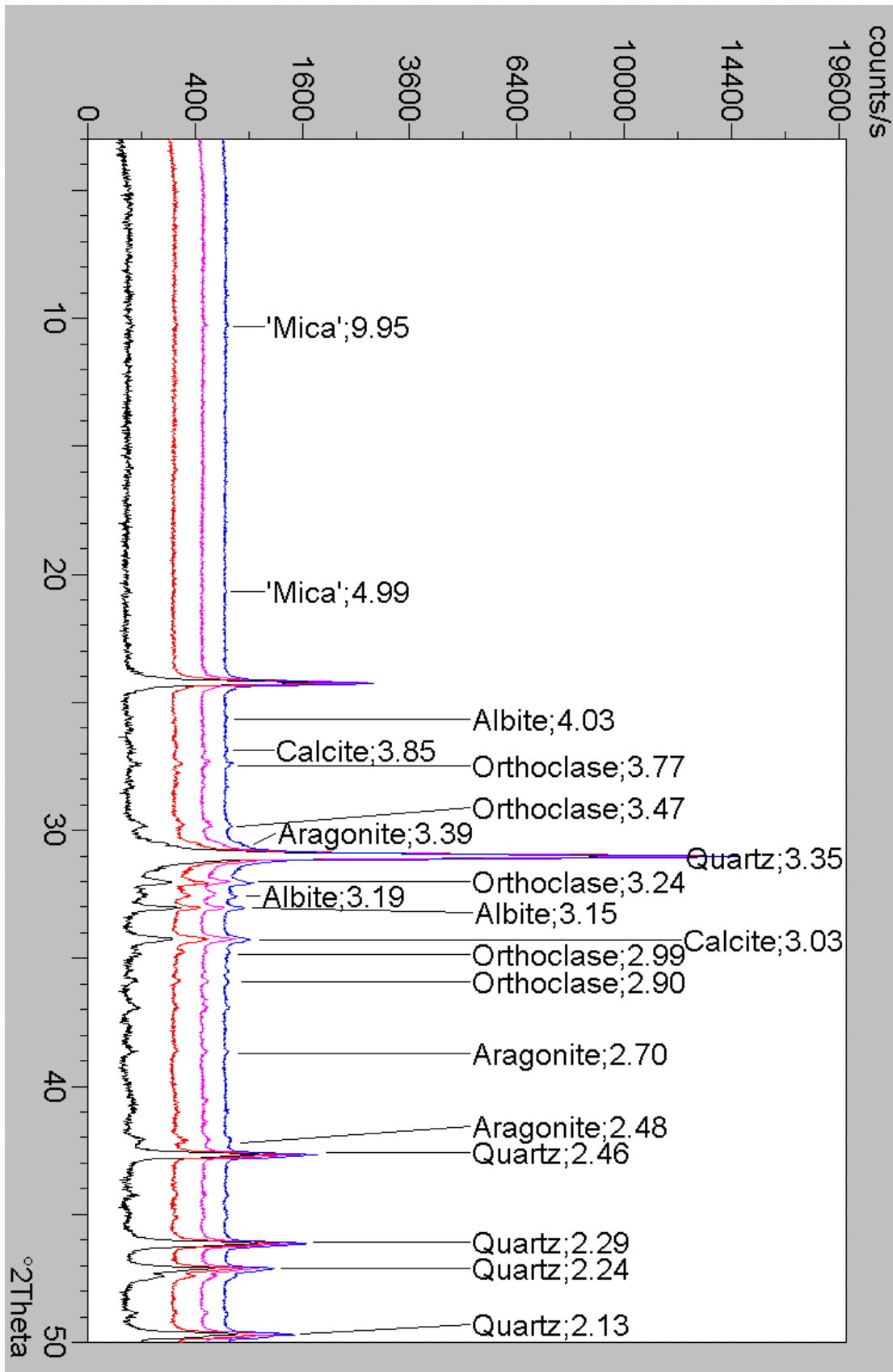


Figure 19. Whole-rock X-ray diffraction traces for samples E641A (black trace), E642 (red trace), E643 (magenta trace) and E644 (blue trace) showing major peak assignments and d spacings. Co-K α radiation.

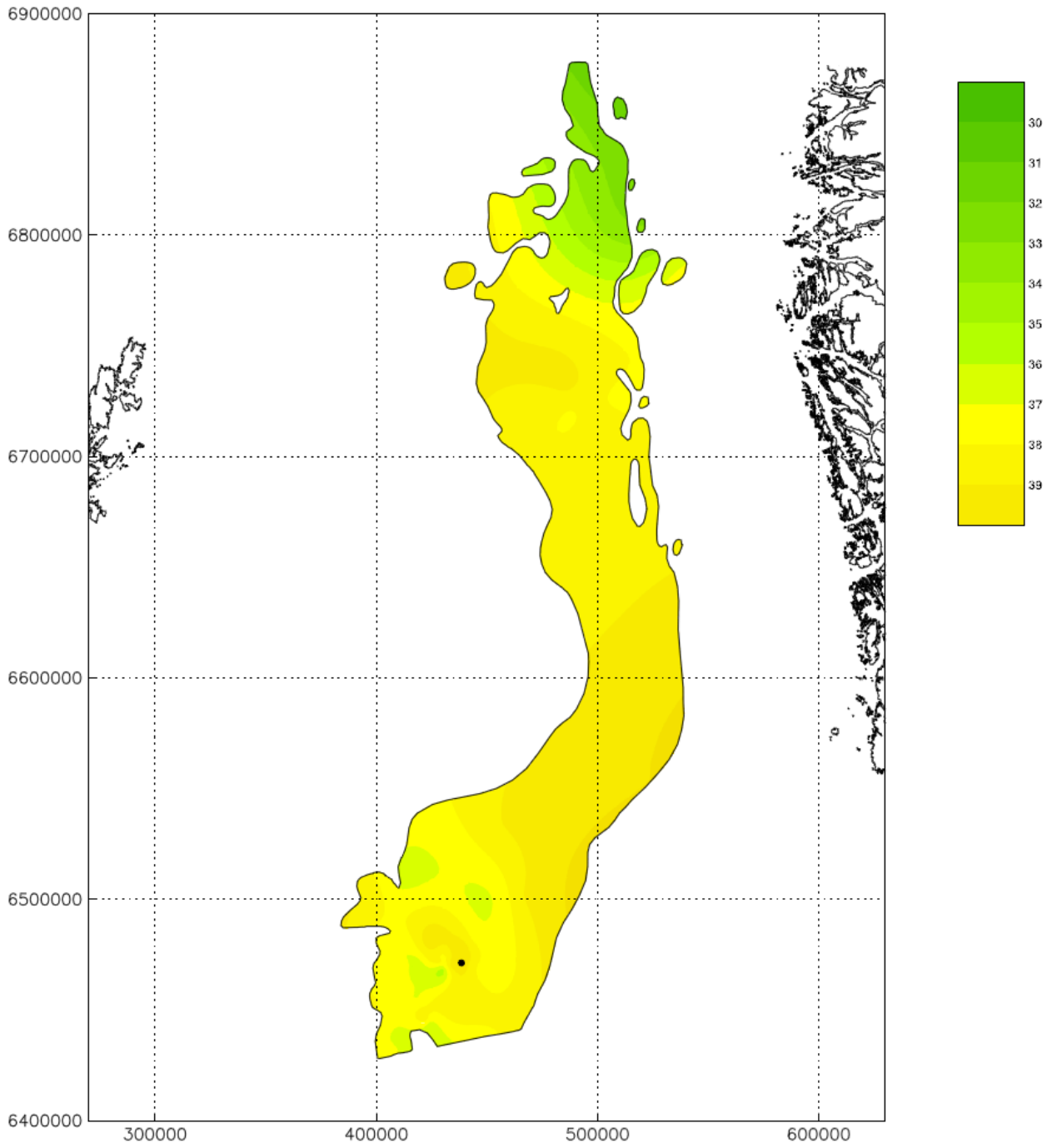


Figure 20. Porosity of the Utsira Sand, computed from well logs (dot denotes CO₂ injection point).

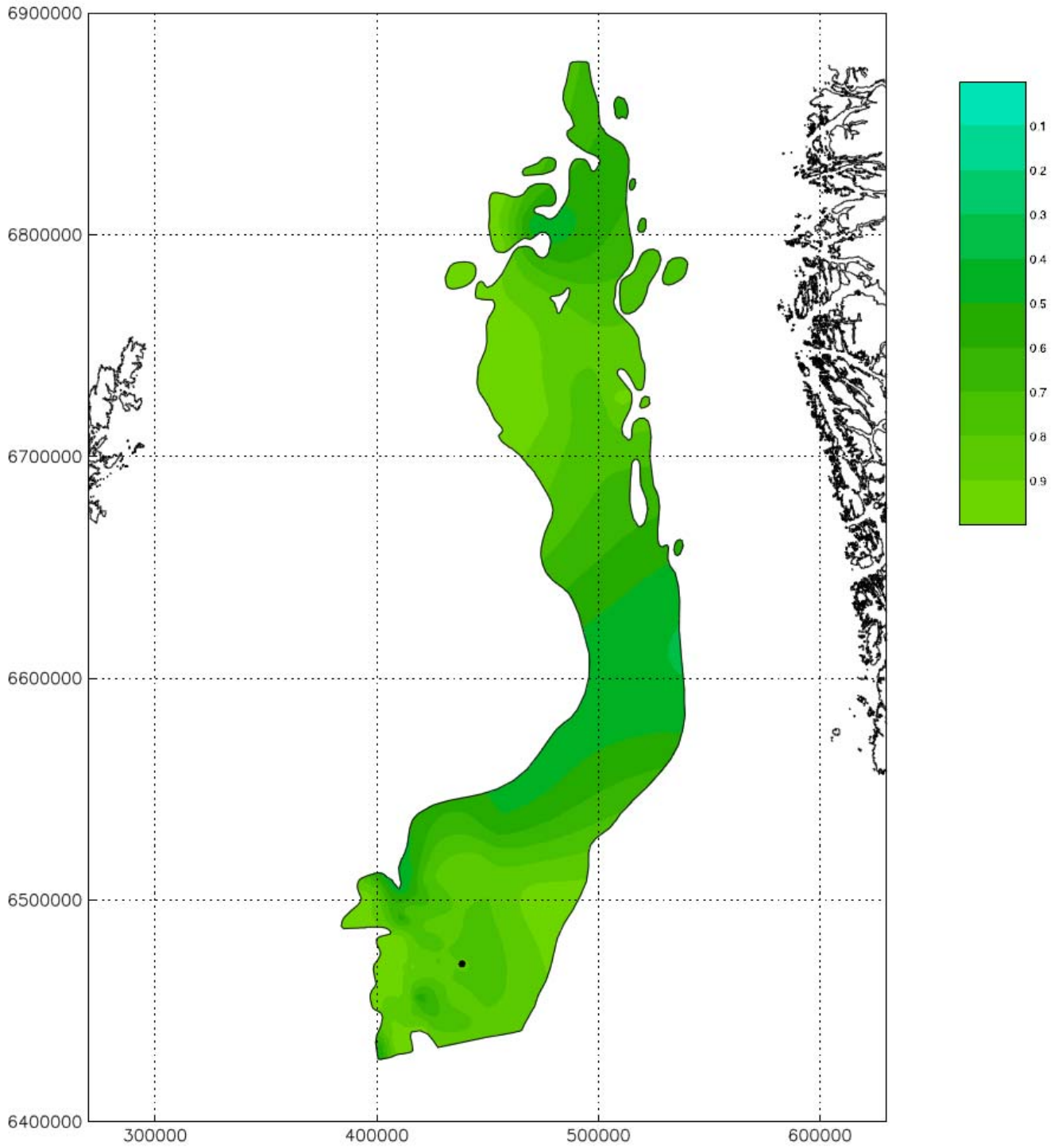
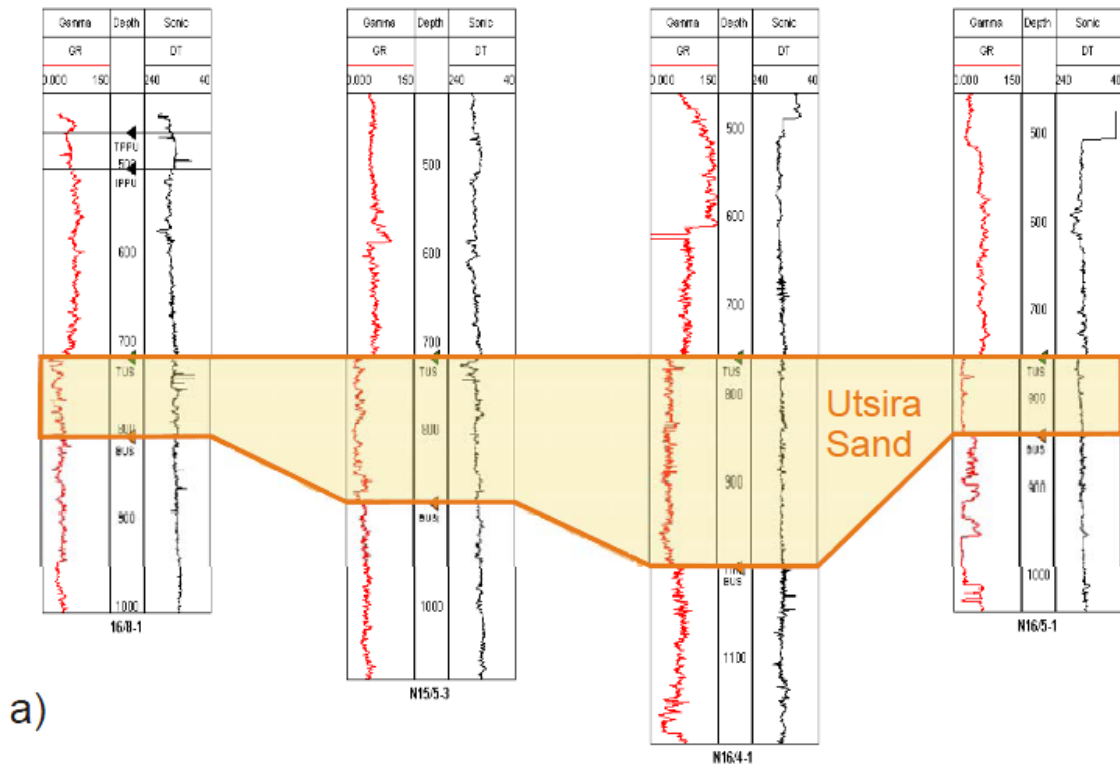
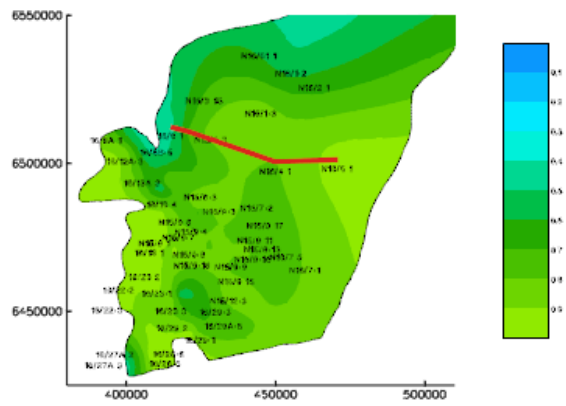


Figure 21. Percentage clean sand in the Utsira Sand, computed from well logs (dot denotes CO₂ injection point).



a)



b)

Figure 22. a) Log correlation cross-section across the southern Utsira depocentre, showing the lateral variation in shale content (percentage clean sand). b) Section location with map of percentage clean sand in southern depocentre.

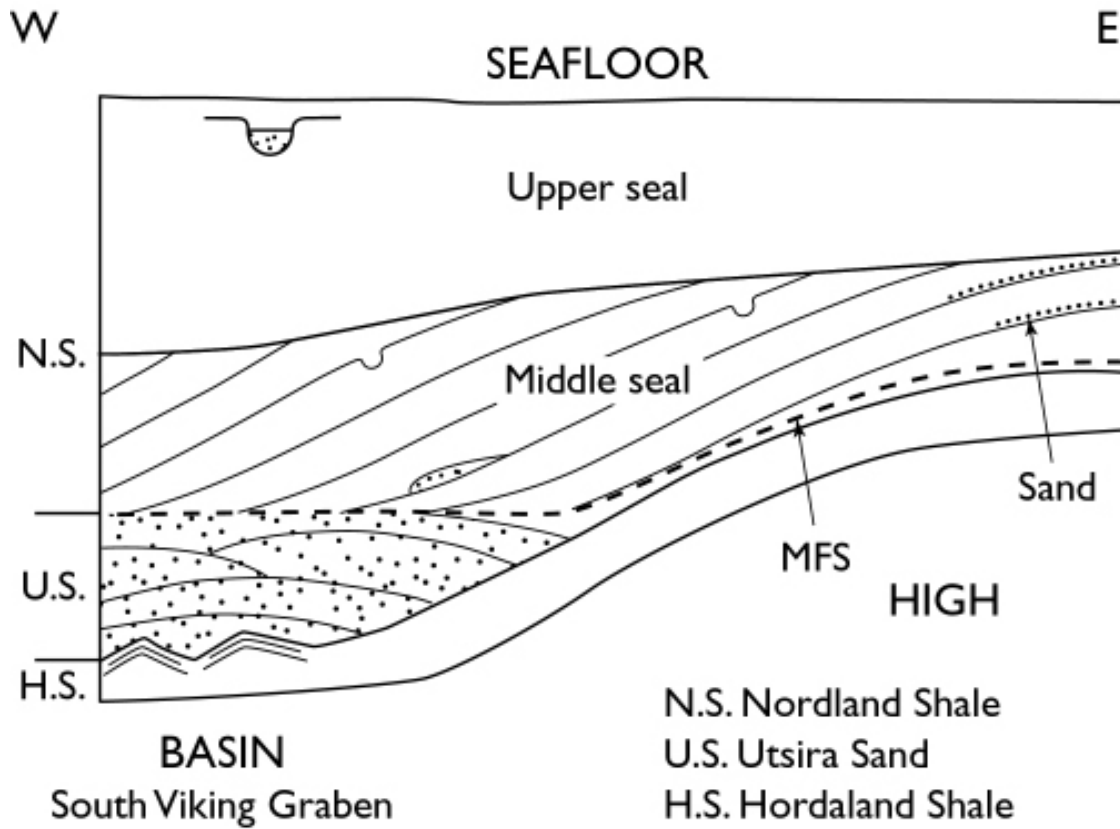
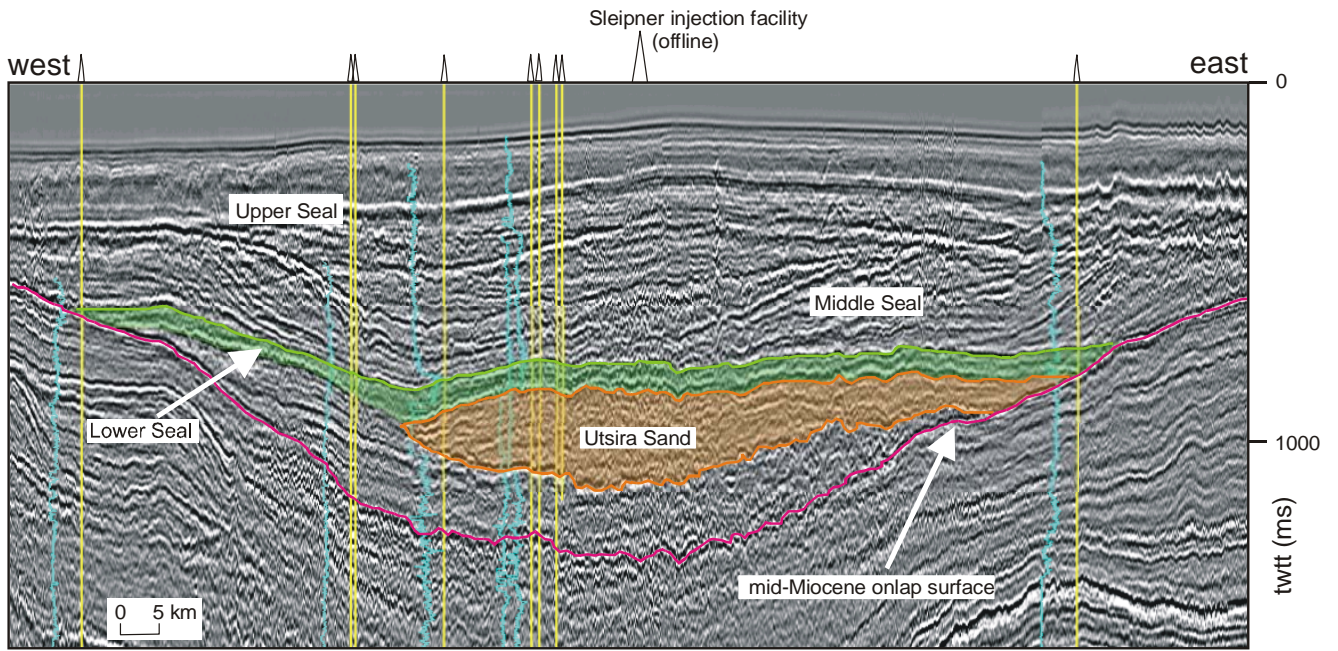


Figure 23. Schematic diagram of Pliocene prograding wedges and possible distribution of lithologies.



a

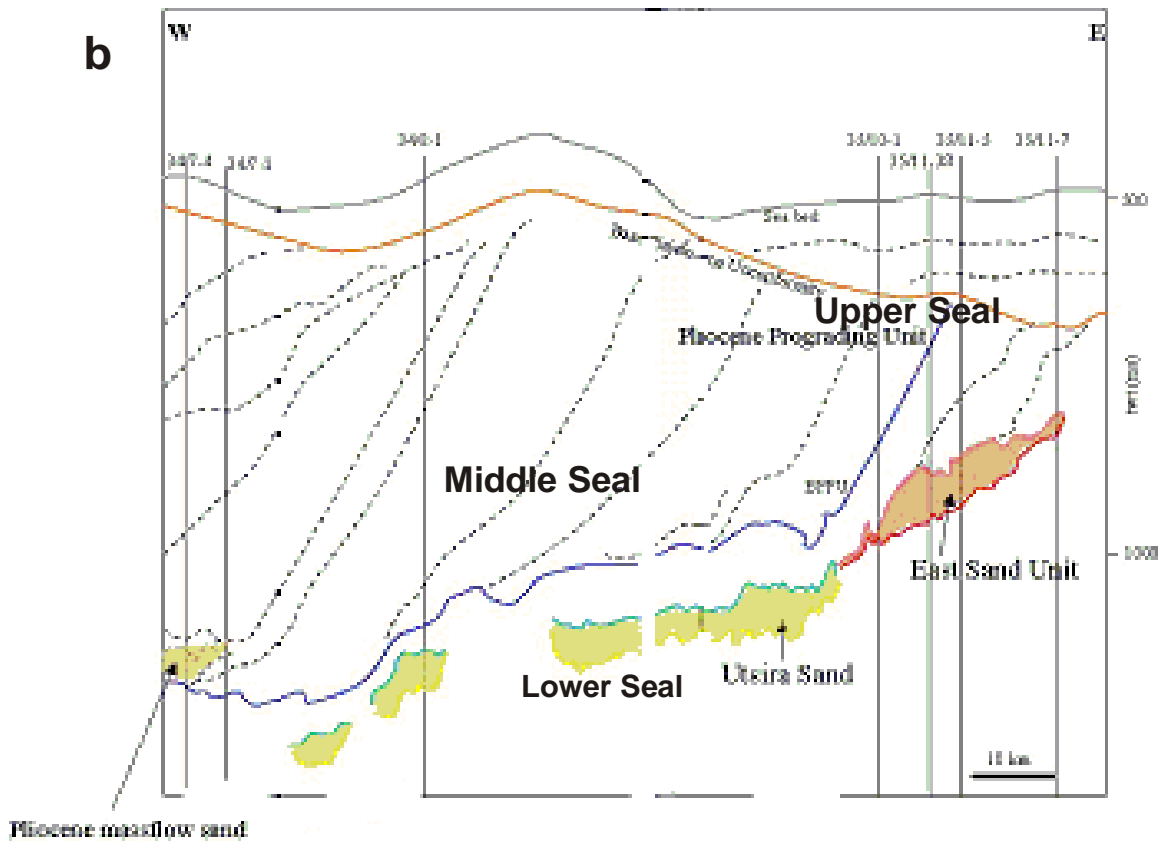


Figure 24. a) Seismic section across the southern Utsira depocentre showing the main caprock units. b) Interpreted geoseismic section across the northern Utsira depocentre showing the main caprock units.

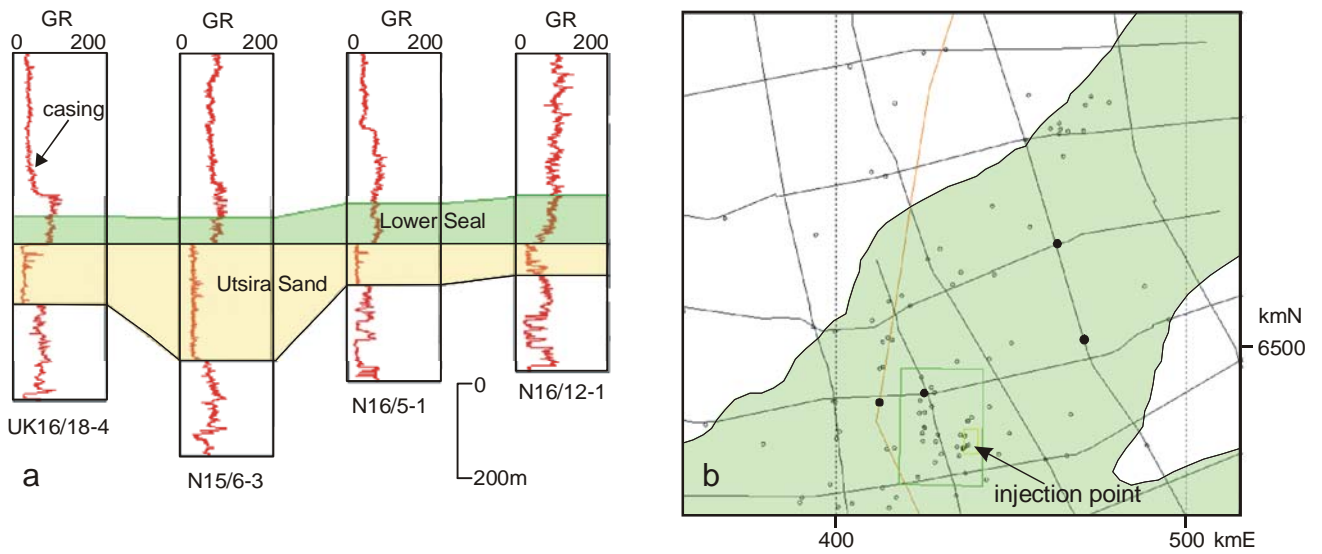


Figure 25. a) Log detail of the Lower Seal around Sleipner b) Extent of the Lower Seal above the southern Utsira depocentre. Larger rectangle denotes survey ST98M11, smaller rectangle denotes 1999 time-lapse survey.

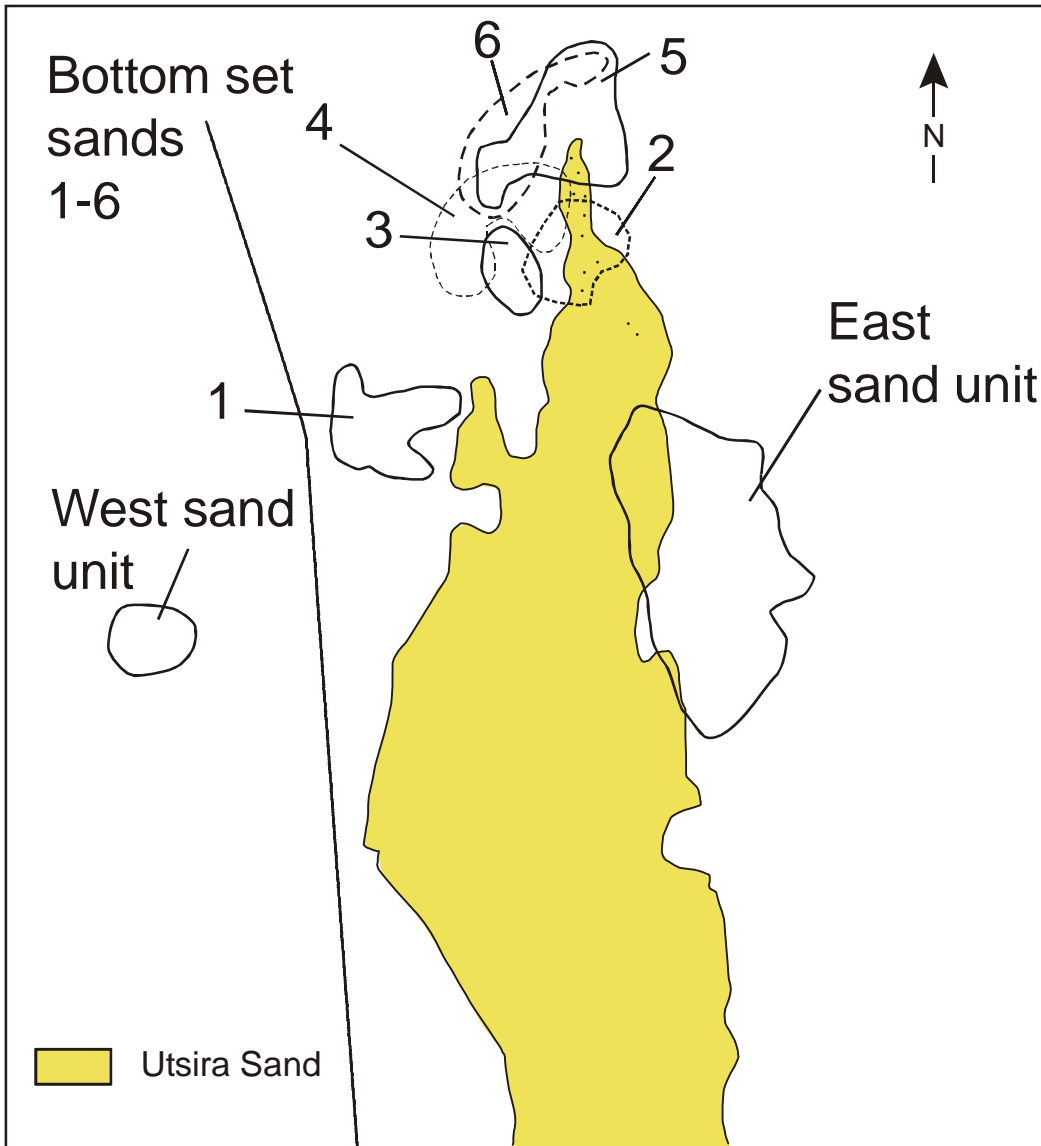
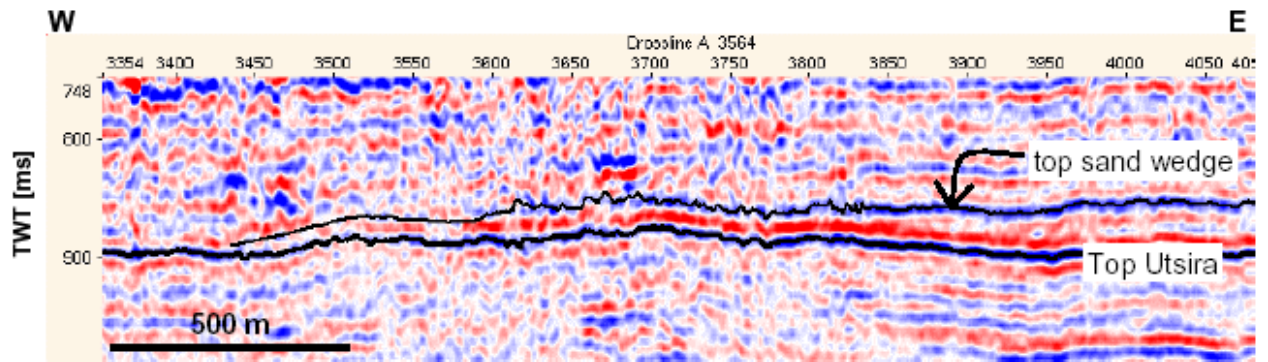


Figure 26. Distribution of minor sand units in the caprock succession.



a

b

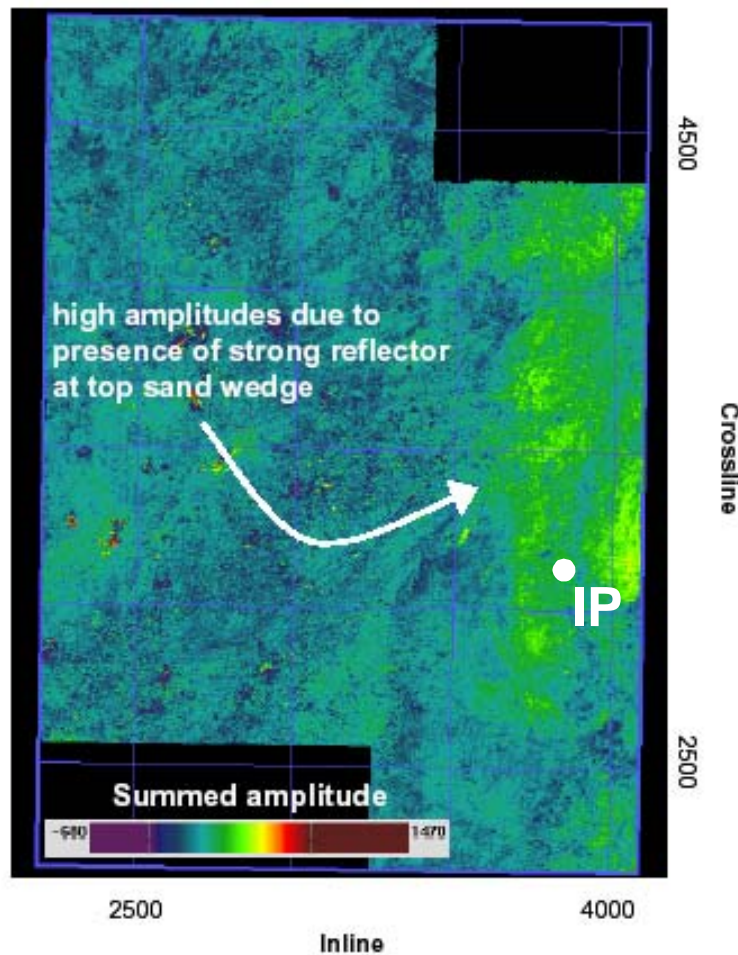


Figure 27. a) The Sand-wedge on seismic b) Approximate extent of Sand-wedge picked out by high amplitudes c) Thickness map (metres) of the Sand-wedge based on seismic mapping and well data.

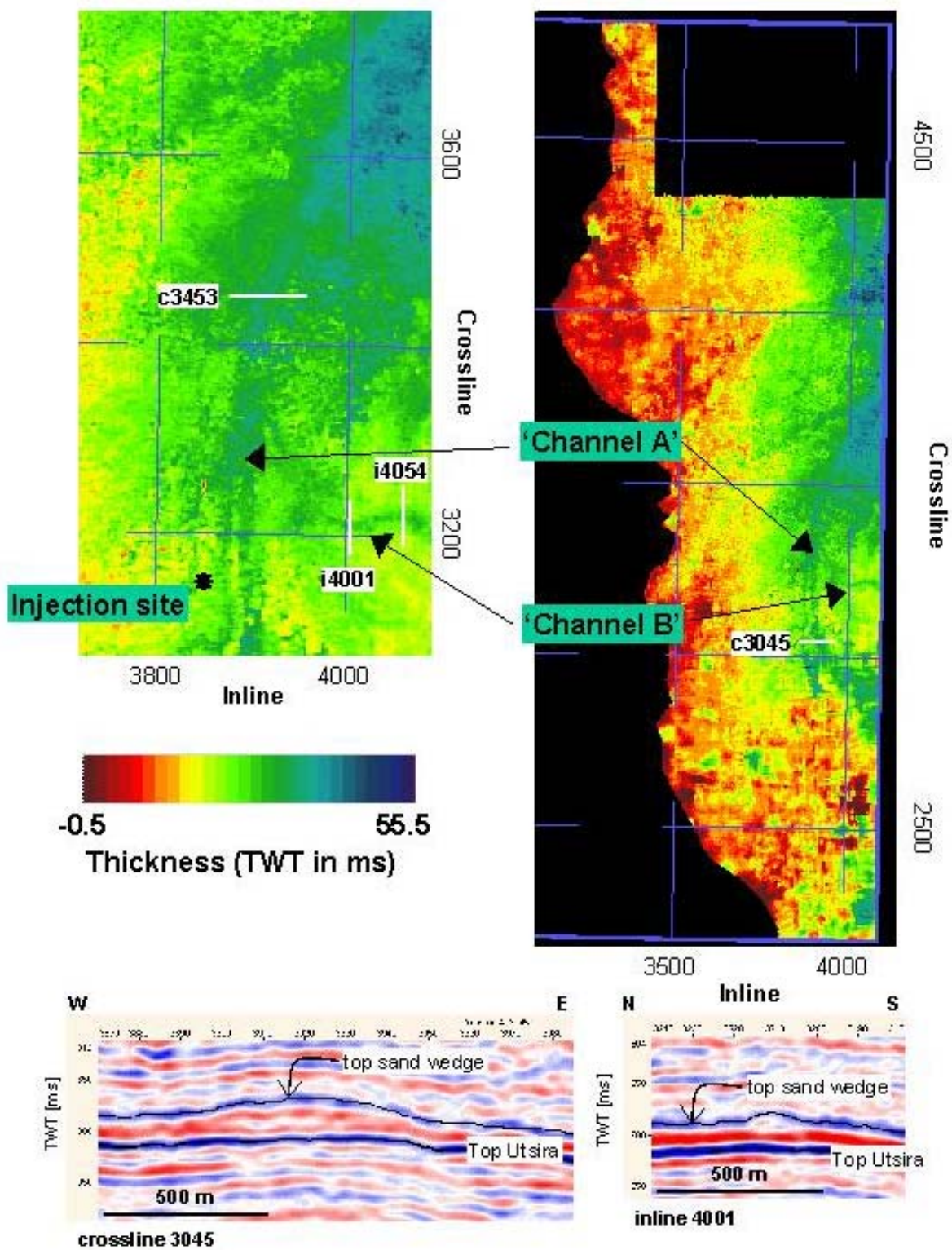


Figure 28. Thickness maps of the Sand-wedge (upper), reveal curved linear features interpreted as channels, also visible on individual seismic lines (lower).

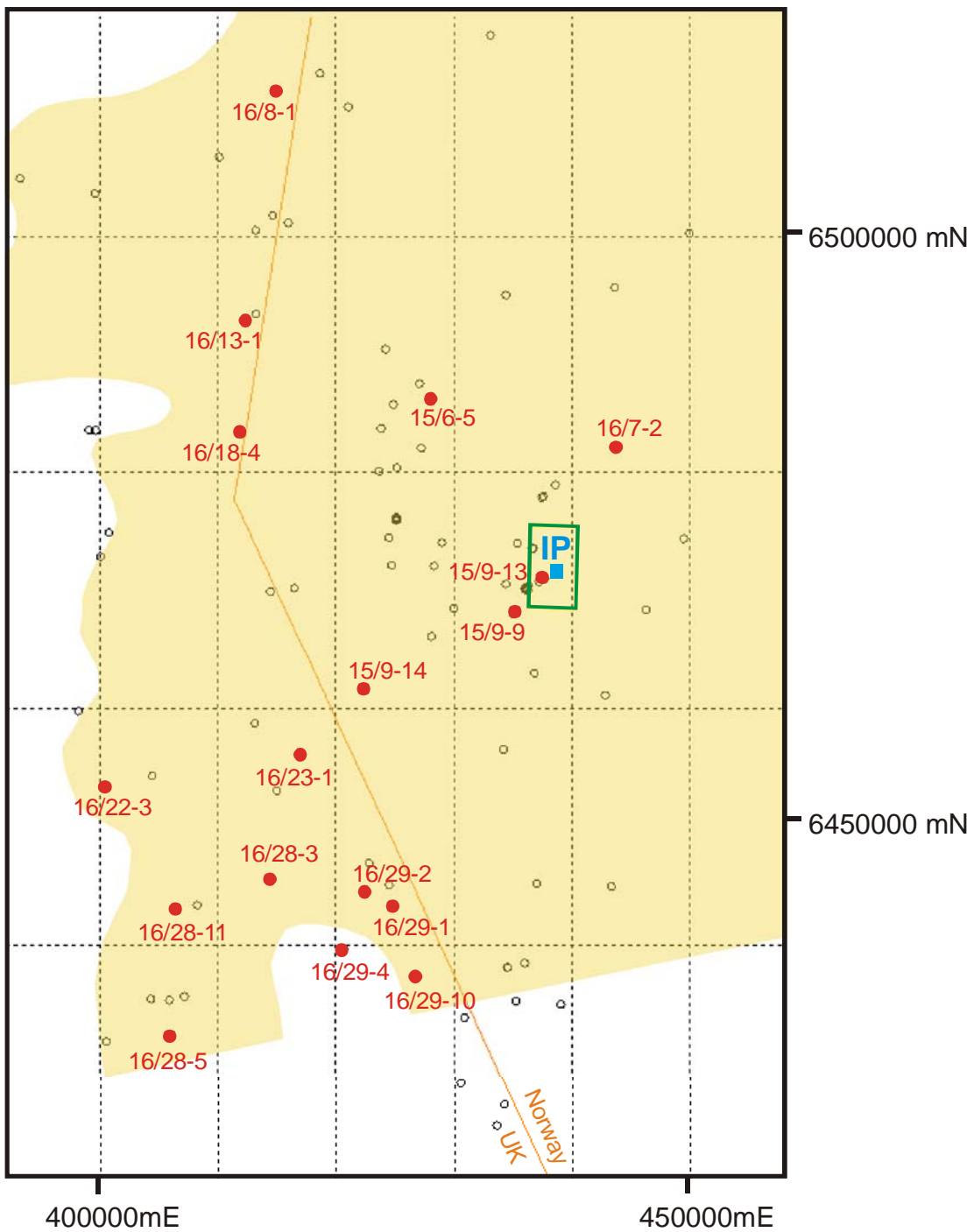


Figure 29. Wells with caprock cuttings samples. IP denotes CO₂ injection point. Green rectangle shows area of 1999 time-lapse seismic survey. Shaded area denotes extent of Utsira Sand.



a



b

Figure 30. Typical examples of caprock cuttings a) shale fragments from Norwegian well 15/9-9, 615 m depth b) grey shale fragments from Norwegian well 15/9-14, 855 m depth.

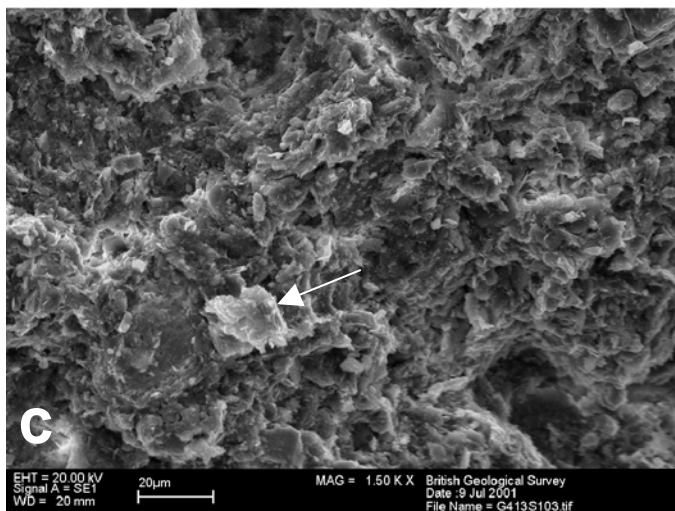
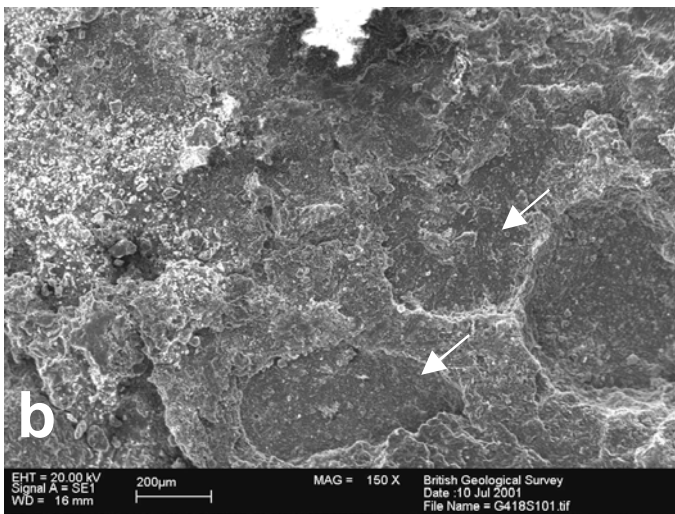
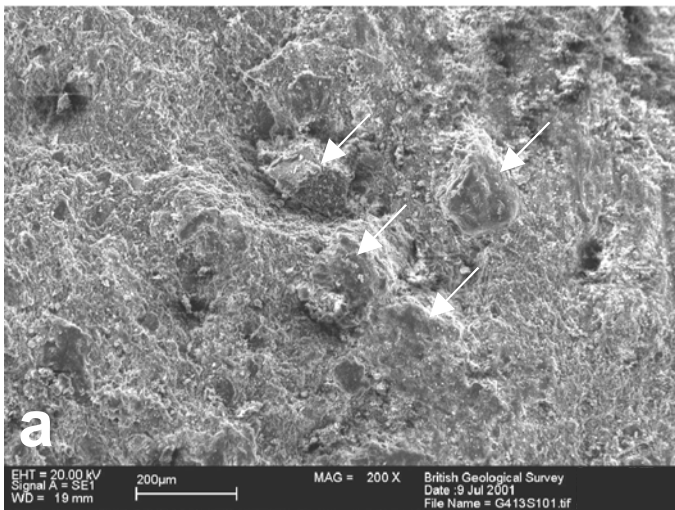


Figure 31. SEM images of caprock cuttings material from wells in the UK sector a) Massive mudrock with several rounded fine-grained quartz grains, UK well 16/29-1, 907 m depth b) Massive mudrock with large (up to 0.5 mm) voids (arrowed) where sand grains have been plucked out, UK well 16/28-3, 990 m depth c) High magnification detail of massive mudrock, showing tightly packed rather randomly-oriented clay particles. Note presence of clay mineral particles (arrowed), up to 20 μm in diameter, UK well 16/29-1, 907m depth.

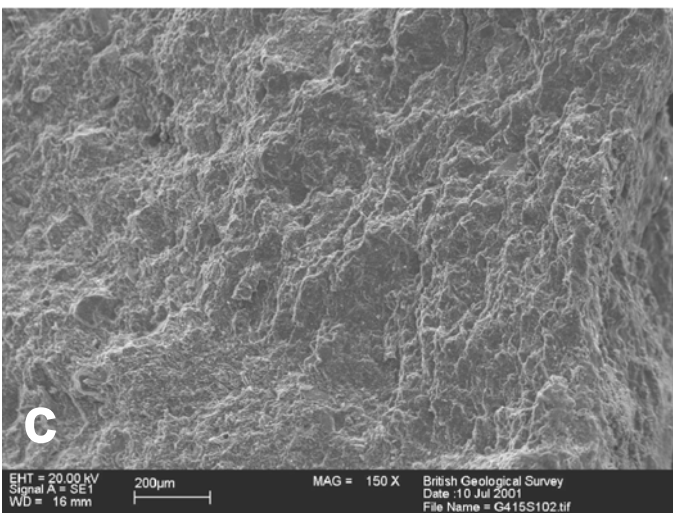
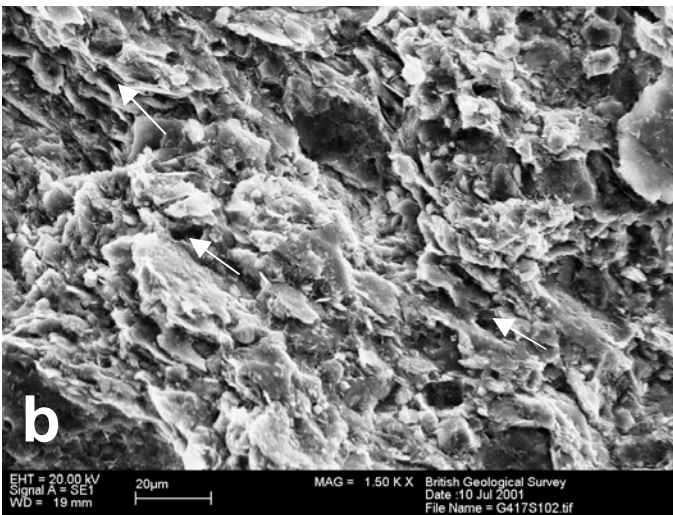
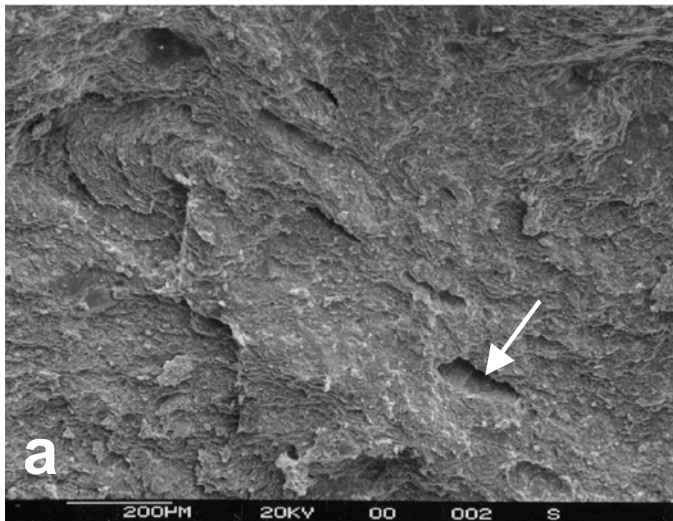


Figure 32. a) Laminated mudrock with holes where fine sand grade grains have been plucked out, UK well 16/29-4, 1055 m depth b) High magnification detail of laminated mudrock showing tightly packed platelets with preferred orientation. Micropores (arrowed) are a few microns in diameter and poorly connected with each other, UK well 16/28-3, 970 m depth. c) Laminated mudrock, lamination defines terraced appearance of sample, UK well 16/29-1, 998 m.

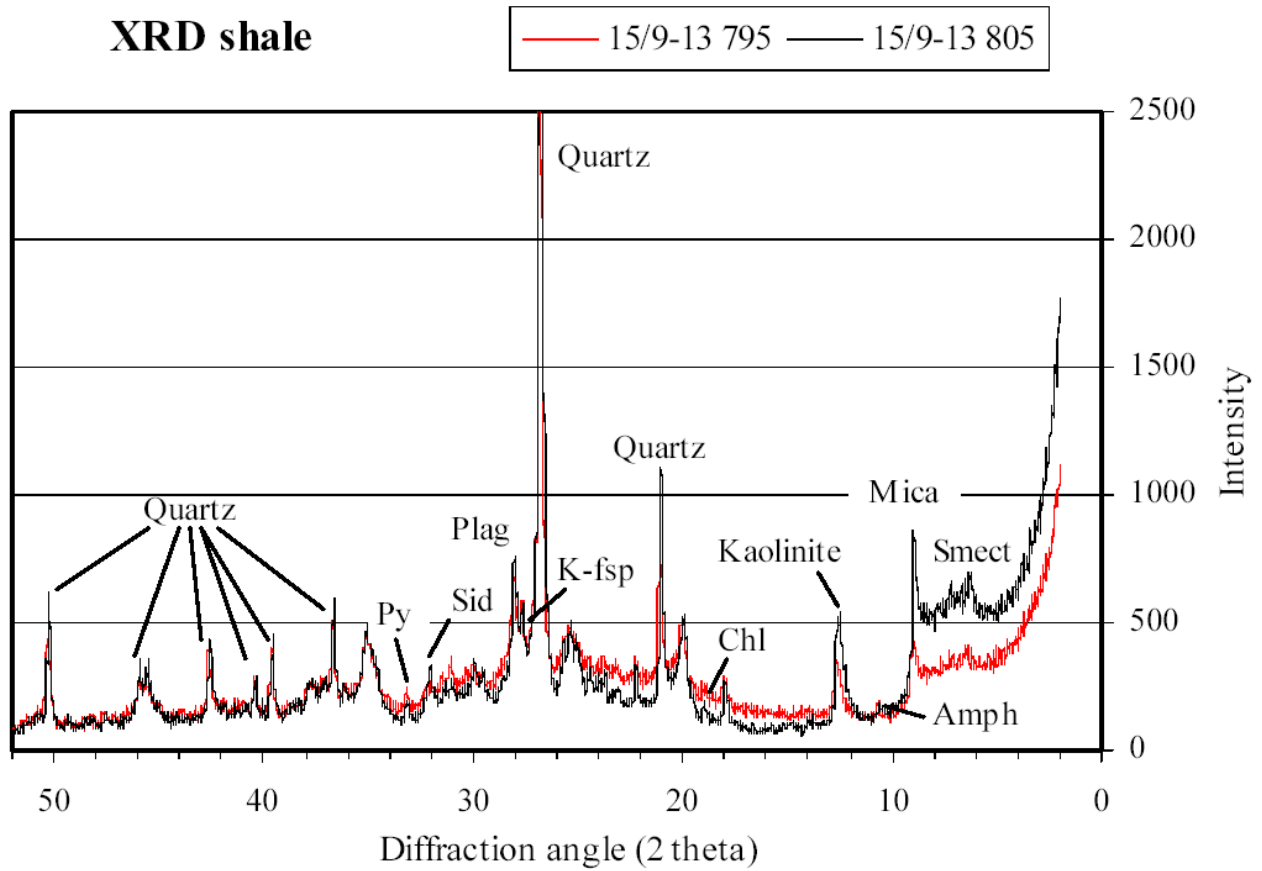


Figure 33. X-ray diffraction traces from two caprock samples from Norwegian well 15/9-13, 795 and 085 m depth.

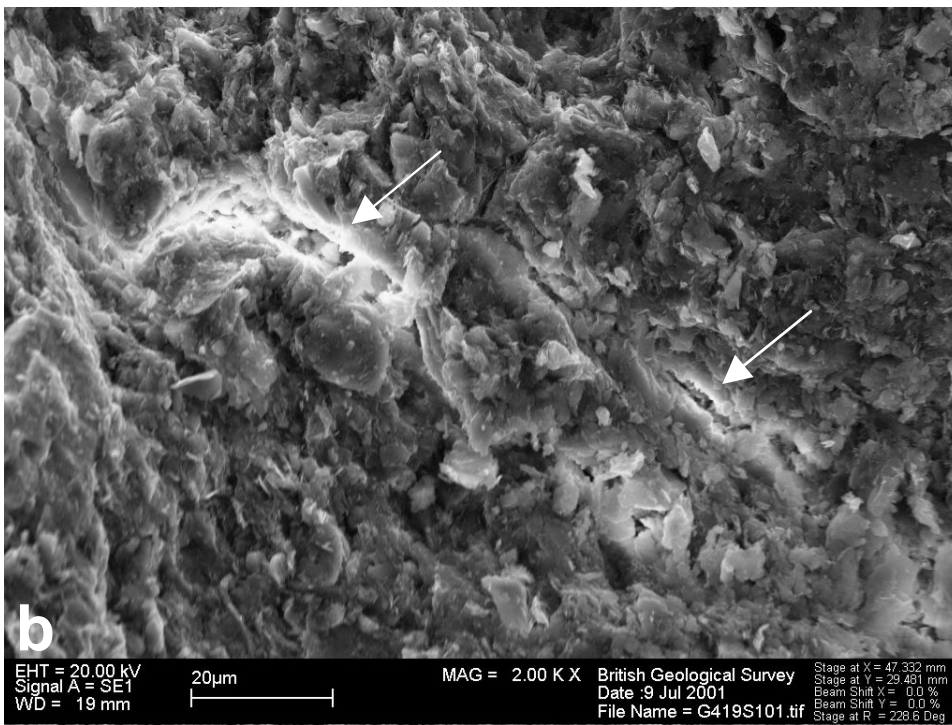
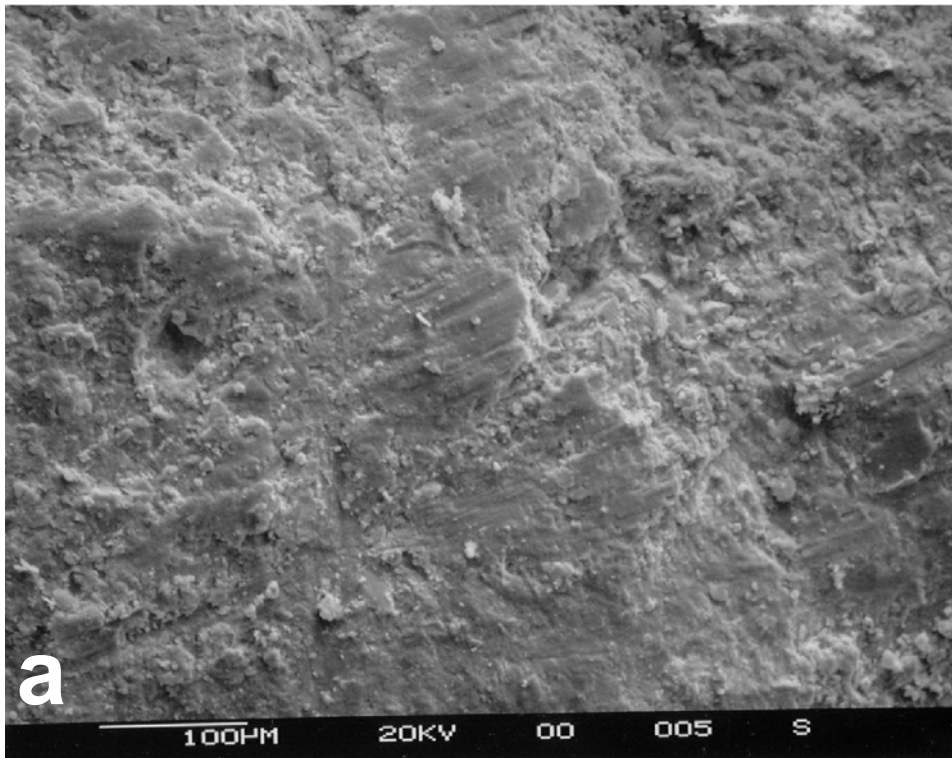


Figure 34. a) Mudrock with well-developed slickensides, UK well 16/28-5, 1100 m depth b) Mudrock with microfractures (arrowed), interpreted to result from sample shrinkage during drying out UK well 16/23-1 945 m depth.

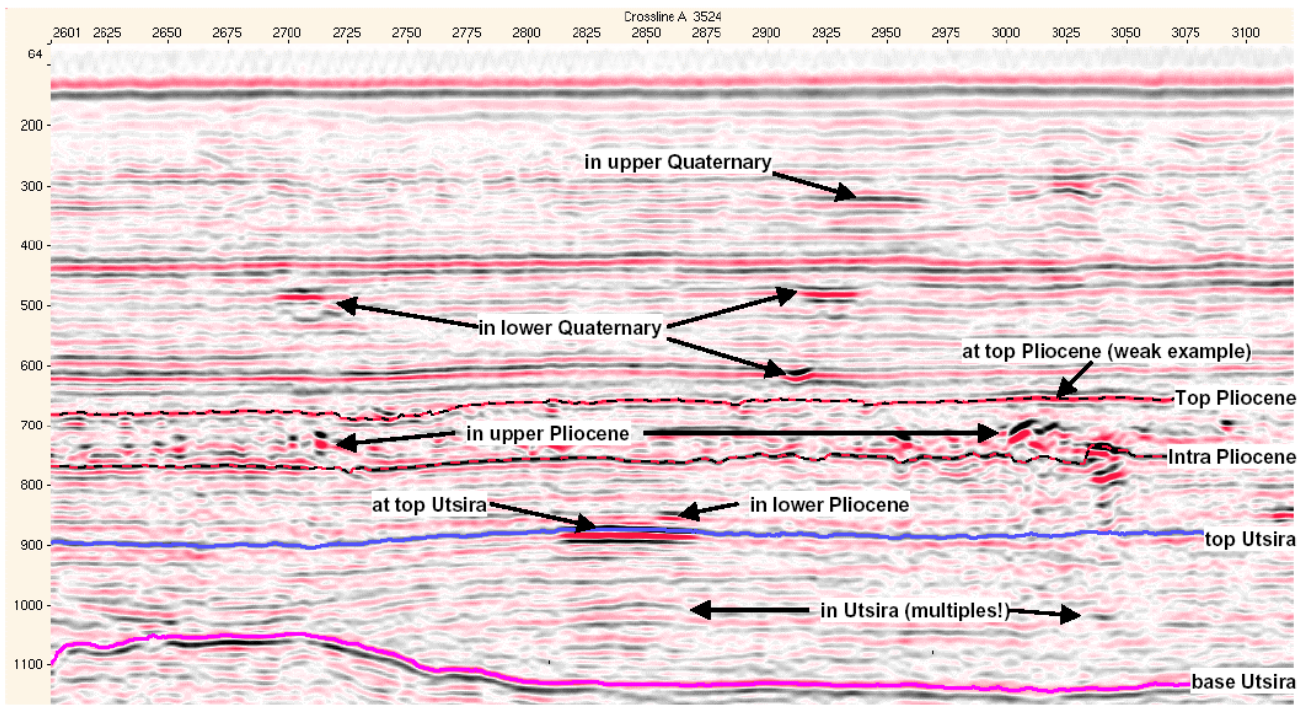


Figure 35. Seismic amplitude anomalies around and above the Utsira Sand

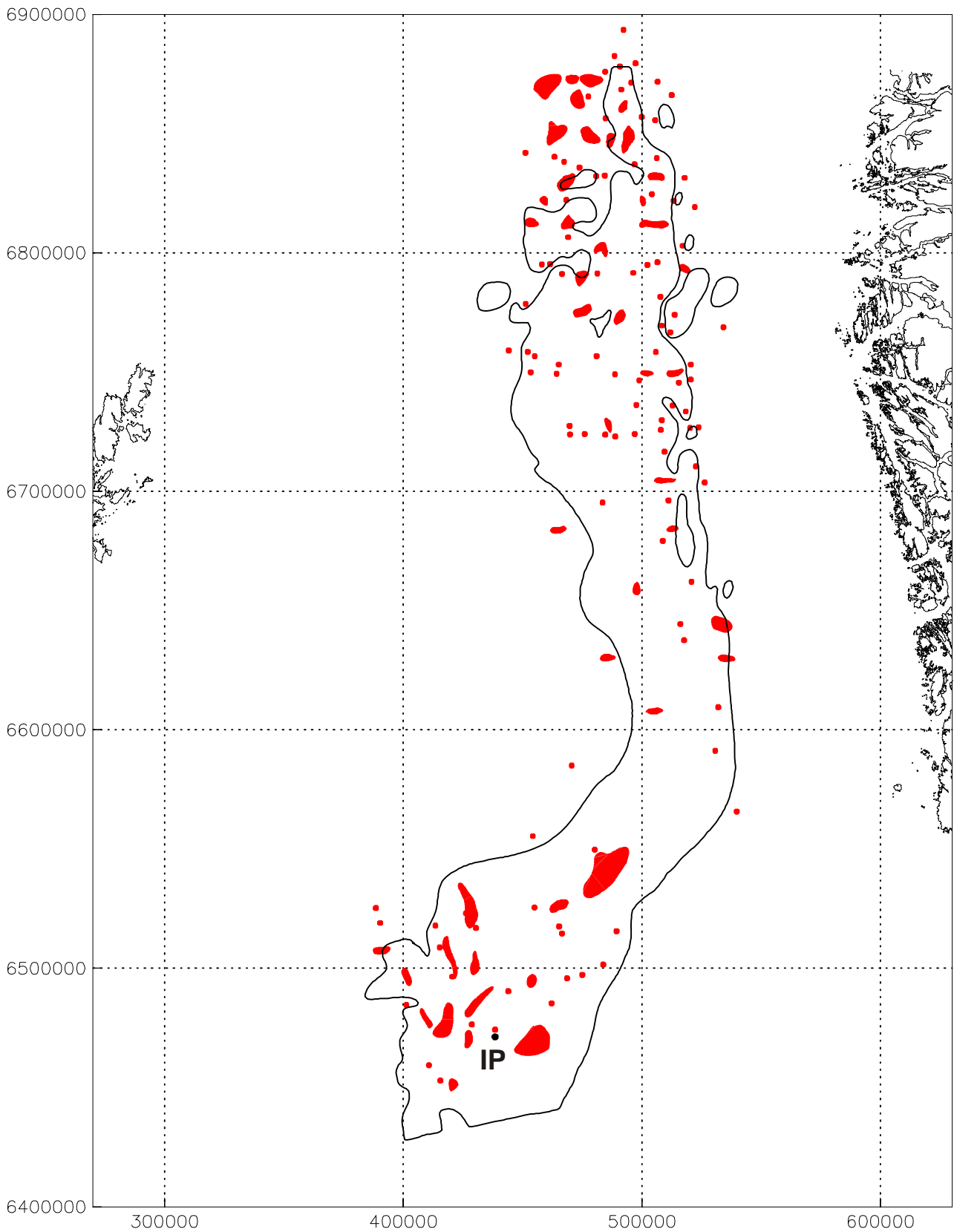


Figure 36. Regional distribution of seismic amplitude anomalies in the Lower Seal

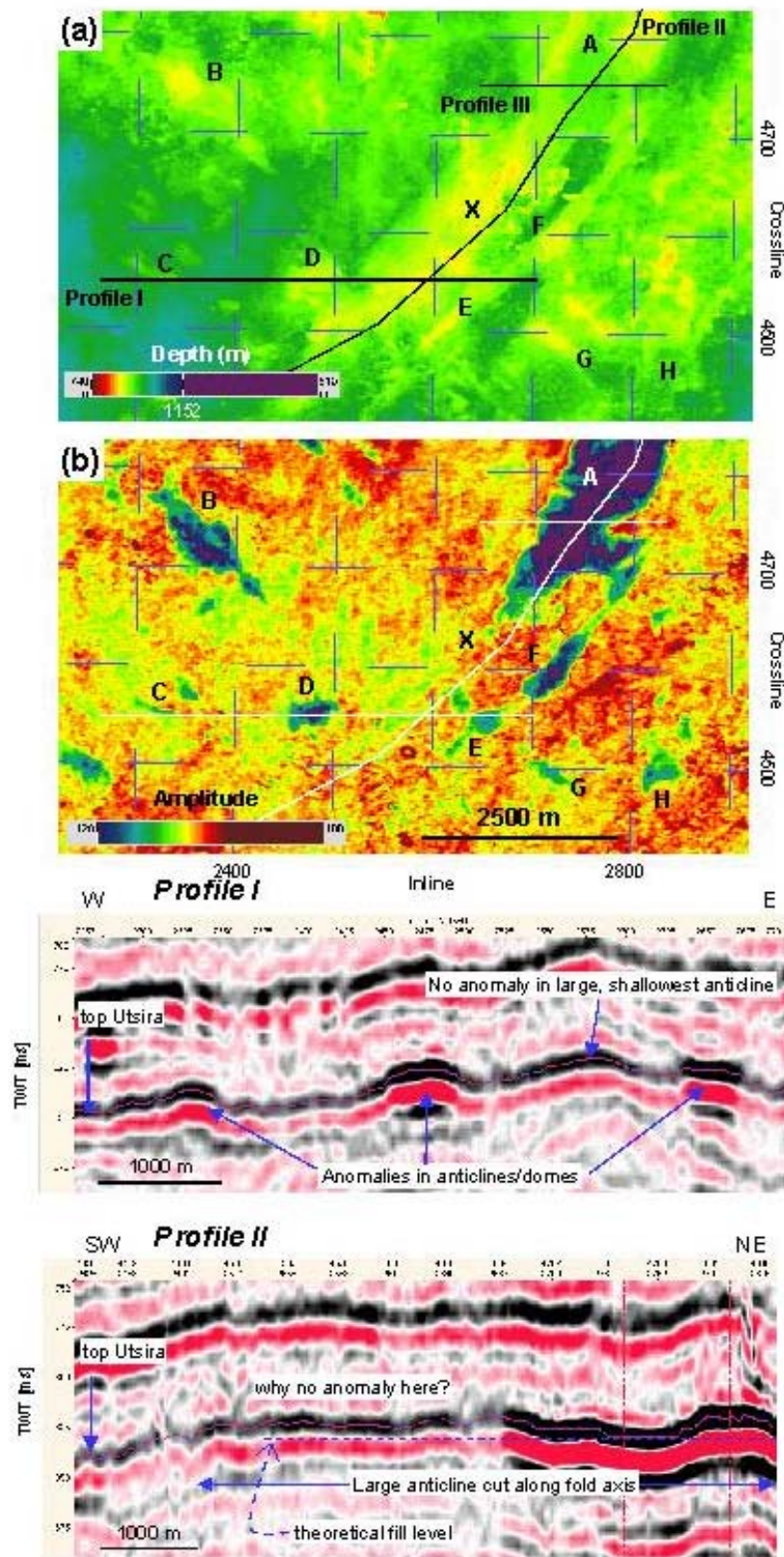


Figure 37. Seismic amplitude anomalies at the top of the Utsira Sand a) depth map b) seismic amplitude map, note prominent blue anomalies c) d) seismic sections through the anomalies, showing structural control of higher amplitudes.

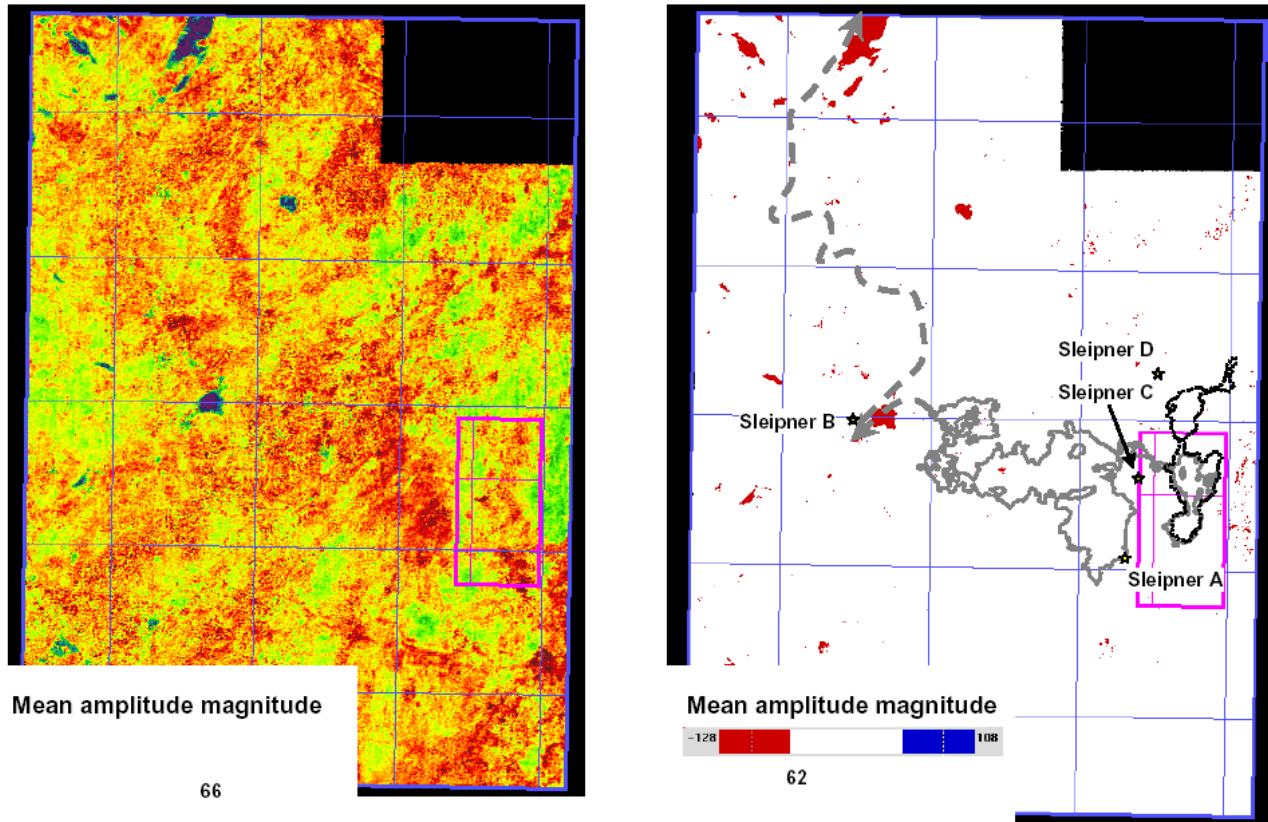


Figure 38. Survey ST98M11, seismic amplitude anomalies at top Utsira Sand

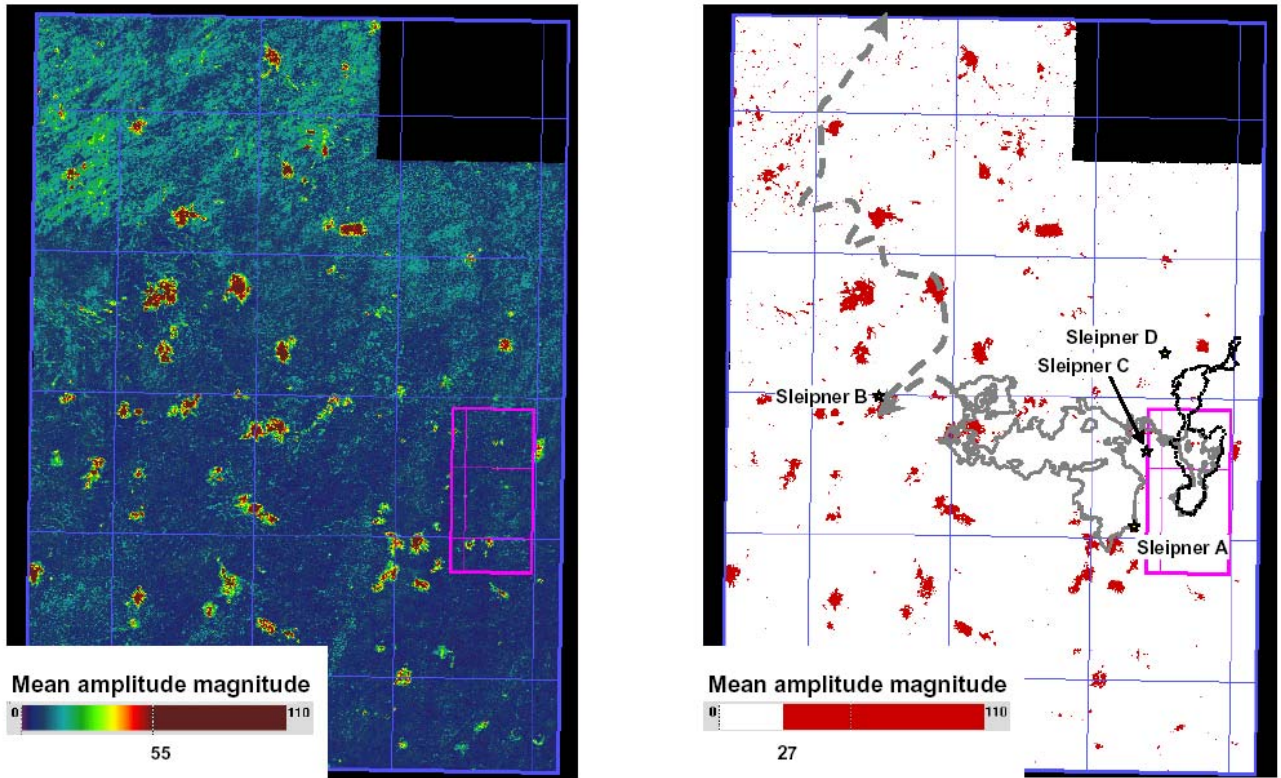


Figure 39. Survey ST98M11, seismic amplitude anomalies in the Lower Seal

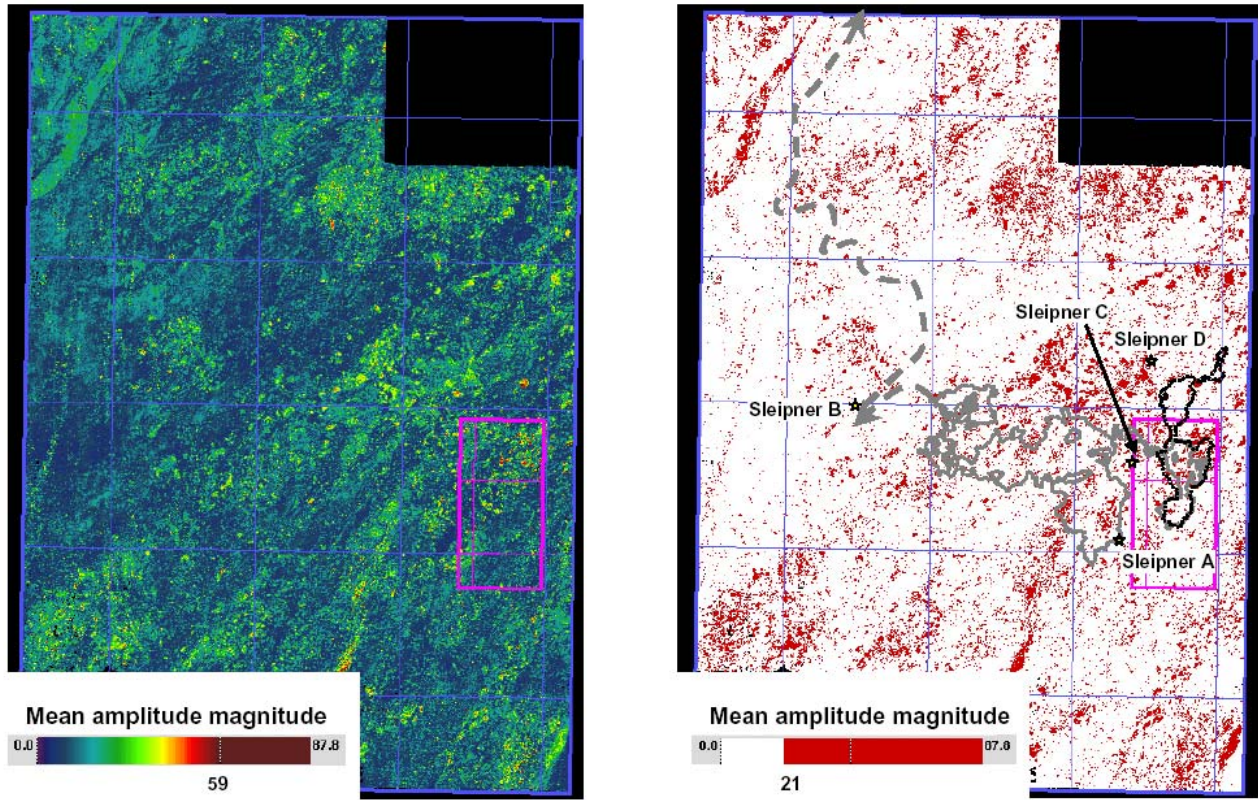


Figure 40. Survey ST98M11, seismic amplitude anomalies in the Middle Seal, note prominent NE-trending grain.

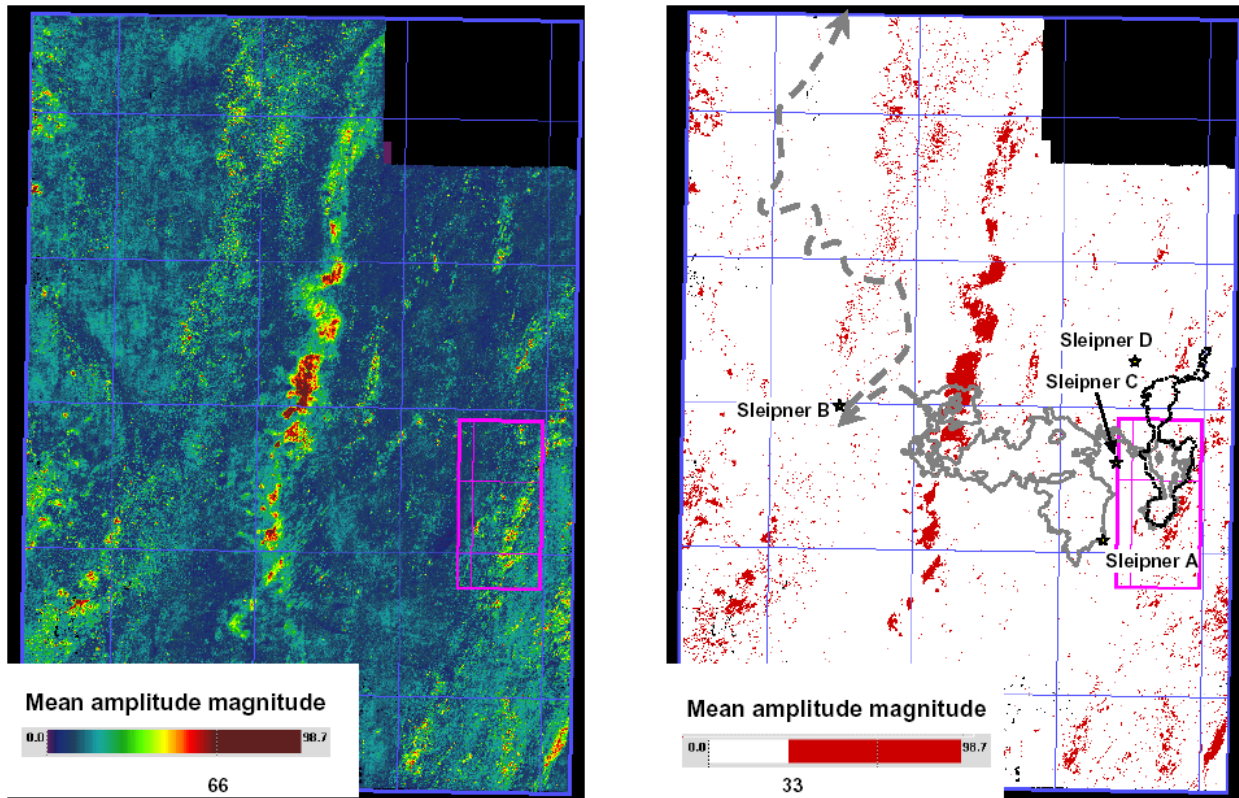


Figure 41. Survey ST98M11, seismic amplitude anomalies from the topmost Middle Seal, note the NNE linear trends, interpreted as channel features.

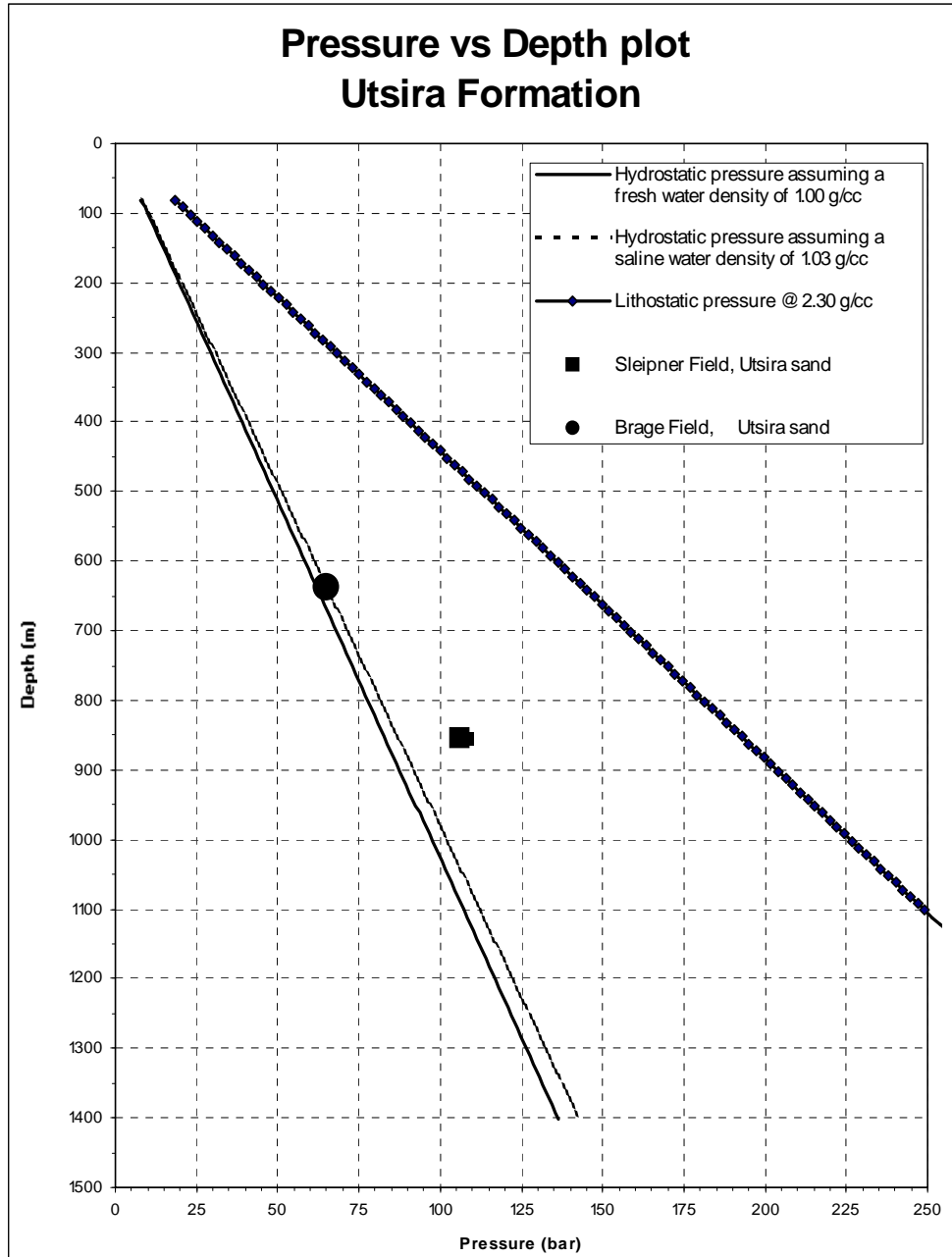


Figure 42. Formation pressure data from the Utsira Sand

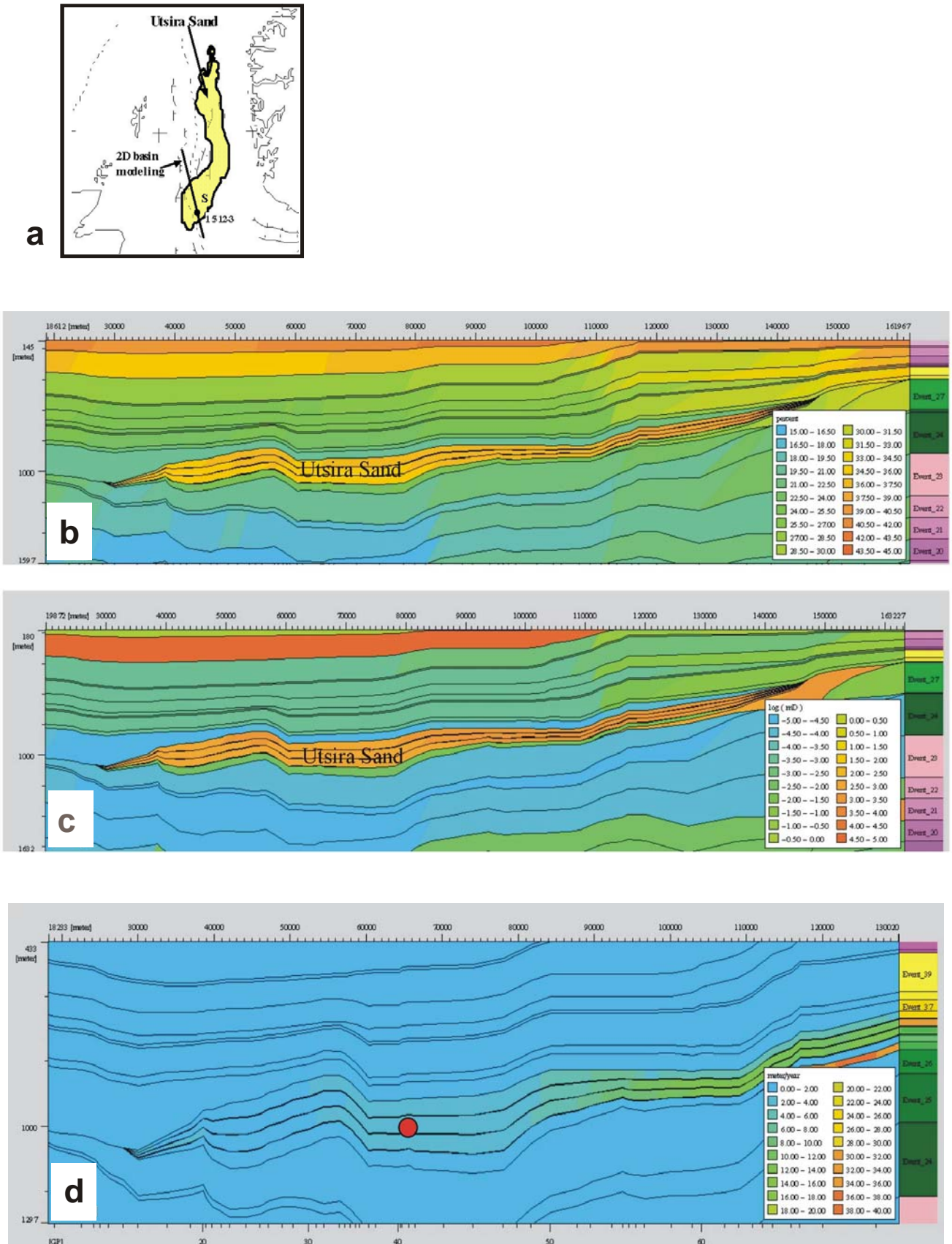


Figure 43. 2D basin model a) Location map b) Porosity of the Utsira Sand and surrounding formations c) Permeability of the Utsira Sand and surrounding formations d) Predicted present-day fluid flow velocity (metresyear⁻¹) due to sediment compaction.

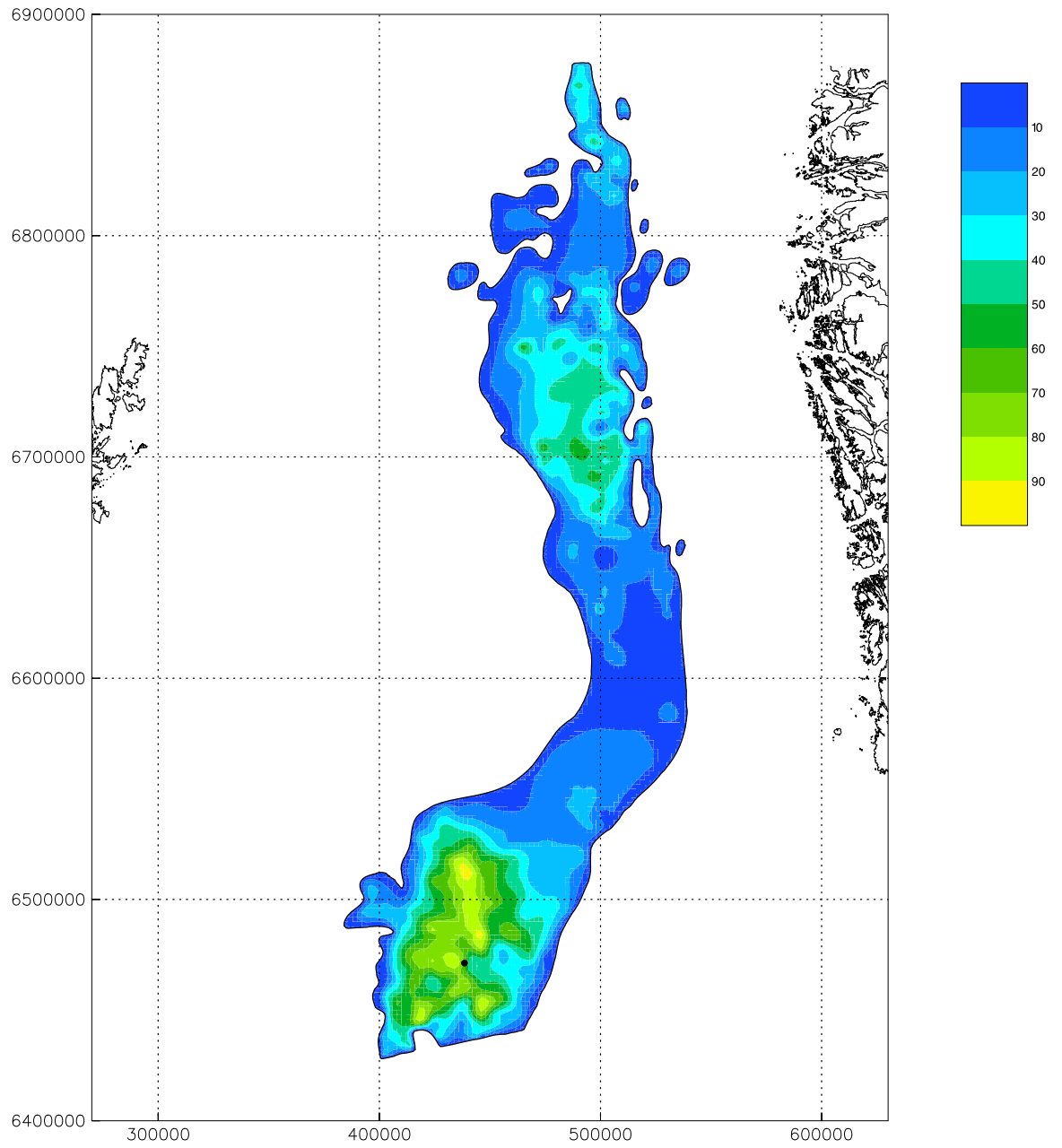


Figure 44. The Utsira Sand, total pore-space thickness (metres). Dot denotes CO₂ injection point.

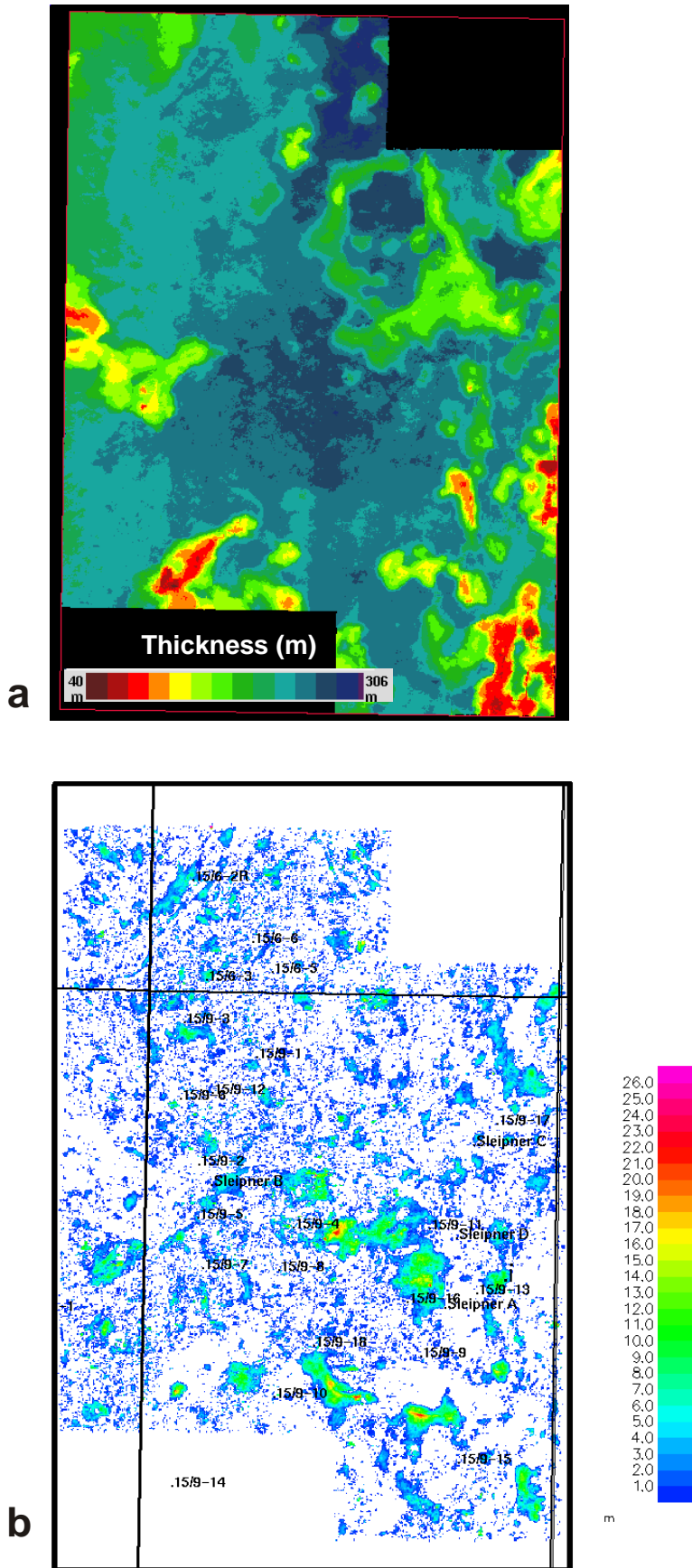


Figure 45. a) Survey ST98MT11 a) Utsira Sand thickness b) Structural traps at the top Utsira Sand. Colour scale gives height (metres) of trapped fluid column.

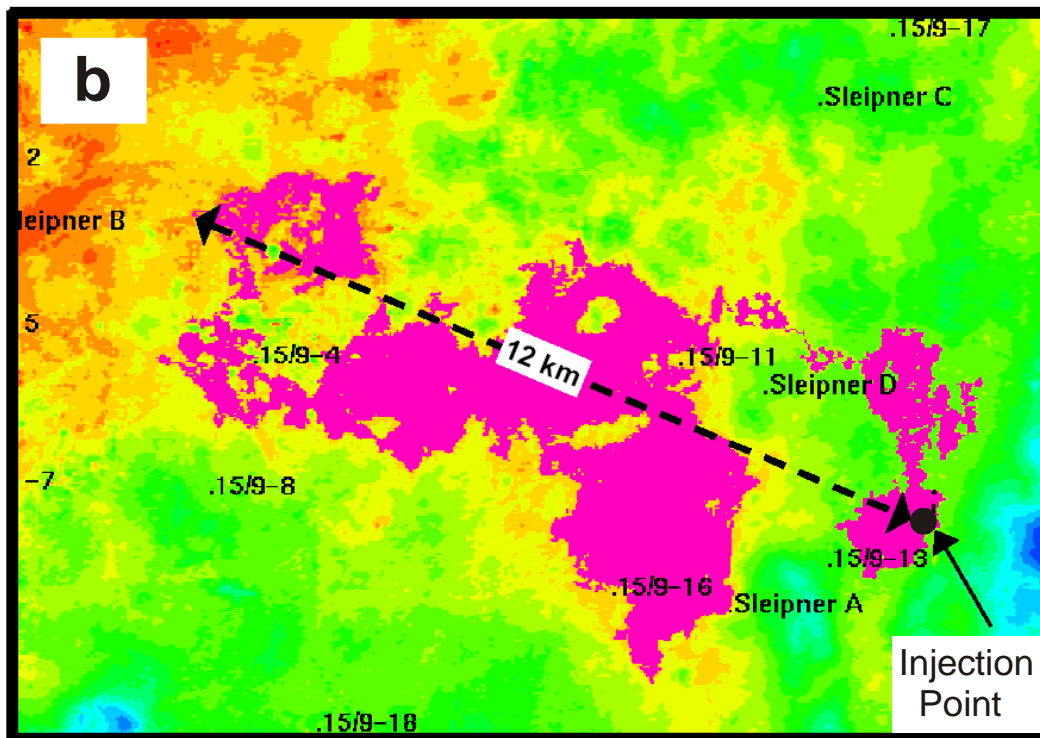
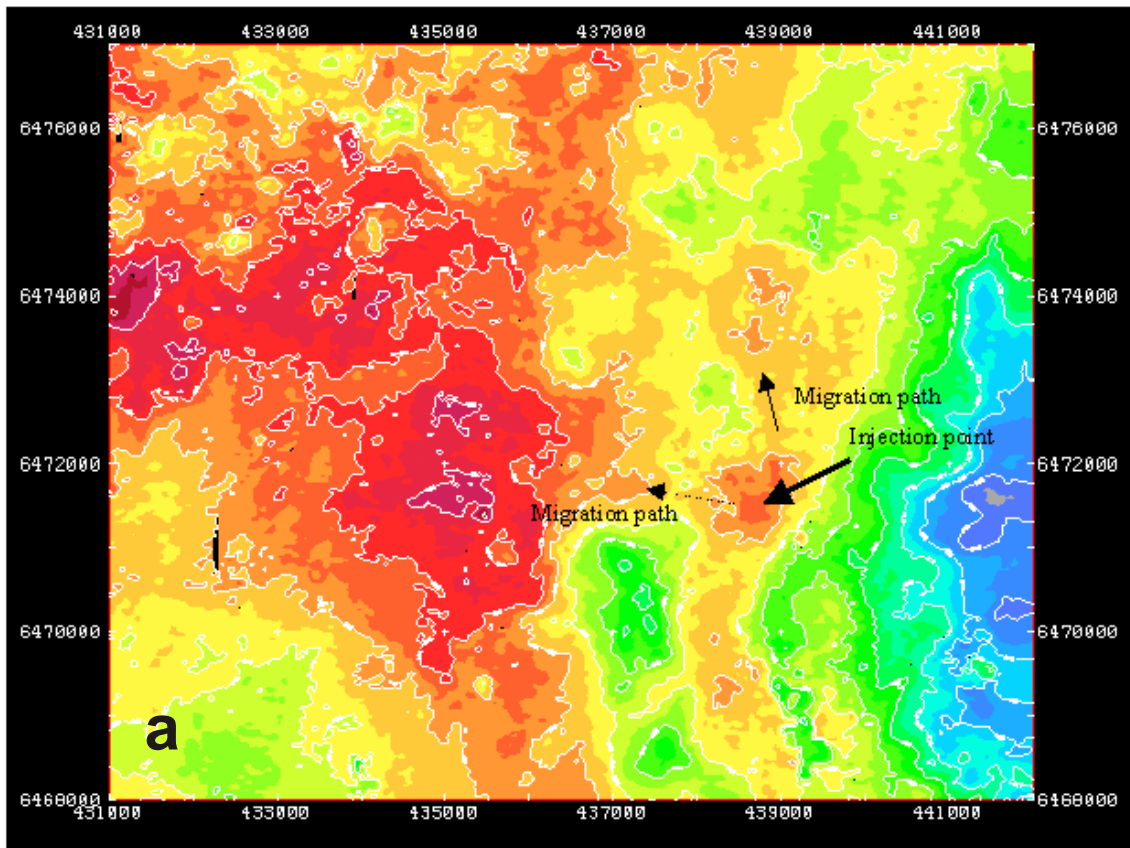


Figure 46. a) Detailed depth map of top Utsira Sand, showing potential initial migration paths from the injection point b) Final distribution of $30 \times 10^6 \text{ m}^3$ (~ 20 MT) of CO_2 assuming migration beneath the top of the Utsira Sand.

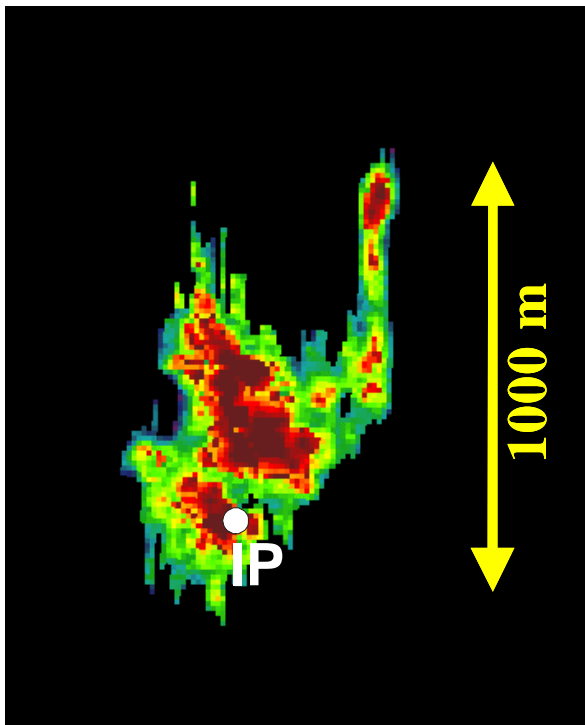
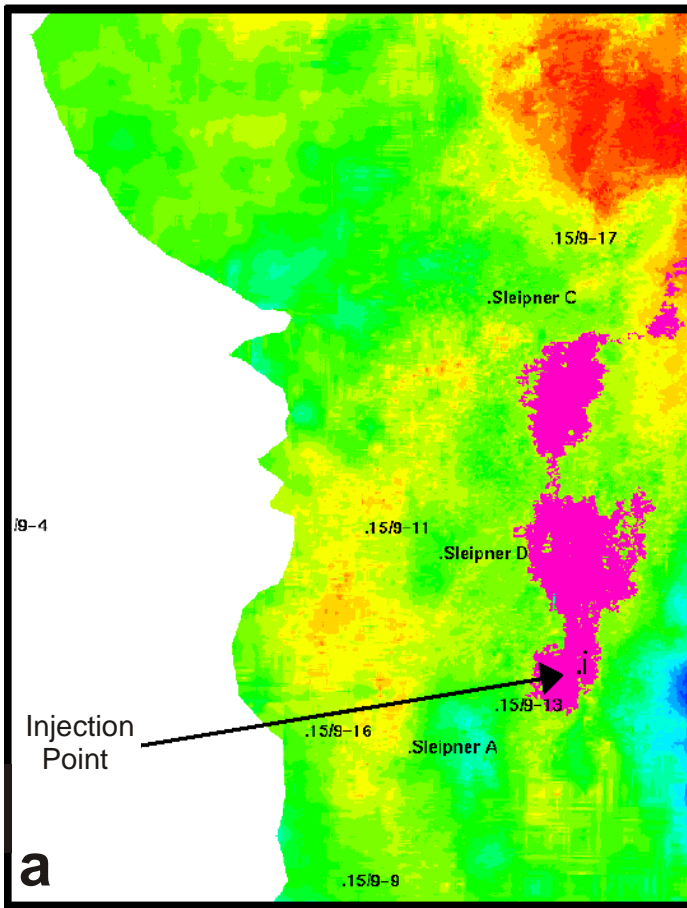


Figure 47. a) Final distribution of $7.4 \times 10^6 \text{ m}^3$ (~ 5 MT) of CO₂ assuming migration beneath the top of the Sand-wedge. Note if more CO₂ is injected it will migrate out of the mapped area. b) Image of the CO₂ accumulation beneath the top of the Sand-wedge from the 2001 time-lapse seismic data. Note linear northward migration feature beneath possible channel-related feature.

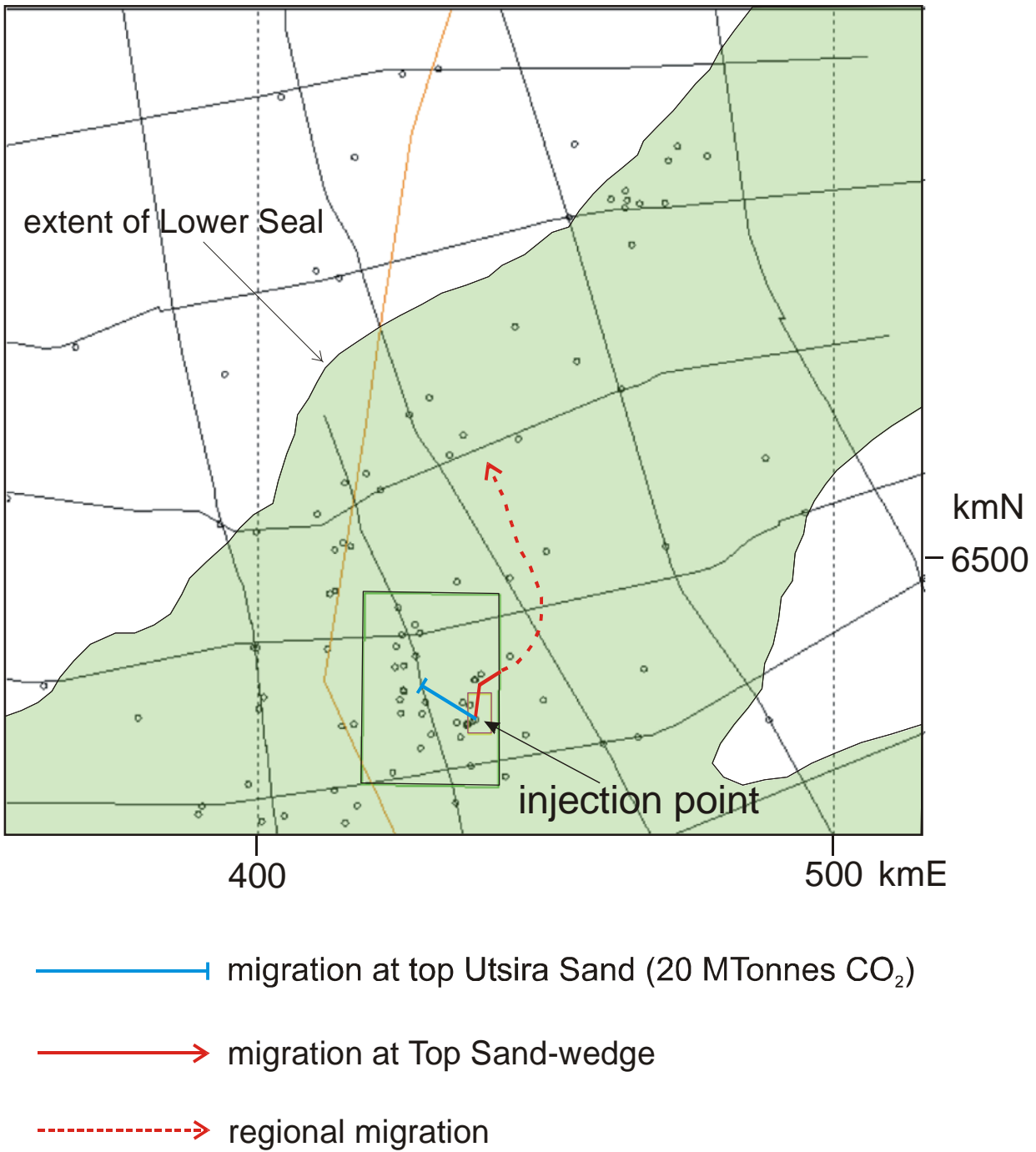


Figure 48. Regional migration trends from the Sleipner injection point. Large rectangle marks extent of ST98M11 survey, smaller rectangle marks 1999/2001 time-lapse surveys.